# Analysis of Seladin-1 Role in Apoptosis and Cholesterol Metabolism

---

**Dissertation**

**zur**

**Erlangung der naturwissenschaftlichen Doktorwürde**
**(Dr. sc. nat.)**

**vorgelegt der**

**Mathematisch-naturwissenschaftlichen Fakultät**

**der**

**Universität Zürich**

**von**
Arames CRAMERI

**von** Poschiavo/GR

**Promotionskomitee**

Prof. Dr. Peter Sonderegger (Vorsitz)
Dr. M.Hasan Mohajeri (Leitung der Dissertation)
Prof. Dr. Josef Jiricny

**Zürich, 2005**

# Contents

# Summary

Accumulation of amyloid-β peptides (Aβ) in the CNS is an invariant feature of the pathophysiology of Alzheimer's disease (AD), the most common form of dementia. Aβ peptides are derived from proteolytic cleavage of the amyloid precursor protein (APP) with the β-secretase cleaving at the N terminus and the γ-secretase(s) at the C terminus of Aβ peptides.

Accumulation of Aβ in the brain has a fundamental role in AD-pathology including the induction of tau phosphorylation and neurofibrillary tangle formation, deficits in synaptic transmission and synaptotoxicity, and leads to age-dependent neuronal loss. Given all the above, concentrated effort has been focused on the identification of regulatory mechanisms that control APP cleavage and are involved in Aβ production, on proteases with the capacity to degrade Aβ, as well as on neuroprotective factors.

A large body of literature indicates that alterations in cholesterol levels affect APP metabolism. Moreover, cholesterol is the major lipid constituent of the detergent resistant cholesterol-rich membrane domains (DRMs or rafts). The functional significance of DRM domains has been shown in cellular trafficking and in signaling events. The disorganization of DRM due to low cholesterol levels have been described in the hippocampus and cortex of a significant number of AD patients. In addition, DRMs are important to restrict APP β-cleavage and reduce Aβ production in primary neurons in culture. Consistently, these alterations also result in diminished activity of the Aβ degrading enzyme plasmin, which is normally produced in these domains.

The majority of studies exploring the biological function of DRMs have been based on pharmacological approaches utilizing drugs that diminish cholesterol or sphingolipids, or based on modifications of DRM proteins in cultured cells. The functions of DRMs in living animals, however, have not yet been shown. It is especially not known how changes in cholesterol levels and distribution affect DRM dependent functions, such as APP processing *in vivo*.

Seladin-1 (the selective Alzheimer's disease indicator-1), encoded by a single gene (DHCR24) on chromosome 1, is an evolutionary conserved gene whose

product catalyzes the reduction of the Δ24 double bond of sterol intermediates leading to cholesterol production. It was shown that seladin-1 levels are lower in affected neurons in AD, suggesting that seladin-1 levels may influence the selective vulnerability of neurons in AD. Overexpression of seladin-1 *in vitro* protected cells from apoptosis induced by oxidative stress and high expression of endogenous seladin-1 was associated with resistance against Aβ-induced toxicity. Moreover, functional expression of seladin-1 resulted in the inhibition of caspase 3 activation after either Aβ-mediated toxicity or oxidative stress and protected the cells from apoptotic cell death. Deficiency in the Dhcr24 gene causes a severe autosomal recessive disorder characterized by elevated levels of the cholesterol precursor desmosterol in plasma. Seladin-1 knock-out mice are viable, although almost no cholesterol was detected in plasma and tissue of these animals.

This study gives insight into the role of seladin-1 in neuroprotection, regulation of cholesterol levels and cholesterol-mediated functions *in vitro* and *in vivo*. We show that seladin-1 expression modulates APP processing and Aβ generation *in vivo*. We substantiated the anti-apoptotic function of seladin-1 in human neuroblastoma cells and show for the first time that elevated seladin-1 expression increases the levels of cellular and membrane cholesterol and therefore affects the distribution and function of rafts in these cells. Furthermore, we demonstrate that the overexpression of seladin-1 leads to reduced amyloidogenic APP processing and decreased generation of the Aβ peptide. In contrast, decreased seladin-1 expression in mouse brain resulted in lower levels of cellular and membrane cholesterol and elevated concentrations of the cholesterol presursor desmosterol. A significant increase of $A\beta_{40}$ and $A\beta_{42}$ was observed in brains of seladin-1 deficient mice overexpressing the human APP carrying the Swedish mutation when compared to littermates with a normal seladin-1 expression. The findings that low expression of seladin-1 parallele a reduction in brain cholesterol levels strengthen the notion that brain cholesterol loss participates in the pathogenesis of AD. Because of its role in cholesterol synthesis and neuroprotection, increasing seladin-1 activity in CNS neurons may therefore represent a putative therapeutical target for AD treatment.

# Zusammenfassung

Die Alzheimer Krankheit ist eine der häufigsten Formen von seniler Demenz bei älteren Menschen. Sie ist durch den Verlust von Gedächtnis und anderen kognitiven Funktionen gekennzeichnet, welcher wiederum auf den Verfall von Nervenzellen zurückzuführen ist. Bisher gibt es noch keine eindeutige Erklärung für diesen zahlreichen Zerfall der Neurone, doch scheint unter anderem die vermehrte Ablagerung von abnormalen Proteinen die Ursache hierfür zu sein. Diese bestehen teilweise aus extra- und intrazellulärem β-amyloid (Aβ), dem Spaltprodukt des Vorläuferproteins (APP). Aβ reichert sich im Krankheitsfall zu Plaques an und ist schädlich für die Nervenzellen. Zum anderen finden sich in Gehirnen von Alzheimer Patienten intrazelluläre Anreicherungen von so genannten „tangles“, das sind hyperphosphorylierte Formen des Zellgerüst-assoziierten Proteins Tau.

In ca. 10% der Alzheimer Fälle wird die Krankheit durch Genveränderungen ausgelöst. In dieser familiären Form der Erkrankung treten die klinischen Zeichen und neuropathologischen Veränderungen bereits in jüngeren Jahren auf. Der wichtigste Risikofaktor für die spontane Form der Alzheimer Krankheit ist eine Genvariante des Proteins Apolipoprotein E, welches am Transport von Cholesterin im Blut beteiligt ist. Tierstudien legen ebenfalls einen Zusammenhang zwischen hoher Cholesterin-Aufnahme und der Entwicklung einer Alzheimer Krankheit nahe. Cholesterin ist ein wichtiger Baustein von Zellmembranen. Innerhalb der Membran existieren flossartige Strukturen, die sogenannten „rafts“, welche von Cholesterin zusammengehalten werden. Diese „rafts“ spielen eine wichtige Rolle bei der Übermittlung von Signalen und werden ausserdem mit der Prozessierung von APP in Zusammenhang gebracht.

Seladin-1 ist ein Protein aus der Familie der Flavin-Adenin-Dinukleotid-abhängigen Oxidoreduktasen und ein wesentliches Enzym im Cholesterinstoffwechsel. Seladin-1 wurde vor einigen Jahren im Rahmen einer Studie entdeckt, in welcher erkrankte Hirnregionen von Alzheimer Patienten mit gesunden Bereichen verglichen wurden. In den kranken Regionen ist das Expressionsniveau von Seladin-1 signifikant geringer, weshalb es auch der selektive Alzheimer's Disease Indikator -1 genannt wird.

In der vorliegenden Studie wurde die Rolle von Seladin-1 während des programmierten Zelltods (Apoptose) und bezüglich des Cholesterinstoffwechsels näher untersucht. Wir konnten zeigen, dass die Überexpression von Seladin-1 Zellen resistenter gegen Apoptose macht und zu einer Zunahme der Cholesterinkonzentration in der Membran führt. Letzteres resultierte in einer massgeblichen Beeinflussung der Zusammensetzung und Funktion der „rafts“. Ebenso konnten wir darlegen, dass höhere Seladin-1- und Cholesterinspiegel die Prozessierung von APP und damit die Aβ Produktion hemmen. Im Gegensatz dazu zeigten Seladin-1 defiziente Mäuse geringere Cholesterinkonzentrationen in der Membran und eine erhöhte Aβ Bildung.

Diese Ergebnisse zeigen zum ersten Mal, dass die Modifizierung der Seladin-1 Expression, und damit einer endogenen Komponente, zu einer Veränderung der Cholesterinkonzentration führen kann und dass Seladin-1 ein essentieller Regulator der Zusammensetzung und der Funktion von „rafts“ ist. Das Resultat, dass die Erhöhung von Seladin-1 die Aβ Bildung reduziert, weist Seladin-1 als möglichen therapeutischen Angriffspunkt in der Alzheimer Behandlung aus.

# Introduction

## Alzheimer's disease

Aging is one of the most significant risk factors for neurological disorders including Alzheimer's disease (AD), the most common form of dementia. AD was first described by the German physician Alois Alzheimer in 1907 and is characterized by progressive atrophy and loss of neurons resulting in cognitive deficits, confusion and dementia, culminating in childlike helplessness and death. The two major pathological hallmarks of the disease are amyloid plaques, which are composed primarily of insoluble β-amyloid fibrils, and neurofibrillary tangles (NFTs), consisting of paired helical filaments (PHF) of hyperphosphorylated Tau. According to a statistical investigation of the World Health Organization, AD and other dementias have an overall prevalence of about 5 % for men and 6 % for women aged above 60 years.

## Amyloid percursor protein (APP) and Aβ-peptide generation

APP is a polypeptide that is cotranslationally translocated into the endoplasmic reticulum via its signal peptide and then posttranslationally modified through the secretory pathway. It is a ubiquitously expressed type I integral membrane protein with a large extra- and a short intracellular domain[6]. The role of APP remains unclear. Both during and after the trafficking of APP through the secretory pathway, it can undergo a variety of proteolytic cleavages to release secreted derivatives into the lumen and the extracellular space. The first proteolytic cleavage identified, made by an α-secretase, occurs 16 amino acids $NH_2$-terminal to the single transmembrane domain of APP[6]. This processing results in the release of the large soluble ectodomain fragment (α-APPs) into the lumen/extracellular space and retention of an 83-residue COOH-terminal fragment (CTF) in the membrane. Alternatively, some APP molecules not subjected to α-secretase cleavage can

be cleaved by an activity designated β-secretase, which principally cuts 16 residues $NH_2$ terminal to the α-cleavage site, generating a slightly smaller ectodomain derivative (β-APPs)[7] and retaining a 99-residue CTF (C99) in the membrane that begins at residue 1 of the Aβ region[8]. It was assumed that Aβ generation was a pathological event, because the cleavage of the C99 fragment resulting from the γ-secretase activity appeared to occur in the middle of the transmembrane domain. Furthermore it was assumed that this would require the release of C99 from the membrane, for example, as a result of some pre-existing membrane injury that allowed access to a soluble protease. However, Aβ was shown to be constitutively released from cells under entirely normal cellular conditions[7,9-11]. Similarly, a peptide fragment designated p3 was discovered to be produced by the sequential actions of the α- and γ-secretases[10,12]. These findings indicate that Aβ production is a normal metabolic event, and indeed, the peptide can be detected in both

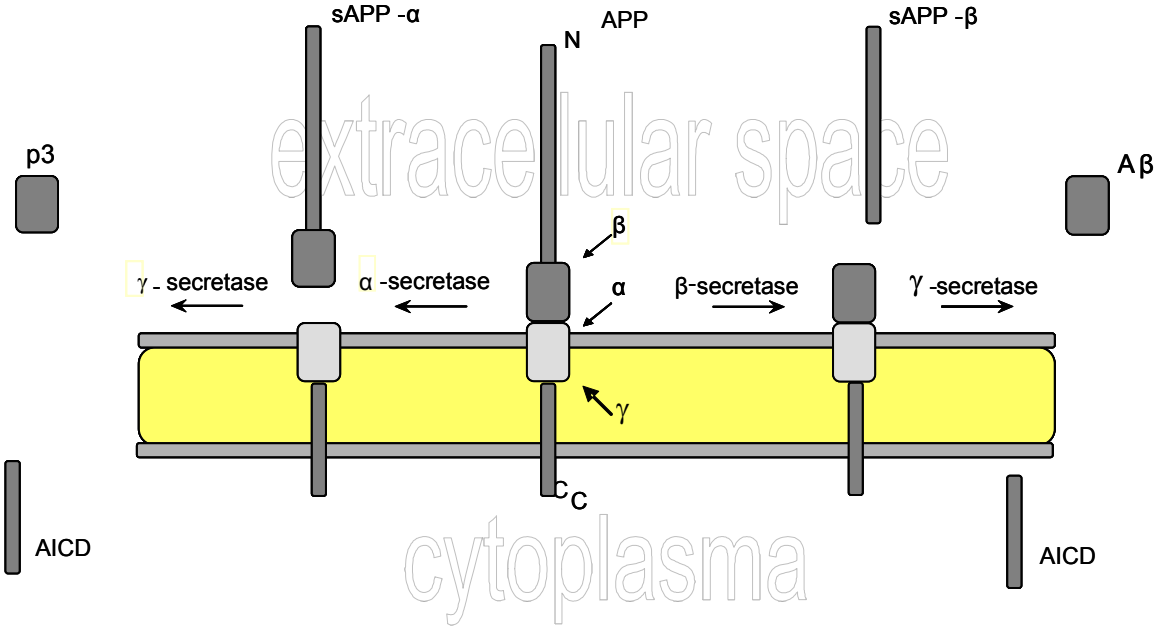


**Processing of APP**

Aβ is derived by sequential proteolytic cleavages: APP is either cleaved by an α-secreatase followed a γ-secretases resulting in the nonamyloidogenic P3 peptide, an N-terminal soluble APP α and an APP intracellular C-terminal domain (AICD), or by a β-secreatase prior to the γ-secretase, producing the amyloidogenic Aβ and soluble APPβ.

cerebrospinal fluid and plasma in healthy subjects throughout life[7,11]. Cleavage by the γ-secretase can occur at position 40 or 42 of the Aβ sequence and gives rise to $A\beta_{40}$ or $A\beta_{42}$, the latter having a higher tendency to aggregate and thus being more amyloidogenic[13]. The γ-secretase is a multiprotein complex, which includes presenilin1 (PS1), presenilin2 (PEN-2)[14], APH-1, and nicastrin[15]. The γ-secretase complex cleaves several type I transmembrane proteins, such as Notch 1[16], ErbB4[17], N- and E-Cadherins [18] following a regulated intramembrane proteolysis process[19]. The shorter form, $A\beta_{40}$, accounts for about 90% of the Aβ in AD brains. This proportion varies depending on the different mutations in presenilins and APP, influencing among others the activity of the secretases. In familial cases of AD (FAD) such mutations are believed to cause AD by increasing $A\beta_{42}$ production, or by increasing the ratio of $A\beta_{42}$ to $A\beta_{40}$ peptides.[20,21]

## Aβ peptide degrading enzymes

The accumulation and polymerization of Aβ are considered to be pathologically important in AD[22]. This hypothesis is supported by the impairment exerted by Aβ on synaptic trasmission and neuronal viability[23]. Numerous studies show the toxicity of Aβ-peptide but the mechanisms how this peptide initiates the cascade of death is not known to the last detail. Whereas higher production of Aβ leads to familial forms of AD (FAD), no indications of increased Aβ generation is observed in sporadic forms of the disease, that constitudes the majority (up to 95%) of AD cases[24]. Therefore, a reduced degradation of the Aβ peptide can lead to its accumulation to AD. Various proteases have been implicated in Aβ degradation, including neprilysin (NEP), a membrane-anchored zinc endopeptidase, involved in digestion of biologically active small peptides such as substance P, enkephalines and somatostatin, and insulin-degrading enzyme (IDE)[25], a thiol metallo-endopeptidase that was discovered based on its activity to degrade

insulin. Whereas IDE exclusively degrades soluble monomeric but not oligomeric Aβ species, NEP is capable of degrading monomeric and oligomeric Aβ. NEP is the rate limiting enzyme for Aβ degradation *in vivo* and its expression is downregulated in AD brains. Another important protease involved in Aβ degradation is the serin protease plasmin[26]. Plasmin activity is regulated by plasminogen-activators and inhibitors as well as plasminogen activator inhibitors and plasmin inhibitors[27]. In addition, plasmin generation is dependent on the binding of plasminogen to the plasma membrane. Plasminogen activators (PAs) are serine proteases, the main function of which is to activate plasminogen into plasmin. There are two types of mammalian plasminogen activators: tissue-type (tPA) and urokinase-type (uPA)[28]. tPA is expressed in various regions of the mouse brain, including the hippocampus, amygdala, cerebellum and hypothalamus[29], where it participates in both normal and pathological events[30]. In particular, tPA is highly expressed in the hippocampus, a region important for learning and memory and often involved in AD pathology. Furthermore, uPA and tPA are also involved in a critical step in the excitotoxin-induced neurodegeneration[31,32]. tPA acts by two known pathways, a proteolytic and a non-proteolytic. The proteolytic one proceeds via its ability to convert plasminogen into plasmin[33,34]. Plasmin is involved in neuronal death, degradating the extra-cellular matrix (ECM) and preparing a gradient of chemoattractants for microglia[34] and contributes to neurite outgrowth by processing the proteoglycans in the ECM. Recent studies have shown that tPA potentiates signaling mediated by glutamatergic receptors through proteolytic regulation of N-methyl- D-aspartate (NMDA) receptors and thus increasing the influx of calcium[35]. In the nonproteolytic pathway, tPA stimulates a cell-surface receptor on microglia, resulting in microglial activation. Once activated after neuronal injury, microglia contribute to neurodegeneration[36] and are associated with several diseases, like AD[37] and stroke [38]. It is evident that Aβ degrading enzymes play an important role in AD – these proteases are logical targets for drugs attenuating AD and are being considered as possible targets for retarding AD pathogenesis.

## Neurofibrillary tangles and the microtubule-associated protein tau

The cytoskeleton plays a major role in establishing and maintaining the regional specialization within neurons. Microtubules are responsible for neurite extension and serve as the tracks for transport within the cells. Microtubule-associated proteins play an important role in the assembly of microtubules, in cross-linking of microtubules to each other and to other filaments. Tau belongs to the family of microtubule-associated proteins and it is involved in microtubule assembly and stabilization. In humans, tau is mainly found in neurons[39]. It is encoded by one single gene on chromosome 17q21 which consists of 16 exons[40] that are alternatively spliced generating six tau isoforms, which differ by the presence of either three (3R-tau) or four (4R-tau) carboxy-terminal repeats[41,42]. Tau can be phosphorylated by different kinases like GSK-β and at least thirty different phosphorylation sites have been described using phosphorylation-dependent antibodies. Tau hyperphosphorylation precedes neurodegeneration because it abolishes its biological function to bind microtubules and promotes microtubule assembly. To regulate the activity and binding property, tau is dephosphorylated by phosphatases, in neurons particularly by protein phosphatase 2A (PP2A), a holo-enzyme found predominatly in the brain[43].

Hyperphosphorylation of tau is believed to be an early event in the pathway that leads from soluble to insoluble and filamentous tau protein, that has the tendency to aggregate to paired helical filaments (PHF). Neurofibrillary tangles (NFTs), the filamentous intraneuronal inclusions which, together with amyloid plaques, define the pathology of AD are composed of PHFs and straight filaments (SFs) and their spreading thoughout the brain cortex correlates with the degree of neuronal loss[44]. Several other neurodegenerative disorders characterized by the presence of filaments composed of hyperphosphorylated tau in glial and neuronal cells, degenerating neurites and Pick bodies are known, collectively referred to as tauopathies. The filamentous Tau aggregates are consistently found in AD, corticobasal degeneration (CBD), progressive supranuclear palsy (PSP),

Pick's disease (PiD) and frontotemporal dementia, including fronto-temporal dementia with Parkinsonism linked to chromosome 17 (FTDP-17)[45]

## The amyloid cascade hypothesis

Since the first description of the disease by Alois Alzheimer, Aβ plaques and NFTs have been the defining neuropathological hallmarks of AD, but still today their pathophysiological relation remains unclear. According to the amyloid cascade hypothesis, accumulation of Aβ in the brain parenchyma is the first step in the development of the disease[46]. Crossbreeding of a mouse

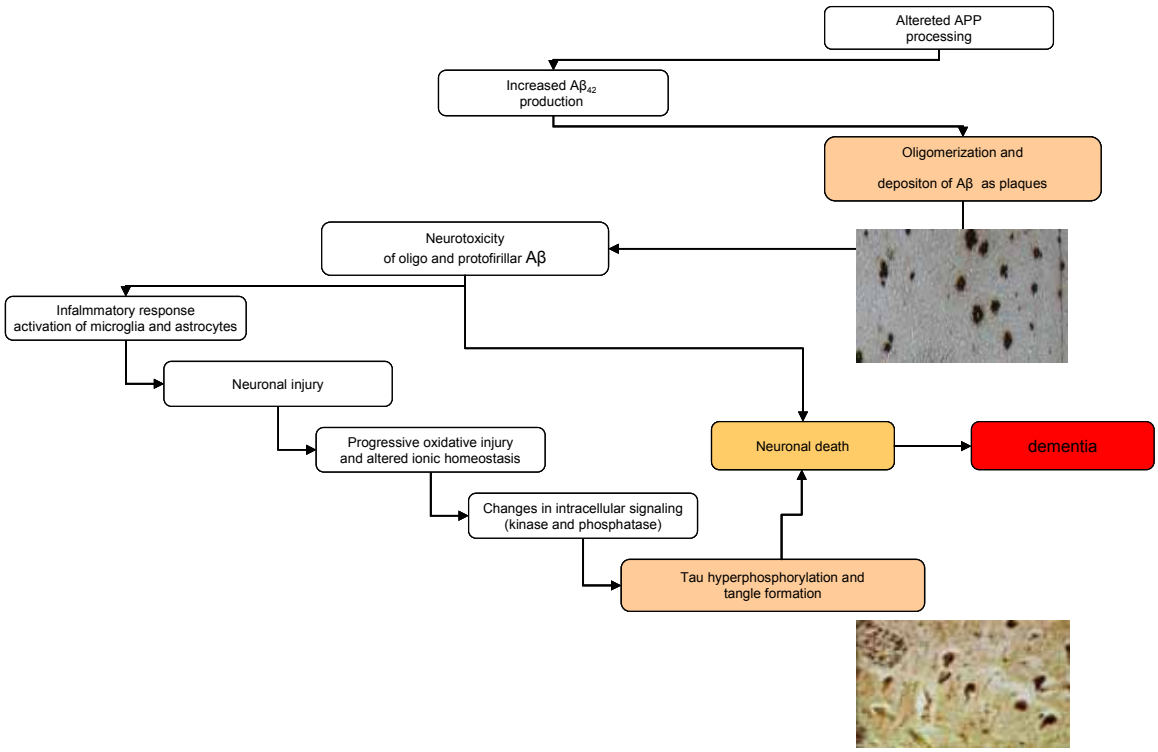


**The amyloid cascade hypothesis:** in AD, an aberrant APP metabolism leads to an increase in Aβ levels and, subsequently, Aβ aggregation and plaque formation. Oxidative stress, gliosis and neurotoxic properties of Aβ induce synaptic loss and neurodegeneration, and according to the hypothesis, Aβ is also the trigger for tau pathology in AD.

line expressing a tau mutation associated with FTDP-17 with mice expressing a mutated variant of APP that causes AD in humans led to a dramatic increase in NFT formation in these mice[47]. Stereotaxic injection of $A\beta_{42}$ fibrils into the brains of another transgenic mouse line expressing the same tau mutation caused a fivefold increase in the numbers of NFTs in cell bodies within the amygdala from where neurons project to the injection sites [48]. Although these experiments failed to dissect a distinct pathway by which Aβ induces NFT formation and neuronal death, they support the evidence that aggregation of Aβ is an initial event in AD pathogenesis and that other features of the disease, including hyperphosphorylation of tau and subsequent tangle formation, result from an imbalance between production and clearance of Aβ[49]. For Aβ-induced neurotoxicity, several mechanisms have been proposed including oxidative stress, free-radical formation, disrupted calcium homoeostasis, induction of apoptosis, neuritic damage, chronic inflammation and formation of amyloid pores[8,50]. Another potential mechanism involves the interaction of Aβ with cell-surface receptors and APP itself, resulting in inhibition or aberrant activation of signal transduction pathways.

## Viable mouse models for Alzheimer's disease

To investigate the pathological process that underly AD, many animal models have been developed. These models are based on the knowledge of proteins involved in the pathology of the disease in humans. Rare autosomal dominant mutations causing early familial forms of AD were described for APP and the presenilin1 (PS1) and 2 (PEN2) genes. Several transgenic mouse-lines overexpressing human APP or one of the FAD-linked APP mutations have been generated, exhibiting an AD-like phenotype[51-53]. For the overexpression of the transgenes, different promotors were shown to drive high expression in the brain (i.e. the Thy1.2 promotor in brain neurons or the PrP promotor more ubiquitously in the CNS). Overexpression of human APP cDNA containing two mutations immediatly before the Aβ sequence (K670M/N671L), first discovered in a FAD case in a familiy from Sweden - further referred as the

Swedish mutation (Sw) – revealed increased Aβ generation by enhanced β-secretase cleavage. These SwAPP-mice develop the first Aβ deposits as early as 6 months after birth in the cerebral cortex and exhibit inflammatory reactions like astrogliosis and microgliosis, which are thought to play a key role in the pathogenesis of AD[54]. Double transgenic mice co-expressing the M146L presenilin 1 (PS1) and K670N/M671L, SwAPP mutations exhibit an earlier Aβ deposition and more profound impairment of working memory and learning than single SwAPP mutant mice[21]. Even though these animal models mimic the Aβ related pathology of AD, none of them develop an AD-like tau pathology nor exhibit any neurofibrillary tangles or threads. Therefore, animal models of the tau pathology were generated by overexpressing wildtype human tau in murine neurons[55]. In this model, transgenic hyperphosphorylated tau was present in nerve cell bodies, axons and dendrites, but no obvious neurolopathological phenotype or neurofibrillary tangles were observed[56]. The subsequent use of stronger promoters to drive transgene expression resulted in a more pronounced phenotype. In addition to numerous abnormal tau-immunoreactive nerve cell bodies and dendrites, large numbers of pathologically enlarged axons were detected[57,58]. Tau protein extracted from transgenic brain and spinal cord became more insoluble with increasing age, whereas NFTs were only found in very aged mice. Mice with expression of mutated P301L tau, a mutation leading to a higher state of tau phosphorylation, showed motor and behavioural deficits and an age- and gene-dose-dependent development of NFTs[59]. Crossing of these mice with mice overexpressing SwAPP gave rise to double mutants with substantial neurofibrillary tangle pathology[47]. Moreover, injection of $A\beta_{42}$ fibrils into the brains of these mice caused fivefold increases in the number of NFTs in cell bodies within the amygdala from where neurons project to the injection sites[48]. As the hyperphosphorylation of tau abolishes its ability to bind to the microtubules and promote their assembly, the function of protein phosphatases that might restore the physiological function of tau has also been investigated using different animal models. An attempt to examine the

function of PP2A in a mouse model by using a knockout technique has been unsuccessful, because the selective knock-out of this enzyme was lethal[60]. This problem could be circumvented by expression of a dominant negative mutant form of the catalytic subunit Cα of PP2A, which gave rise to mice with a substantially reduced PP2A activity and tau hyperphosphorylation[61].

## Apoptosis in central nervous system

Mature neurons are the longest living among mammalian cells. In contrast, immature neurons die in large numbers during development. The induction of developmental cell death is a highly regulated process that is dependent on a variety of trophic factors and can be suppressed by various extracellular stimuli. A chemical or electrical feedback from the neighboring tissue is important for neuronal survival[62]. Developing neurons compete for the restricted trophic factors provided and only such neurons, which complete successfully their connections have a higher probability for survival. Neuronal apoptosis often occurs via an intrinsic apoptotic cascade triggered by the translocation of Bax, a pro-apoptotic Bcl-2 family member, to mitochondria. In response to signals generated by Bcl-2 family members, such as Bim and Bid, Bax oligomerizes at the outer mitochondrial membrane and forms a pore that releases cytochrome c from the mitochondria[63]. Cytosolic cytochrome c then interacts with Apaf-1 and pro-caspase-9 to form a functional apoptosome that ultimately activates downstream executioner caspases like caspase-3[64]. The Bax-dependent mitochondrial pathway is often used to model apoptosis [65-67]. Numerous caspases which are cysteine aspartate-specific protease play a major role in neuronal apoptosis[68]. Caspase-8 and caspase-10 contain death-effector domains which bind to the intracellular domain of receptors like CD95 (Fas) and tumor necrosis factor (TNF) receptors and initiate programmed cell death. Caspases, like caspase-1,-2,-4,-5, which contain a caspase activating recruitment domain (CARD) are mostly activated by the complex caspase9-cytochromc-Apaf1. Caspases that have a short active pro domain like

caspase-3 and -6 are activated by all caspase pathways. Observations that caspases-11 and -12 can be activated in particular pathological terms are of great interest to therapeutic approaches against cellular degeneration[69,70]. Examining several knock-out mice for caspases like caspase-3,-9 and for Apaf-1 show the importance of caspases in the context of neuronal death.

## Neuronal survival and cell death

The survival of developing immature neurons depends on the availability of neurotrophic factors. Neurotrophins generally activate and ligate the tyrosine kinase receptors (TrkA, TrkB and TrkC) which are cell-surface receptors with intrinsic tyrosine kinase activity. The receptors can autophosphorylate[71]. For instance, the binding of nerve growth factor (NGF) to TrkA leads to the phosphorylation of several tyrosine residues within the cytoplasmic tail of TrkA. These phosphotyrosines in turn serve as docking sites for other molecules such as phospholipase C$\gamma$, phosphoinositide 3-kinase (PI(3)K)[72] and adaptor proteins such as sonic hedgehog (Shc), coordinate neuronal survival. The Akt protein is another important kinase implicated in the neuronal death. It is responsible for the inhibition and activation of different proteins involved in the survival of the cell. Akt acts in the phosphatidylinositide 3'OH kinase (PI(3)K)/c-Akt kinase cascade. c-Jun pathway is activated after NGF withdrawal, and blocking this pathway inhibits neuronal cell death. The overexpression of PI(3)K or of its downstream effector Akt kinase blocks cell death in neurons after NGF withdrawal, even though the c-Jun pathway is activated. Stimulation of the PI(3)K pathway is sufficient to allow cells to survive in the absence of NGF[73] . From three isoforms, c-Akt3 is the major one expressed in neurons and its binding to phospholipids and proteins supports neuronal survival. Akt phosphorylates Bad, a pro-apoptotic protein, and inhibits its activity during deprivation of trophic factors. Akt has been shown to affect, directly or indirectly, three transcription factor families, forkhead, which transcribes CD95L protein,

cAMP-response element-binding protein (CREB) and NF-κB, which are all involved in regulating cell survival. It is obvious that Akt is a potent kinase that keeps neurons alive in various ways and certainly additional targets of Akt will be identified. Neurotrophins can not only activate PI(3)K and Akt, but also they can activate Trk receptors which in turn trigger small GTP–binding protein Ras and the downstream MAP kinase cascade, which includes Raf, MAP kinase/ERK kinase (MEK) and the extracellular signal regulated protein kinase (ERK)[74]. The involvement of MAP in the neuronal survival is at least partially linked to the activation of the ribosomal S6 kinase (RSK) family members. Together with Akt, these kinases are responsible for the the phosphorylation of Bad and therefore for its inactivation. RSK also activates CREB transcription factors. CREB activates in turn the transcription of bcl-2, and, therefore, can directly stimulate cell survival. Neurotrophins suppress apoptosis via activation of different inhibitors of death factors. Deprivation of growth factors leads to a decrease of kinase activities like MAP kinase and PI(3)K and to reduced glucose uptake and protein synthesis. In parallel, several other kinases are upregulated, c-Jun amino-terminal kinase (JNK) and p38 MAP kinase are the two most common in this context. It is shown that a permanent generation of pro-apoptotic proteins is required[66]. Understanding the role of neurotrophic factors in the complex events of apoptosis is necessary to accumulate enough knowledge to design drugs against neurodegeneration, as it occurs in AD and Parkinson's disease (PD).

## Neuronal cell death in Alzheimer's disease

The neuronal degeneration in AD can be described as an apoptotic event, although the underlying process is not known to the last detail. Compared to the massive and progressive neuronal loss in brains of AD patients, only few neurons were detected in apoptotic stages in post-mortem analysis. These findings suggest that apoptosis may not be the only process causing neuronal death in AD[75,76]. It is generally believed that Aβ production and aggregation is responsible for disease progression, as high Aβ levels are toxic to the brain[77], but the question how this accumulation of the peptide causes cognitive decline is still unanswered. It has been shown that Aβ peptides actually kill

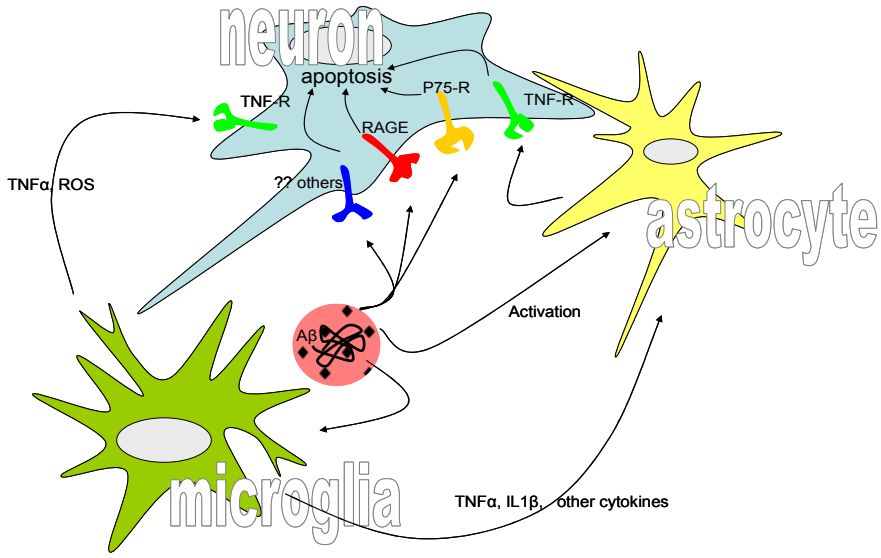


**Possible induction of apoptosis by the Aβ peptide in neurons**

Different receptors on the neutonal membrane can be activated by Aβ in different manners and consequently induce programmmed cell death through different pathways. Aβ can also activate astrocytes, and microglia which in turn activate certain neuronal receptors and induce apoptosis.

neuronal cells *in vitro*, induce oxidative stress and increase the intracellular concentration of $Ca^{2+}$-ions [78,79]. The interaction between Aβ and neuronal receptors like p75 neurotrophin receptor, a tumor necrosis factor receptor (TNF-R) or receptor for advanced glycation endproducts (RAGE) are shown to induce apoptosis *in vitro*[80,81]. In support of the notion that *in vitro* neurotoxicity of Aβ is not an artifact, this cytotoxicity is mediated by defined intracellular

signaling mechanisms, including the destabilization of calcium homeostasis[79], oxidative stress relevant pathways[78], calpain-activated cdk5 pathway[82], caspase-dependent pathways[83] and the c-Jun N-terminal kinase (JNK) pathway[84]. Moreover, neurons with elevated Aβ generation exhibit a higher vulnerability to additional toxic stimuli *in vivo*; in addition, anti-Aβ immune therapy reduces Aβ and protects neurons against exitotoxicity.

## Cholesterol and other sterols in the CNS

The cellular needs for cholesterol in the periphery is covered by *de novo* synthesis and by cellular uptake of liproprotein-associated cholesterol from the circulation. The blood-brain barrier effectively prevents cholesterol uptake from the circulation, and *de novo* synthesis is responsible for practically all cholesterol present in the brain. Cholesterol synthesis and degradation is highly regulated in the CNS. Essentially all (99.5%) cholesterol is unesterified, and the majority of cholesterol present in the CNS is believed to reside in two different pools: one represented by the myelin sheaths (e.g. oligodendroglia) and the other by the plasma membranes of astrocytes and neurons[85]. A noteworthy characteristic of myelin is that it contains approximately 70% lipid and 30% protein, whereas most other cell membranes are composed of more than 70% proteins and 30% lipids. It has been estimated that up to 70% of the brain cholesterol is associated with myelin. Cholesterol synthesis in the developing mamalian CNS is relatively high, but declines to a very low level in adults. This can be explained by an efficient recycling of brain cholesterol. As a consequence, brain cholesterol has an extremely long half-life of about 5 years in humans[86]. In mammalian brain, cholesterol is synthesized mainly in astrocytes, tranlocated to the cell surface by the ATP-Binding Cassette Transporter A1 (ABCA1)[87] and tranported to the neurons by apolipoprotein E (apoE). Although the recycling system seems quite efficient, there are two mechanisms known at present for the excretion of cholesterol from the brain to maintain the steady state. There is some excretion of apoE-bound

cholesterol via the CSF, whereas the precise sites and mechanism of the elimination remain to be conclusively established. A quantitatively more important mechanism involves conversion of cholesterol to 24OH-cholesterol, a reaction catalized by the 24OH-hydroxylase, a brain specific protein encoded by the *CYP46* gene. This oxysterol is able to traverse the blood-brain barrier and has been demonstrated to be a very specific and the most important excretion mechanism for cholesterol in the brain[88]. 24OH-cholesterol is not only a degradation product of cholesterol but also a regulator for the key enzymes in cholesterol transcription and post-translational events, as well as a precursor for steroid hormones[89]. All genes regulated by sterols contain a sterol-responsive element (SRE) within the 5'-flanking region. Through the binding of SRE binding proteins (SREBP), sterols control the transcription of these genes. Cholesterol is mostly synthetized in the endoplasmatic reticulum (ER) and transported to the membrane. A very small amount of cholesterol is stored as cholesterol-esters in the brain, esterified by ACAT1, a brain specific enzyme. Cholesterol is known to be an essential modulator of the physicochemical state and functional activity of physiological membranes[90] and thus plays an essential role in the regulation of synaptic function and cell plasticity[91]. In the past, decade evidence of a possible link between cholesterol and neurodegeneration has accumulated. Some of the earliest observations of this link were the recognition of ε4 isotype apoE as an important risk factor for late-onset Alzheimer's disease[92] and that hypercholesterolemia was associated with increased brain Aβ immunoreactivity in rabbits[93]. In Niemann-Pick Type C (NPC) disease, an autosomal recessive disorder, abnormal intracellular accumulation of cholesterol and glycosphingolipids is found, leading to progressive neuropathology, neurodegeneration, and premature death. In Smith-Lemli-Optiz syndrome, a defective 7-dehydrocholesterol-7-reductase leads to the abnormal accumulation of 7-dehydrocholesterol, a direct precursor of cholesterol. Patients with desmosterolosis have a reduced activity of the 3β-hydroxy-σ5-steroid-24 reductase, also named seladin-1, leading to the

pathological accumulation of desmosterol and to premature death[4,94]. Several *in vitro* and numerous mouse models have been generated to study the different diseases correlated to the pathological changes in cholesterol homeastasis and metabolism.

## Apolipoprotein E

Apolipoproteins are lipid carrier molecules. They play an important role in the coordination of the metabolism of lipids following peripheral and central nervous system injuries[95,96]. Apolipoprotein E (apoE) in particular is unique

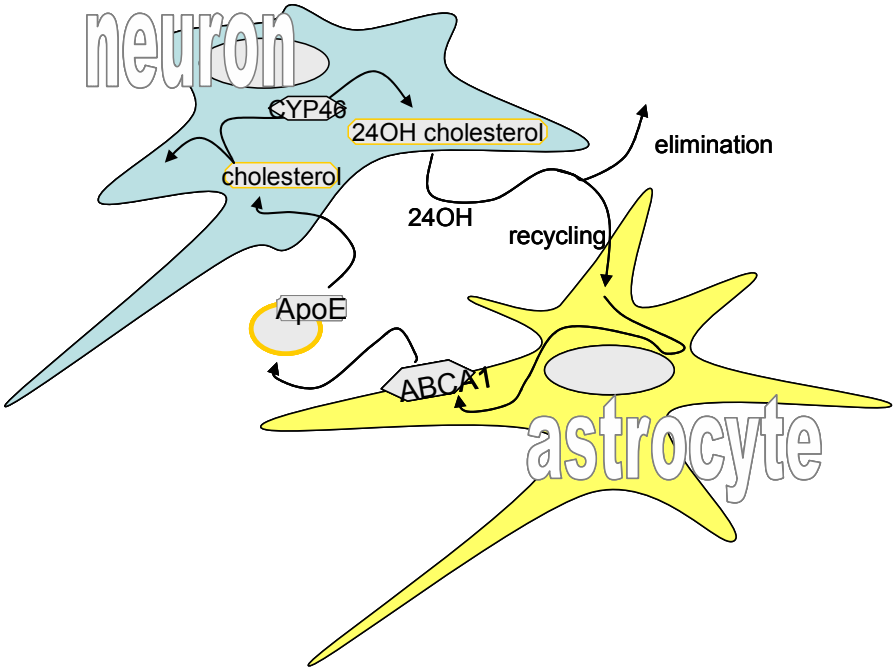


**Interactions of astrocytes and neurons in cholesterol homeostasis according to Pfrieger and collegues[2,3].**

Although neurons are capable of synthesizing cholesterol, it has been suggested that neurons rely on delivery of cholesterol from nearby cells such as astrocytes.

among apolipoproteins in that it has a special relevance to nervous tissue. The 34 kDa glycosylated protein is encoded on chromosome 19 and plays a pivotal role in the mobilization and redistribution of cholesterol and phospholipid during membrane remodelling associated with synaptic plasticity[95]. Three common alleles are known for apoE, ε2, ε3 and ε4, are

present in 7%, 78% and 15% of the population, respectively[97]. ApoE has been associated with AD since carriers of the apoE ε4 allele have an enhanced risk of developing AD, whereas carriers of ε2 are protected[98].

This apoE effect is explained by its physiological function in lipid clearance, which is inversely correlated with Aβ deposition. apoE is found in Aβ plaques in AD patients and is correlated with Aβ deposition around blood vessels and in the brain parenchym[26]. Deposition of Aβ is also observed in ε4 allele carriers even in the absence of AD causing mutations[99]. Controversially, co-expression of APP and the ε4 allele does not lead to a significant variation in the production of Aβ in cell culture[100]. *In vitro* studies have shown that ε4 increases fibrillogenesis of Aβ, supporting the hypothesis of a direct role of apoE in amyloid deposition[101]. In apoE knock-out mice crossed with mice transgenic for a mutant form of APP, the plaque load is decreased compared with single APP transgenic mice. These results indicate that the ApoE ε4 allele enhances the aggregation and/or decreases the clearance of the Aβ peptide in the brain[102,103]. Furthermore, ε4 may also directly affect nerve cells. Primary neurons derived from transgenic mice expressing the ε4 allele show a decrease in neuritic outgrowth and maintenance of neurites[104]. Astrocytes provide the brain with apoE, and although it is mostly considered a lipid transport molecule, data suggest that it plays additional roles in the brain regulating astrocyte and neuronal function, like, for example, calcium homeostasis[105]. ApoE modulates transmitter release and sequestration and enhances the rate of glutamate uptake and prevents excitotoxicity[106,107]. These diverse functions may be due to the variations in the ability of the isoforms to transport lipids, bind receptors or influence other cellular functions such as cholesterol homeostasis and microtubule stabilization[108].

### Detergent Resistent Membrane Microdomain (DRM) or Raft

Most cellular cholesterol resides within plasma membranes, which consist of two leaflets that are asymmetric in lipid distribution, electrical charge, fluidity,

function and possibly the localization of lipid rafts[109-111]. Within the plasma membane 70%-85% of free cholesterol resides in the cytofacial bilayer leaflet, whereas only 15-30% join the exofacial leaflet[112]. Exofacial cholesterol builds up lateral membrane domains such as kinetic pools of lipid rafts[111]. The existence of lipid rafts was postulated more then 10 years ago[113]. These membrane domains were shown to be resistant to Triton X-100, a nonionic detergent, and are therefore also named Detergent Resistant Membrane-domains (DRMs). DRMs are specialized plasma membrane microdomains highly enriched in glycosphingolipids and multiple membrane proteins[114]. There is strong evidence to suggest that cholesterol condenses the packing of sphingolipid molecules and thus cholesterol-sphingolipid microdomains form a separate lipid-ordered phase in the exofacial leaflet[115]. Functionally, lipid rafts are thought to be involved in intracellular trafficking of proteins and lipids, secretory and endocytic pathways, as well as in cell-surface proteolysis and signal transduction pathways[115]. Extracellular ligands can initiate DRM assembly which in turn can influence strength, duration and quality of intracellular signaling. For example, in neurons, the signal transduction is, among others, determined by GAP-43 like proteins (e.g. growth-associated protein-43 (GAP43), cytoskeleton associated protein of MW23kDa (CAP23), myristoylated Ala-rich C-kinase substrate (MARCKS) and dependent of lipid rafts[116]. DRMs are believed to steer efficiency and reliability of extracellular signals by concentrating specific proteins, like flotilin 1, in special regions of plasma membranes. Other important raft components are sphingolipids like sphingomyelin and the ganglioside GM1. Sphingomyelin is a major source of ceramides, lipid mediators that are generated when sphingomyelin is cleaved by sphingomyelinases. Sphingomyelinases are activated by inflammatory cytokines[117] and oxidative stress *in vivo* [118]. The ganglioside GM1 was shown to bind to the Aβ peptide and perhaps change the latter's conformation[119].

## Seladin-1

Seladin-1 shares homologies to a family of flavin-adenine-dinucleotide-dependent oxidoreductases and is the human homologue of the Diminuto/Dwarf1 gene, described in plants (i.e *Arabidopsis thaliana*) and in *Caenorhabditis elegans*[120]. In plants, Diminuto/Dwarf1 is required for the


**Seladin-1 aminoacids sequence**

| | |
|---|---|
| red | animoacids homologe to mdm2 binding site to p53[1] |
| green | animoacids homologe to p53 binding site to mdm2[1] |
| blue | mutations leading to desmosterolosis in human[4] |
| black italic | caspase cleavage sites[5] |
| | flavin-adenin-dinucleotide (FAD) binding site homologous region[5] |

synthesis of brassinosteroids, which are plant sterols essential for normal growth and development[121,122]. In humans, the seladin-1 (the selective Alzheimer's disease indicator- 1) mRNA has been found to be downregulated in brain neurons affected in AD, suggesting that seladin-1 levels may influence the selective vulnerability of neurons in this disease[5]. Greeve and colleagues showed that overexpression of seladin-1 in human H4 neuroglioma cells protected cells from apoptosis induced by oxidative stress, and high expression of endogenous seladin-1 was associated with resistance

against Aβ-induced toxicity. Moreover, seladin-1 was linked to tau-related neuronal degeneration in AD, showing a close inverse correlation between the seladin-1 expression level and the presence of neurofibrillary tangles, neuritic plaques and paired helical filaments in temporal cortices of AD cases when compared to non-demented subjects[123]. The function of seladin-1, encoded by a single gene (DHCR24) on chromosome 1, was investigated in 1979 using radioactive acetates. Seladin-1 was shown to catalyze the reduction of the Δ24 double bond of lanosterol and other obligatory sterol intermediates leading to the production of cholesterol[124]. Deficiency in the *Dhcr24* gene causes a severe autosomal recessive disorder characterized by elevated levels of the cholesterol precursor desmosterol in plasma of the patients tested[4,125]. In tumors seladin-1 expression is elevated, suggesting a role of seladin-1 in the suppression of apoptosis[126]. Seladin-1 knock-out mice are viable, even though plasma and tissue of these animals containe almost no cholesterol, and desmosterol was shown to account for 99% of all sterols[94]. Homozygous knock-out pups were born at a lower than predicted Mendelian frequency, indicative of some prenatal death and were about 25% smaller in size. This relatively mild phenotype contrasts dramatically with the severe abnormalties observed in patients with desmosterolosis. This discrepancy may be due to the fact that maternal cholesterol is not available during human embryogenesis[127], as it is in mice. Recent findings give evidence of an interaction between seladin-1 and the tumor suppressor protein p53[1]. Following oncogenic and oxidative stress, seladin-1 binds to p53 amino terminus and displaces E3 ubiquitin ligase Mdm2 from p53, thus resulting in p53 accumulation, suggesting an unanticipated role for Seladin-1 in integrating cellular response to oncogenic and oxidative stress[1].

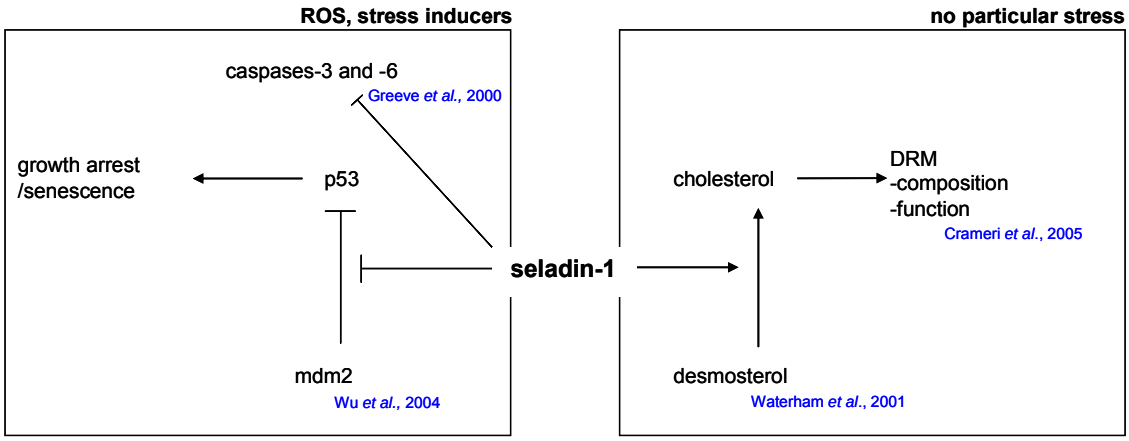


**Postulated functions of seladin-1**
Stress induced by reactive oxigen species (ROS) or other similar stress factors induces the upregulation of seladin-1, which inhibits the ubiquitination of p53 and its degradation. Under Aβ stress, seladin-1 can inhibit caspase-3 and -6 . The second function is related to the reductase property of seladin-1, which enzymatically reduce desmosterol to cholesterol. Cholesterol in turn regulates DRM in composition and function.

# Methods

## Molecular methods

### Restriction analyses

The plasmid DNA was analysed using type II restriction endonucleases. These restriction enzymes recognize palindromic sequences within the DNA. Digestions were performed in 1x cleavage buffer by addition of the restriction endonuclease to the DNA and incubation at 37°C for at least 1 hour. The resulting DNA fragments were analysed by agarose gel electrophoresis.

### Rapid ligation kit

The ligations were performed in a volume of 20µl for 20 minutes at room temperature. DNA was purified from an agarose gel slice using the Qiagen gel extraction kit (Qiagen). Quantitative agarose gel analysis was used to estimate the amount of DNA fragments. 200ng of DNA were diluted in 8µl $H_2O$, 2µl of 5x dilution buffer, 10µl T4 ligation buffer and 1µl T4 ligase, according to the manufacturer's protocol (Roche).

### Preparation and transformation of chemically competent cells

To transform DNA into *E. coli* the cell membranes have to be porous. This can be achieved by treating the cells with $Ca^{2+}$. The addition of DNA leads to the formation of DNA-$Ca^{2+}$ complexes, that enter the cells following a short heat-shock.

To generate chemically competent bacteria, cultures of DH5α or XL1Blue cells were grown in LB-medium at 37°C overnight and harvesterd at an $OD_{600nm}$ of 0.375. The cells were pelleted by centrifugation at 4,000g at 4°C for 15 minutes, resuspended in 10 ml of a 0.1 M $CaCl_2$ solution and kept on ice for 1 hour. Cells were collected by centrifugation at 4,000g at 4°C, resuspended in 0.1 M $CaCl_2$, 0.02 M $MgCl_2$, and 15% glycerol. Aliquots of competent cells were immediately frozen in liquid nitrogen and stored at –80°C.

To transform cells, diluted plasmid DNA or an aliquot of a ligation reaction were added to 100µl competent *E. coli* and incubated on ice for 20 minutes. Following a heat shock for 90 seconds at 42°C the cells were chilled on ice for one additional minute. After adding 1ml LB-medium, the cells were incubated on a shaker for 1 hour at 37°C. Cells were plated on LB-agarose plates containing the appropriate antibiotics.

**Agarose gel electrophoresis**

To analyze or isolate DNA fragments or PCR products these were separated by agarose gel electrophoresis. Due to the negatively charged phosphate groups in the backbone of nucleic acids, DNA migrates towards the positive anode when exposed to an electric field. The migration of linear DNA fragments depends mainly on their size. Using ethidium bromide (Sigma), which intercalates in the major groove of the DNA and allows visualization under UV-light, the length of DNA fragments can be determined by comparison with a DNA ladder marker.

**Gel extraction**

DNA fragments to be used for ligations, transformations or transfections were purified from the agarose slices by the Qiagen gel extration kit according to the company's protocol (Qiagen).

**DNA dephosphorylation**

In order to prevent self-ligation of the vector, alkaline phosphatase was used to remove terminal 5'-phosphate groups before using the plasmid vector DNA in a ligation reaction. Calf intestinal phosphatase (CIP) was used according to the manufacturer's instructions (Promega).

**Preparation of plasmid DNA**

The principle of plasmid isolation from *E. coli* is based on alkaline lysis of the cells in combination with the anionic detergent SDS[128] that breaks down the cell walls and denatures the proteins as well as genomic DNA. In contrast, the

strands of closed, much smaller, circular plasmid DNA stay in solution and can be recovered from the supernatant. Plasmid DNA was isolated from small scale (1-2ml), intermediate scale (20-50ml) and large scale (500ml) bacterial cultures using QIAGEN plasmid purification protocols. Briefly, after a modified alkaline lysis procedure negatively charged phosphates of the DNA backbone are bound to an anion-exchange resin (QIAGEN) and plasmid DNA can be purified from RNA and proteins. To avoid a possible contamination of DNA with bacterial endotoxins, DNA fragments that were planned to be injected into oocytes for generation of trangenic mice were purified using the QIAGEN EndoFree Maxi kit following the manufacturer's instructions.

**Ethanol precipitation of DNA**

The addition of ethanol to nucleic acids depletes their hydration shell and exposes the negatively charged phosphate groups in the backbone of the DNA. $Na^+$-ions bind to these groups so that a precipitate can form. To 1 volume of DNA solution 1/10 volume of 3M Na-Acetate (pH 5.2) and 2.5 volumes of 100% ethanol were added and mixed on a vortex. The DNA was precipitated at –20°C for 1 hour, pelleted by centrifugation at 20,000g and washed with 1ml of 70% ethanol. The DNA pellet was dried for 5–10 minutes at room temperature and resuspended in 10 mM Tris (pH 8.0).

**Polymerase chain reaction (PCR)**

The polymerase chain reaction is a method to amplify DNA-sequences of interest [129]. To produce multiple copies of DNA two specific primers are used that are complementary to one of the two strands. Denaturing of the DNA is followed by a fall in temperature so that the primers can anneal to their complementary sequence on the DNA. Taq-DNA polymerase catalyzes the replication of the DNA by adding nucleotides (dNTPs) to the 3'-ends of the primer sequences. By repeating these steps several times the DNA-sequence of interest is amplified exponentially. 1ng of plasmid DNA or 10 to 200ng of genomic DNA were diluted in 1x reaction buffer and used as a template for the PCR. After addition of 10pmol forward primer, 10pmol reverse primer, 10mM dNTPs and 1Unit of Taq-polymerase the PCR was run on a Perkin

Elmer 9700 PCR machine. The reaction was started by denaturing the DNA for 5-10 minutes at 95°C followed by 35 cycles of denaturing for 1 minute, annealing of primers at 55-70°C for 1 to 1.5 minutes and extension of the sequence at 72°C for 1 to 3 minutes, followed by a final incubation at 72°C for 10 minutes. The times, temperatures and number of cycles were chosen according to the polymerase used, the melting point of the primers and the sequence to be amplified (Sigma).

**Site-directed mutagenesis**

A modified PCR protocol was routinely used to mutate one or more nucleotides in a given sequence in a plasmid. In brief, primers were designed in the region that was supposed to be mutated, in both directions, containing the desired changes in the nucleotide sequence. After the PCR the reaction mixture was incubated with *DpnI* restriction enzyme, which digests only methylated DNA. A newly synthetized plasmid containing the mutation is not methylated and therefore remains intact and can therefore be isolated on a agarose gel. The QuikChange Site-Directed Mutagenesis Kit was used according to the manufacturer's instructions (Stratagene).

**DNA sequencing**

DNA cycle sequencing is based on the dideoxy method developed by Sanger[130]. In the cycle sequencing reaction all four dideoxynucleotides (A, T, G, C) labeled with different dyes were added to an excess of deoxynucleotides. When one of the labelled dideoxynucleotides is incorporated, the elongation of the chain is terminated because the labelled nucleotides lack the 3'-hydroxyl group. The reaction mixture is then applied to a ABI Prism gel capillary and separated according to their molecular weight (ABI Prism 7700 Sequence Detector). Different wavelengths are used to excite each dye and thus to identify the sequence of the DNA. 1µl DNA containing 200-500ng plasmid DNA, 1µl primers (10pmol end concentration), 4µl Ready Mix and 6µl $H_2O$ were mixed in a reaction tube. The DNA cycle-sequencing reaction was carried out using the following program: 96°C 15 seconds; (96°C 30 seconds, 50°C 30 seconds, 60°C 4 minutes) for 25 cycles;

4°C. DNA was precipitated in ethanol and washed with 70% ethanol. The DNA pellet was resuspended in 12µl Template Suppression Reagent and prior to sequencing incubated on a shaker platform for 5 minutes. For the capillary gel run and detection of fluorescent dyes the ABI PRISM 310 Genetic analyzer was used.

**Northern blotting**

Northern blotting and hybridization is a tool to measure the amount, abundance and size of RNAs. RNA was separated according to its size by electrophoresis through a formamid denaturing agarose gel. The RNA was transferred from the gel to a nylon HyBond $N^+$ membrane (Amersham) by upward capillary transfer overnight and immobilized on the membrane. To identify RNAs of interest the membrane was incubated with a radioactive labeled probe that binds to complementary RNA sequences. Results were analyzed by autoradiography.

**RNA extraction**

RNA extraction was performed as described by Chomczynski[131]. A monophasic lysis reagent is used to lyse cells. The addition of chloroform to the lysate generates an organic phase into which DNA and proteins are extracted while the RNA stays in the aqueous supernatant. The RNA is precipitated from the supernatant with isopropanol. The RNA is resuspended in RNase free water and stored at –80°C. Total RNA from brain tissue and eukaryotic cells was extracted using Trizol reagent (Gibco) as described previously[132], according to the manufacturer's protocol. Briefly, tissues were homogenized in 1ml Trizol; to the homogenate were added 0.2ml chloroform and centrifuged for 15 minutes at 12,000g at 4°C. The upper aqueous phase was transferred into a fresh tube and incubated with 0.5ml isopropyl alcohol for 10 minutes at room temperature. The samples were then centrifuged again at 12,000g at 4°C for 10 minutes. The supernatant was removed and pellets were mixed with 1ml 75% ethanol and centrifuged at 7,500g for 5 minutes at room temperature. Pellets were then air dried and dissolved in 10µl RNase free water and stored at -80°C for further detection.

**Preparation of RNA for electrophoresis**

20µg RNA were resuspended in 32µl sample buffer, heated at 68°C for 10 minutes, chilled on ice and 8µl 5x sample buffer was added. The gel was pre-run for 3 minutes at 60V, then run at 6V/cm until the bromphenol blue dye band had migrated one-half the length of the gel. The gel was examined on an UV transilluminator to visualize the RNA and photographed with a ruler. 28S RNA corresponds to a mRNA size of 4718 bp, 18S RNA to 1874 bp.

**RNA Transfer**

The gel was rinsed in DEPC-treated $H_2O$ to wash out formaldehyde and soaked twice in 10x SSPE for 15 minutes. The membrane was soaked in 10x SSPE for 5 minutes. The separated RNA was blotted by capillary transfer with 10x SSPE overnight on a Hybond-N+ membrane (Amersham). After the transfer the membrane was washed twice in 5x SSPE for 15 miutes. The RNA was covalently bound onto the membrane by irradiation (120,000 microjoules/$cm^2$; Stratagene UV-Crosslinker). Then the membrane was incubated in 5% glacial acid for 1 minute stained with methylene blue for 3 minutes. The membrane was washed with DEPC treated water.

**Generation of radioactively labelled DNA probes by random prime labelling**

Random labeling of cDNA was carried out using the random prime labeling system rediprime II (Amersham Pharmacia Biotech). The target cDNA was used as a template for a random synthesis of DNA fragments in the presence of short primers (hexanucleotides) and α32P-radiolabeled dCTP, so that newly synthesized DNA harboured the radioactive nucleotide. 10 ng of target DNA was denatured in 45 µl TE-buffer at 99°C for 5 minutes. The sample was chilled on ice for 5 minutes and added to the reaction tube, containing hexanucleotides, dATP, dGTP, dTTP and the Klenow fragment of DNA polymerase I. After the addition of 5 µl α32P-dCTP with a specific activity of 3000 Ci/mmol the solution was incubated at 37°C for 30 minutes. The QIAGEN Nucleotide Removal Kit was used to remove nucleotides that were not incorporated during the reaction and short oligonucleotides (< 100 bp).

**Hybridization**

The membrane with the cross-linked RNA was placed in a roller bottle and pre-hybridized in 10 ml ExpressHyb (Clontech) containing salmon sperm (10 µg/ml) for 2 hours at 65°C. The labeld probe was denatured for 5 minutes at 99°C, chilled on ice for 5 minutes and added to the pre-hybridization solution. The hybridization was carried out at 65°C for 20 hours. The hybridization solution was discarded and the blot was washed in wash buffer for 10 minutes at room temperature and twice for 30 minutes at 65°C. The membrane was exposed to a Biomax MR film for 10-60 hours at -80°C.

**Quantitative RT-PCR**

Primers specific to human and murine seladin-1, 5'-CCGTCCGAAAACTCAG-3'; 5'-GCGGTGGTAGTAGTGT-3' and 5'-CATCGTCCCACAAGTATG-3'; 5'-CTCTACGTCGTCCGTCA-3' were designed using the program *LC probe design software* (Roche). Seladin-1 mRNA was quantified in three independent cell cultures or mouse brains (n=5 for each group). The housekeeping genes phosphoglucokinase (PGK) and porphobilinogen deaminase (PBGD) were used as reference genes. These two genes were selected based on our unpublished results showing a constant expression of these genes in various experimental conditions both *in vitro* and *in vivo*. Light Cycler quantitative real time PCR (LC-PCR) was performed with a RNA SYBR Green kit following the manufacturer's instructions (Roche Diagnostics). In brief, one microliter of 10µM primers and 150ng of total RNA was used for each reaction. Reverse transcription was performed at 55°C for 10 minutes. Amplification was carried out for 45 cycles, each consisting of 1 second at 95°C, 10 seconds at 58°C followed by 13 seconds at 72°C. Melting curve analysis was carried out by heating the reaction up to 95°C with a temperature transition rate of 0.1°C/second followed by a stepwise cooling process with a temperature transition rate of 20°C/second.

## Biochemical methods

### Western blotting

Western blotting is a method to identify a protein of interest in an extract or homogenate. Proteins are electrophoretically separated by SDS-polyacryl gel electrophoresis (SDS-PAGE) and transferred from the gel to a nitrocellulose membrane where they can be detected with specific antibodies.

### Measurement of protein concentration

Protein concentrations of cell or tissue extracts were measured as described by Lowry *et al.*,[133] using the BioRad *DC* Protein Assay Kit. Proteins react with an alkaline copper tartrate solution and reduce folin reagent. The reduced folin species have a characteristic blue color with an absorption maximum of 750 nm.

### Preparation of cell and brain samples for Western blot analysis

Cells were homogenated with lysis buffer containing by 20 passages through a 16G and a 26G needle, on ice. The homogenization of mouse brains was done in a glass homogenizer using a Heidolph electronic homogenizer at 240rpm. 30-60µg protein of the homogenates were mixed with 3x loading buffer and heated to 84°C for 5 minutes. After 2 minutes incubation on ice the samples were centrifuged at 20,000g for 3 minutes at room temperature.

### SDS-polyacrylamide gel electrophoresis (SDS-PAGE)

Separation of proteins was carried out by SDS-PAGE analysis. Proteins were dissociated into their polypeptide subunits using the anionic detergent SDS in combination with a reducing agent and heat. SDS binds to hydrobhobic regions of the polypeptides so that they become negatively charged and migrate to the anode. Because the amount of SDS bound is proportional to the molecular weight of the protein subunits, the SDS-polypeptide complex migrates in the gel according to the size of the polypeptide. For seperation of proteins 10-20% and 10% Tris-Tricine gels (Invitrogen) were used following

the manufacturer's instructions. Gels were usually run at 90V for 2-3 hours at room temperature.

**Transfer of proteins**

Following SDS-PAGE the resolving gel was equilibrated in transfer buffer for 3 minutes on a shaker platform. Whatman papers and nitro-cellulose membranes were cut to the size of the gel and soaked in transfer buffer. The gel and the membrane were sandwiched between soaked pieces of a sponge, Whatman paper and perforated plastic plates. Blotting was carried out in a blotting tank (BioRad) for 2 hours at 300 mA at 4°C.

**Detection of glycosylation pattern of proteins**

Protein homogenates were run on a polyacrylamid gel (PAAG) and transferred to a nitrocellulose membrane using the above protocol. For the detection of glycosylation pattern the DIG Glycan Differentiation Kit (Roche) was used. The assays were performed according to the manufacturer's protocol (Roche). Briefly, different carbohydrates bound to proteins were characterized using digoxigenin labelled lectins like GNA, SNA, MAA, PNA and DSA. Each of these lectins recognizes a specific carbohydrate.

Specificities of the lectins:

*GNA (Galanthus nivalis agglutinin)*: recognizes terminal mannose, α(1–3), α (1–6) or α (1–2) linked to mannose; thus it is suitable for identifying "high mannose" N-glycan chains glycoproteins.

*SNA (Sambucus nigra agglutinin)*: recognizes sialic acid linked α (2–6) to galactose; thus it is suitable for identifying complex, sialylated N-glycan chains in combination with the lectin MAA; correspondingly linked sialic acids in O-glycan structures are also recognized.

*MAA (Maackia amurensis agglutinin)*: recognizes sialic acid linked α (2–3) to galactose; in combination with SNA (see above) it is suitable for identifying a) complex, sialylated carbohydrate chains and b) sialic acid linkage. Lectin MAA also identifies α (2–3)-linked sialic acids in O-glycans.

*PNA (Peanut agglutinin)*: recognizes the core disaccharide galactose α (1–3) N-acetylgalactosamine and is thus suitable for identifying O-glycosidically linked carbohydrate chains (with exception of yeast glycoproteins). Should the disaccharide be substituted, it is necessary to split off the substitute group forst (e.g. sialic acid) with the aid of neuraminidase [neuraminidase from Arthrobacter or from Vibrio cholerae].

*DSA (Datura stramonium agglutinin)*: recognizes Galβ-(1–4)GlcNAc in complex and hybrid N-glycans, in O-glycans and GlcNAc in O-glycans.

**Enzyme-linked immunosorbent assay (ELISA)**

Total extracts of cells were analyzed by a modified sandwich ELISA that detects specifically either $A\beta_{40}$ or $A\beta_{42}$ according to the provider's protocol (Takeda, Japan)[134]. Aβ was captured with a specific anti Aβ antibody (BNT77). Aβ species ending in residue 40 or 42 were measured using horseradish peroxidase-coupled monoclonal antibodies specific for $A\beta_{40}$ (HPR-conjugated BA27) and $A\beta_{42}$ (HPR-conjugated BC05).

**Lactate dehydrogenase assay (LDH)**

To determine the cell viability in different culture conditions an LDH assay was used. This assay is based on the reduction of Nicotinamide-Adenine-dinucleotide (NAD) by the activity of the enzyme Lactate dehydrogenase (LDH), resulting in a colored compound which is spectrophotometrically analysed. The medium of cultured cells in the desired condition was collected and centrifuged. It was then mixed with a half volume of assay mixture and incubated for 20 minutes at 37°C in the dark. The reaction was then blocked using 1/10 volume 1N HCl. The absorbance was detect at of 490nm. All the steps were performed according to the manufacturer's protocol (Sigma, TOX-7).

### Immunocytochemistry

Cells were washed twice with phosphate buffered saline pH7.4 (PBS) and fixed for 5 minutes with 4% paraformaldehyde (PFA) pH7.4 at room temperature. After two washes with PBS cells were permeabilized with PBS containing 0.1% Triton X-100 for 10 minutes and blocked for 3 hours with 5% sheep serum and 1% BSA diluted in PBS at room temperature. Cells were then washed twice with 1% BSA and 0.05% Triton X-100 diluted in PBS. The primary antibody was diluted in blocking buffer and incubated overnight in a wet chamber at 4°C. The cells were then washed twice with 0.05% Tween-20 in PBS for 5 minutes. The secondary antibody (Amarsham), conjugated with a fluorescence marker was diluted in blocking buffer, added to the cells and incubated for 2 hours at room temperature in the dark. The cells were then washed three times with PBS for 5 minutes and embedded in Moviol.

### Immunohistochemistry for brain sections

Frozen sections were washed twice with PBS and fixed for 30 minutes with 4% PFA pH7.4 at room temperature. After two washes sections were permeabilized with PBS containing 0.1% Triton X-100 for 20 minutes and blocked for 5 hours with 5% HS diluted in PBS at room temperature. Sections were then washed twice with 5% HS and 0.05% Triton X-100 diluted in PBS. The primary antibody was diluted in blocking buffer and incubated with the sections overnight in a wet chamber at 4°C. The brain slides were then washed twice with 0.05% Tween-20 in PBS for 10 minutes. The secondary antibody (Amarsham), conjugated with a fluorescence marker, was diluted in blocking buffer, added to the sections and incubated for 2 hours in the dark. The sections were then washed three times with PBS for 5 minutes and embedded in Moviol.

### Terminal deoxynucleotidyl transferase mediated dUTP nick end labelling assay (TUNEL)

TUNEL staining was performed on cells fixed in 4% PFA. Briefly, cells were incubated with 0.1% Triton X-100 (Sigma) in PBS at 4 °C for 2 minutes, blocked with 3% $H_2O_2$ in methanol for 10 minutes, washed in PBS and

incubated with 50µl TUNEL mix solution containing terminal deoxynucleotidyl transferase and digoxigenin-labelled dUTP (Roche) at 37°C for 90 minutes. Cells were then washed with stop/wash buffer and incubated with 50µl Converter-POD at 37°C for 30 minutes. The cells were rinsed twice with PBS, incubated with 100µl DAB substrate for 10 minutes at room temperature and mounted with Moviol.

**Annexin-V staining**

During early apoptosis, most cell types translocate the membrane phospholipid phosphatidylserine (PS) from the inner face of the plasma membrane to the cell surface. Once on the cell surface PS can be detected by staining with a fluorescent conjugate of Annexin V, a protein that has a strong natural affinity for PS. Annexin V can therefore be used as an early indicator of apoptosis[135]. Annexin-V staining was performed on fresh trypsinized cells in suspension. $10^4$-$10^5$ cells were incubated in 500µl binding buffer (LabForce) containing 5µl Annexin-V Cy3 fluorescence conjugated (LabForce) for 5 minutes at 4°C in the dark. Apoptotic cells were detected using cytometry as described below.

**Cytometry**

Seladin-1 overexpression was detected by intracellular staining of the HA-tagged transgene. Prior to staining cells were fixed in 4% PFA for 10 minutes, washed and permeabilized using 0.1% Triton X-100 for 5 minutes at room temperature. The cells were incubated with an FITC conjugated anti-HA antibody (MBL Int. Co.) for 20 minutes at 4°C in the dark. After washing, cells were resuspended in PBS containing 0.2% fetal calf serum (FCS) and analyzed in a FC500 cytometer using CXP software.

**Analysis of lipids contents**

SH-SY5Y cells or mouse brains were homogenized in PBS containing 9% sucrose and protease inhibitors (CLAP: pepstatin, antipain, chymostatin, each at a final concentration of 25µg/ml) using a dounce homogenizer and 10

passages through a 22 gauge syringe on ice. The samples were centrifuged at 700g for 10 minutes at 4°C and the supernatants were considered as total extracts. A further centrifugation was performed at 100,000g for 1 hour at 4°C to pellet the membrane fraction.

Lipids were extracted from membrane pellets according to Bligh and colleagues[136]. Extracted lipids (cholesterol and sphingomyelin) were subsequently analyzed by thin-layer chromatography (TLC) on silica gel 60 HPTLC plates using a two-step system (hydrophilic running solvent: chloroform/acetone/acetic acid/methanol/water (50:20:10:10:5) (Sigma) and hydrophobic solvent: Hexane/ethyl acetate (5:2)) (Sigma). The ganglioside GM1 was analyzed by slot-blot using cholera toxin subunit B peroxidase linked (Sigma). Quantification was done by densitometry of the scanned TLCs or autoradiograms using the NIH-image software.

To determine the sterol concentration, cells were washed once with ice-cold PBS containing 2mg/ml BSA (Sigma) and twice with PBS. The sterols were extracted twice from confluent cells grown in a tissue culture dish (diameter 10cm) or from frontal brain regions expanding from interaural regions 6 to 4 using 4ml hexan/isopropanol (3:2) containing 1µg epicoprostanol as internal control. Gas Chromatography-Mass Spectroscopy analysis was performed as described to determine the total levels of the extracted sterols[137]. In addition, cholesterol was measured in total and membrane extracts containing equal amount of protein (40µg) using the Ecoline 25 cholesterol kit (Merck). Ecoline relies on the enzymatic oxidation by cholesterol oxidase of cholesterol and its esters producing $H_2O_2$. This is converted into a colored quinonimie in a reaction with 4-aminoantipyrine and salicylic alcohol catalyzed by peroxidase. The optical density was measured at 500nm. Pure cholesterol (Sigma) diluted in 95% ethanol were used as standards.

**DRM isolation**

Total SH-SY5Y cell extracts were incubated for 1 hour at 4°C in 1% Triton X-100, 25mM MES pH7.0, 5mM DTT, 2mM EDTA and CLAP. The extracts were mixed with 90% sucrose prepared in MBS buffer to reach a final concentration

of 60% and overlaid in an SW40 centrifugation tube (Sorvall) with a step gradient of 35 and 5% sucrose in MBS. After centrifugation at 100,000g (Sorvall) for 18 hours at 4°C, eleven fractions were collected from the top of each tube. Fractions 4-6 were identified as the DRM fraction[138] by the presence of the detergent resistent microdomain markers flotillin 1 and GM1 in the control samples.

#### Plasminogen binding and plasmin activity

Plasmin enzymatic activity was assayed using the chromogenic substrate S-2251 (Chromogenix) specific for this protease. 200µg of freshly prepared membrane extracts from SH-SY5Y cells were resuspended in Hank's balanced saline solution (HBSS) and 0.1% Ovalbumin (Sigma). They were placed in a 96 multiwell plate in the presence of 2mM chromogenic peptide to measure endogenous plasmin activity. Absorbance was measured at 37°C and 405nm in an ultra microplate reader Elx808iu (BioteK, instruments, INC) every 5 minutes for 45minutes. To determine plasminogen binding, 2µM human plasminogen was also added to the membrane fractions and plasmin activity was measured.

## Cell biology methods

#### Cell culture

Human neuroblastoma (SH-SY5Y) cells were cultured in DMEM-F12 medium, 2 mM L-glutamine, 1 mM sodium pyruvate, 10% fetal calf serum (FCS), 5% HS, 50U/ml penicillin and 50µg/ml strepomycin. Cells were cultivated at 37°C, 5% $CO_2$ and 95% humidity. Confluent cells were washed with PBS, trypsinized with trypsin/EDTA (Invitrogen) and passaged. Cells were resuspended in freezing medium and stored in liquid nitrogen. Human SH-SY5Y neuroblastoma cells were transfected either with HA tagged wildtype or mutant seladin-1 cDNA constructs using LipofectAmine 2000 (Invitrogen) according to the manufacturer's protocol, followed by a selection with 125µg/ml G418 for 30 days. Pools of selected clones were seeded on

collagen type I (Sigma) coated dishes at a density of 0.3-2.0 x $10^4$ cells/$cm^2$, depending on the type of experiment (low density culture for immunocytochemistry, and high density culture for Western blot analysis).

**Tissue preparation**

Mice were perfused transcardially under deep anesthesia (with an overdose of Rompun Bayer Veterinaria) using a peristaltic pump connected to two reservoirs containing saline and fixative solution. A cut along the sternum was made in order to expose the end of the sternum, then, with sharp scissors, a cut was made through the skin, diaphragm and laterally on both sides upward across the ribs parallel to the lungs; the cannula was then inserted through the left ventricle into the ascending aorta. The right auricle was cut with a surgical pair of scissors to allow the escape of return circulation. Perfusion was performed initially with PBS, pH 7.4 for 10 minutes at room temperature, followed by 4% PFA in PBS on ice. Brains were removed and immersion-fixed in 4% PFA overnight at 4°C. Immunohistochemistry was performed either on thick (12µm) cryostat (Leica) sections or on thin (5µm) paraffin sections (Leica). For cryostat sectioning, brains were subsequently incubated in 10%, 20% and 30% sucrose for cryprotection. For paraffin sections, tissue was subsequently dehydrated in an ascending ethanol series followed by xylol incubation prior to paraffin embedding.

**Primary neuronal cultures**

Primary neuronal cultures were prepared from c57Bl/6 wildtype mice. The cortex was dissected and kept in ice-cold Hank's balanced salt solution (HBSS; 10 mM HEPES, pH 7.3) (Gibco) and then incubated at 37 °C for 30 minutes in $Ca^{2+}$/$Mg^{2+}$-free HBSS containing 0.25% trypsin (Gibco) and 0.2 mg/ml deoxyribonuclease (Sigma). The cortical tissues were dissociated to single cells by gentle trituration. The cell suspension was mixed with Neurobasalmedium supplemented with B27 (Gibco), 0.5mM glutamine, 50 U/ml penicillin, and 50µg/ml streptomycin. The cell suspension was centrifuged at 310g for 3 minutes and the resulting pellets were resuspended in the medium described above and plated onto polyornithin/laminin (Sigma)

coated 12-well plates with one coated glass cover slip in each well. The cells were cultured in a $CO_2$ incubator (5% (v/v), 37 °C) for 5 days before treatment with SFV.

**Semliki Forest Virus preparation**

Semliki Firest virus (SFV) is a positive strand RNA virus of the alphavirus genus that can infect differentiated neurons. A heterologous gene in the 'vector RNA' replaces the viral structural protein genes that are required for encapsidation of viral RNA. Vector RNAs are self replicating and referred to as 'replicons'. Replicons must be cotransfected with a 'helper RNA' to be packaged into infectious particles. Kits for the production of packaged SFV are commercially available (SFV, Life Technologies). In short, seladin-1 cDNA

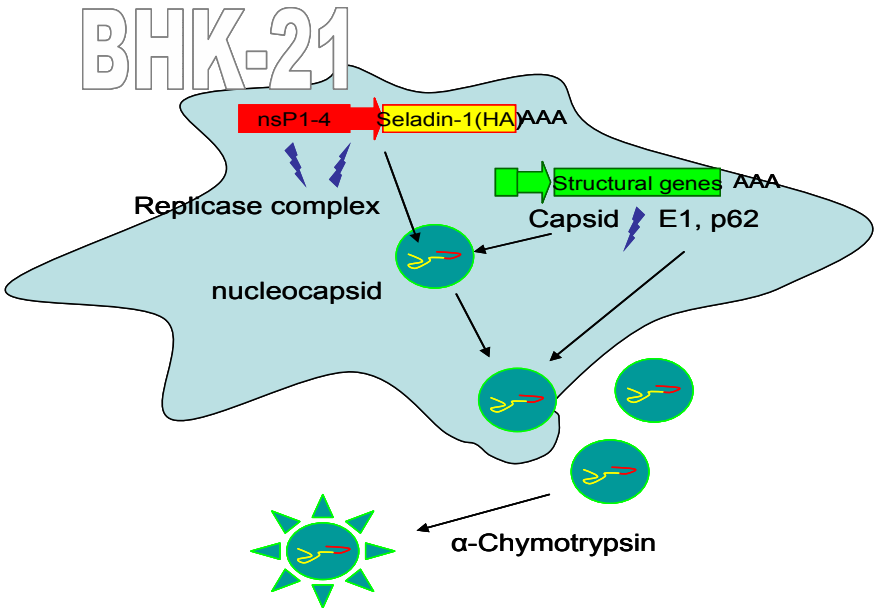


**Production of Selmiki Forest Viruses modified to express the human seladin-1**

BHK-21 cells are cotransfected with a nsP1-4 viral replicon containing seladin-1 mRNA and a helper RNA expressing the structural genes of the virus. Cells transfected with both RNAs produce an inactive virus, which contain the seladin-1 mRNA. The virus is activated after an α-Chymotrypsin digestion.

was cloned into pSFV2 plasmid using BamHI/XhoI restriction sites. The plasmid was transfected into XL-2 Gold bacteria (Invitrogen) and DNA was extracted. The purified plasmid was linearized using NruI restriction enzyme and purified. The plasmid containing the cDNA for the production of structural

genes (helper RNA) was linearized using SpeI. Both linearized plasmids were reverse transcribed to RNA as described by Lundstrom and colleagues[139] using the *in vitro* transcription SuperScript kit (Gibco). To produce the virus, baby hamster kidney (BHK-21) cells (kindly provided by Markus Ehrengruber) were cultured to 80% confluency and transfected with both RNAs in a ratio of 1:1 using LipofectAmine (Invirogen). After 2-3 days the medium was collected. The virus was activated by adding 500µg/ml α-Chymotrysin (Sigma) to the medium containing the packaged replicons, after 30 minutes incubation at room temperature the reaction was stopped with 250µg/ml aprotinin (Sigma). α-Chymotrysin cleaves the spike precursor protein p62 at a leucine residue, resulting in the formation of mature E2 and E3 spike protein, which lead to the activation of the virus.[140]

**Alphavirus mediated gene transfer into neurons**

Primary neuronal cultures were prepared as described above. The activated SFV was added directly to the medium with an approximate titer of $10^4$ infectious units. Cells were incubated during 48 hours in a tissue culture incubator (5% $CO_2$, 37°C). During this time the virus can activate its replicase

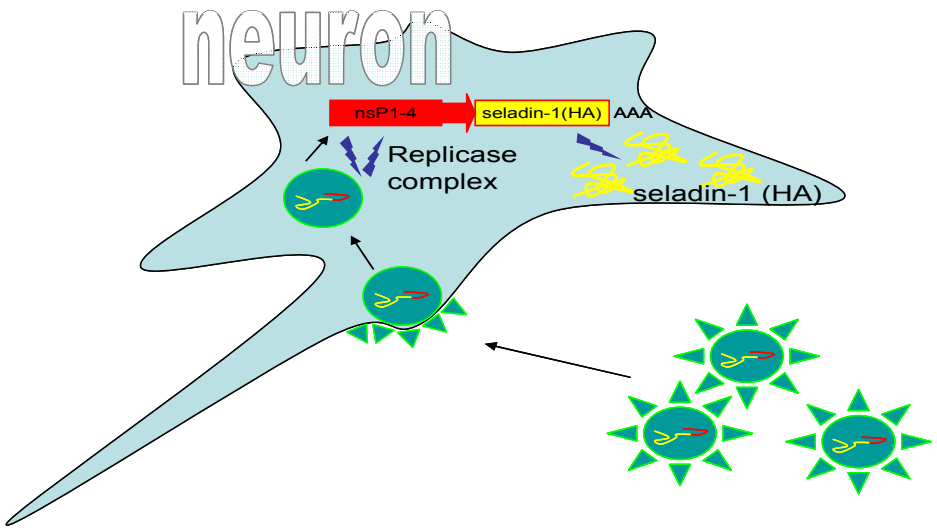


**Selmiki Forest Virus infection of postmitotic neurons**

Selmiki Forest Virus infects the neurons via viral E2 and E3 spike proteins. Once the RNA has been released into the cytoplasma of the neuron, it can express the exogenous seladin-1(HA).

machinery and transcribe the cloned gene using the neuronal transcription and translation factors. An incubation period of two days was optimized for neuronal cultures.

**Intracranial stereotaxic injection**

Four month-old c57Bl/6 mice were anesthetized with Ketalar/Rompun, placed in a Kopf stereotaxic instrument, and an incision was made along the midline to expose the skull. The calvarium was perforated with a dentist borer and 1µl of a suspension of cells in MEM was injected into the hippocampus, according to Bregma coordinates defined as caudal, lateral and ventral measures (-1.9; -1.0; -1.9) over a period of 5 minutes using a 10µl Hamilton syringe positioned with a stereotaxic instrument. The syringe was slowly withdrawn, and the wound was closed with surgical staples.

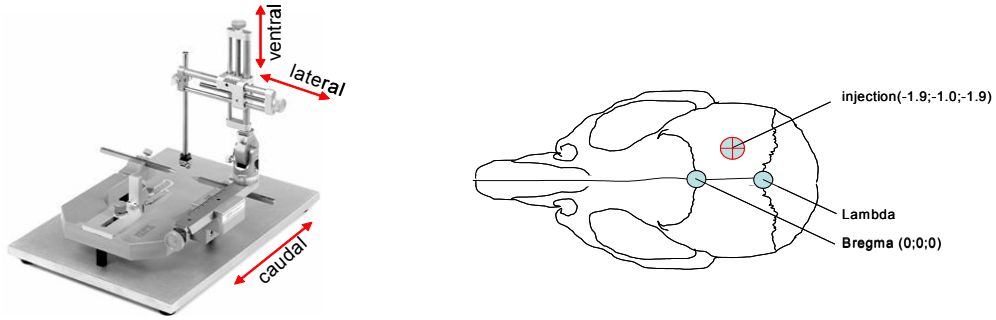


http:// www.kopfinstruments.com

**Schematic figure for stereotaxic injections**

Left panel: Kopf stereotaxic apparatus. The mouse is placed and fixed by means of two ear bars and a mouth-piece, the exact coordinates for injection can be red on an appropriate scale (caudal, lateral and ventral). Right panel: Representation of a mouse skull. Once the skull is exposed by incision with a scalpel, the Bregma and Lambda points are visible, starting from the Bregma, the appropriate coordinates are calculated (e.g. -1.9:-1.0:-1.9 for the CA1 region of the hippocampus).

**Statistical analysis**

Data were collected and statistically analyzed by non-parametric Mann–Whitney U test using theSPSS program. In all graphs mean ± SE (standard deviation of the mean) are shown. P values <0.05 were considered statistically significant. Statistical significance is indicated by asterisks:

*P =0.01-0.05, **P=0.001-0.01, ***P=0.0001-0.001.

# Results

### Cloning and mutagenesis of human seladin-1

To study the effect of seladin-1 overexpression *in vitro* we subcloned the open reading frame (ORF) of the human seladin-1 cDNA in neuroblastoma cells. Since seladin-1 is a putative substrate for caspases[5] we generated two additional constructs with point mutations at the presumed cleavage sites of either caspase-3 at AA 122 (D474E) or caspase-6 at AA 182 (D1256E) (**Fig 1**). Both point mutations block caspase activity because the amino acid aspartate, which is necessary for caspase cleavage, was substituted by glutamate. All three constructs were tagged with a haemagglutinin (HA) sequence at the 3'-OH end and were cloned into the expression plasmid pcDNA3 driven by a CMV promoter. As control construct we cloned EGFP in pcDNA3.

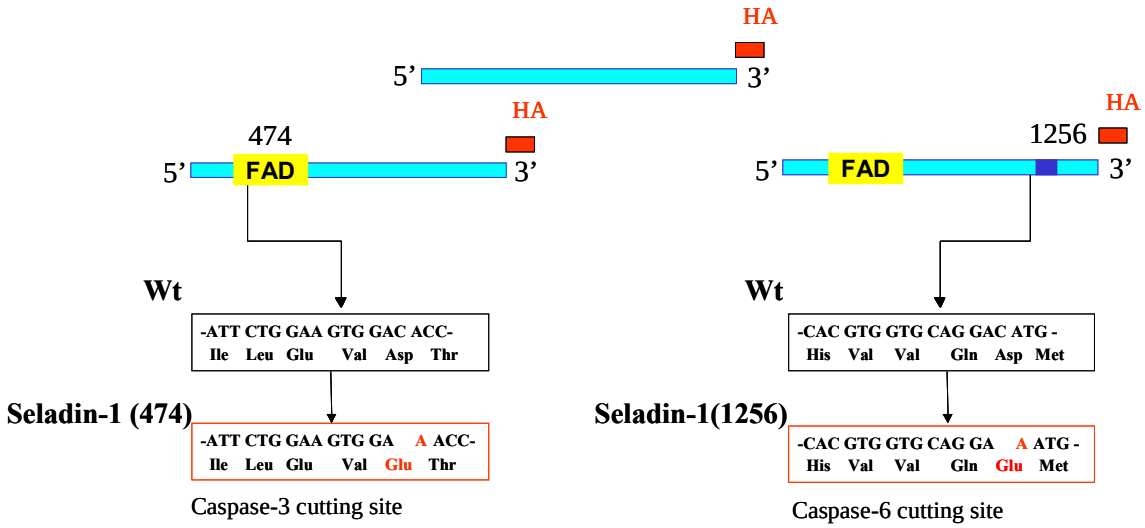


**Figure 1 Cloning, mutations and tagging of human seladin-1 cDNA**

The human seladin-1 cDNA was tagged with an haemagglutinin sequence at the 3'-OH end and subcloned. Point mutations were inserted at the two putative caspase cleavage sites (caspase-3, D474E and caspase-6, D1256E).

### Analysis of transgene expression

Human neuroblastoma (SH-SY5Y) cells were transfected with the wildtype seladin-1 cDNA construct (sel) and the constructs mutated at the putative caspase-3 (474) and caspase-6 (1256) cleavage sites. As control cultures we

transfected the EGFP construct (EGFP) and for mock-transfected control cells we transfected the pcDNA3 vector (control). To obtain stable expression we selected the cultures for five weeks with neomycin. The expression of the transgene was analysed by Western blotting using a polyclonal anti rat antibody against the HA tag. The transgenes were visible at the size of 60kDa confirming the expression of the transfected cDNAs (**Fig 2a**). Control cells did not show any transgenic expression. The loading was controlled by a β-actin staining. The different intensities of the HA-bands in Figure 2 implied a certain difference in the percentage of transfected cells between the three cultures. Cytometry and immunohistochemistry confirmed these differences and revealed that in the seladin-1 overexpressing culture 30% of the cells stably expressed the transgene. In the two mutant cell lines we found 22% of the cells expressing the 474 and 16% expressing the 1256 construct (**Fig 2b**).

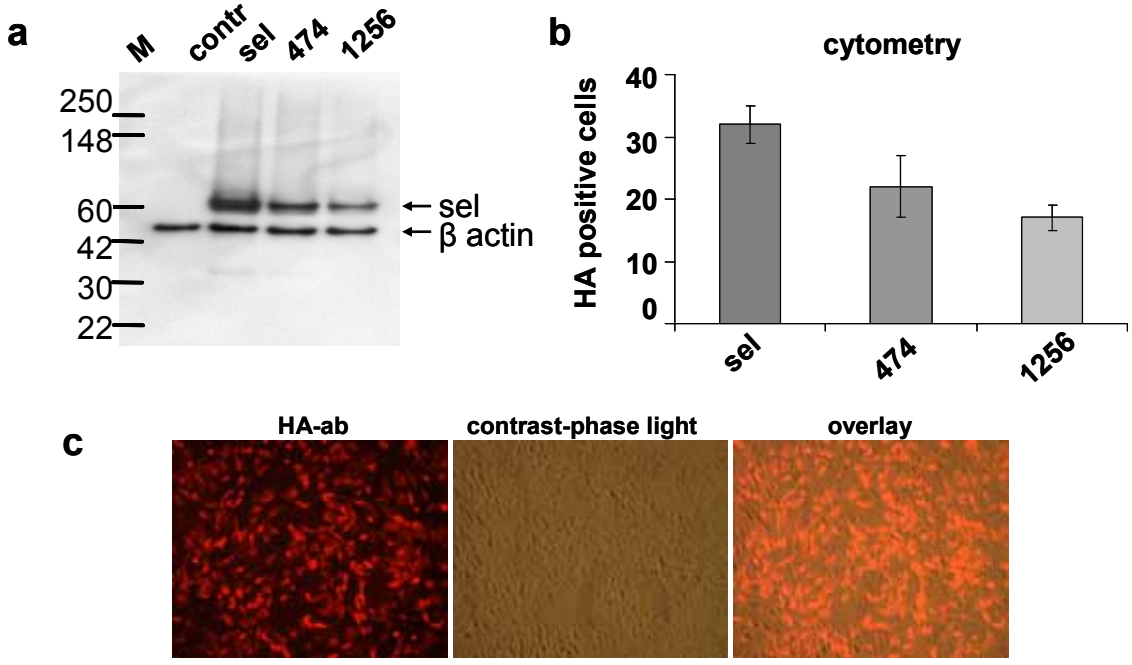


**Figure 2 Analysis of SH-SY5Y cells expressing different seladin-1 constructs**

(**a**) Western analysis of seladin-1 overexpressing cells (lane 2), 474 cells (lane 3) and 1256 cells (lane 4) using an anti HA antibody show the expression of the transgenes. No specific band corresponding to HA could be detected in control cells (lane 1). β-actin staining showed that similar amounts were loaded on the gel. (**b**) Cytometric analysis of seladin-1HA expression. In seladin-1 overexpressing cultures 30% of the cells are stably expressing the transgene. In 474 and 1256 cultures 22% and 16% of the cells are expressing the mutated transgenes, respectively (**c**). Immunocytochemistry. HA-staining and phase images of SH-SY5Y cells transfected with human seladin-1. The overlay shows that ± 30% of the cells stably expressed the transgene.

**Induction of apoptosis and analysis of surviving cells**

To analyze the anti-apoptotic function of seladin-1 and the possible role of caspases in this process we subjected seladin-1 overexpressing wildtype cells, mutated cells lines 474 and 1256 and mock transfected control cells to apoptotic stimuli. Since there are many insults which can trigger a variety of mechanisms leading to the induction of programmed cell death we treated the cells with four different substances. $H_2O_2$ results in general oxidative stress by the production of oxygen radicals whereas tunicamycin selectively induces ER stress. Etoposides block the function of the topoisomerase II during DNA replication and therefore induces apoptosis during cell division. The Aβ peptide is thought to be the primary toxic agent responsible for nerve cell death in AD. The mechanisms involved in Aβ are not known completely and include protein oxidation and lipid peroxidation.[141] For assessment of cell viability, we measured lactate dehydrogenase (LDH) in the supernatant of the cells. LDH is a mitochondrial protein which is released when the cell membrane is damaged, and the assay is based on the reduction of NAD by the action of LDH. For the detection of apoptotic cells we used the terminal deoxynucleotidyl transferase, which catalyses the addition of labeled nucleotides to free 3'-OH DNA ends in a template independent manner (TUNEL-reaction). For cytometric analysis of apoptotic cells we labelled membrane phosphatidylserine using Annexin-V. During early apoptosis, most cell types translocate the membrane phospholipid phosphatidylserine (PS) from the inner face of the plasma membrane to the cell surface. Once on the cell surface, it can be detected by staining with a fluorescent conjugate of Annexin V, a protein that has a strong natural affinity for PS[135]. Double staininig using FITC labeled Annexin-V and TRITC marked anti HA antibody was performed for quantification of the survival rate of apoptotic cells expressing seladin-1 or its mutated forms. To evaluate the protective function of our transgene product, we assessed cell viability after treatment of seladin-1 overexpressing and control cells with 100µM $H_2O_2$ for 30 minutes and 2 hours. LDH measurements revealed that cell viability in seladin-1 overexpressing cells was only slightly affected by the $H_2O_2$ treatment, whereas after 30 min viability in control cultures was reduced to 47% and this

effect increased after 2 hour of treatment (23%) when compared to non treated controls (**Fig 3a**).

Given that wildtype seladin-1 overexpression is protective against induced cell death we next analyzed the cultures containing the caspase mutations 474 and 1256 to evaluate the role of caspases in this process. After 5 hours of $H_2O_2$ treatment we performed TUNEL staining to assess cells undergoing apoptosis. Seladin-1 overexpressing cells were significantly more resistant to the toxic insult than control cells (mortality rate 53%±9.3% and 85%±3.3%, respectively, mean±SE, $P<0.05$), confirming the anti-apoptotic function of seladin-1. The surviving rate of 474 cells was also significantly increased (mortality rate 57%±4.1%, mean±SE, $P<0.05$) whereas the 1256 cells did not significantly differ compared to control cells (**Fig 3b**). Similar results were obtained when comparing TUNEL positive cells of sel, 474, 1256 and control cultures after treatment with etoposides, an inhibitor of topoisomerase 2. Wildtype seladin-1 overexpressing cells were significantly less affected than control cells (mortality rate 23%±10.4%, mean±SE, $P<0.05$). A trend towards less apoptotic cells but no significant reduction was evident in 474 cultures. In 1256 cultures the number of apoptotic cells was similar to control cultures (**Fig 3c**). We next treated the cells with oligomeric and fibrillar forms of $A\beta_{40}$ peptide for 24 hours and did cytometric analysis of the Annexin V staining for assessment of apoptotic cells. After treatment with oligomeric and fibrillar $A\beta_{40}$ peptide the percentage of apoptotic cells in the wildtype seladin-1 overexpressing and 474 cultures was smaller compared to 1256 and control cultures, but only a border-line significance was found. After treatment with oligomeric $A\beta_{40}$ the overall number of apoptotic cells in all groups was greater when compared to the treatment with fibrillar $A\beta_{40}$ (**Fig 3d,e**).

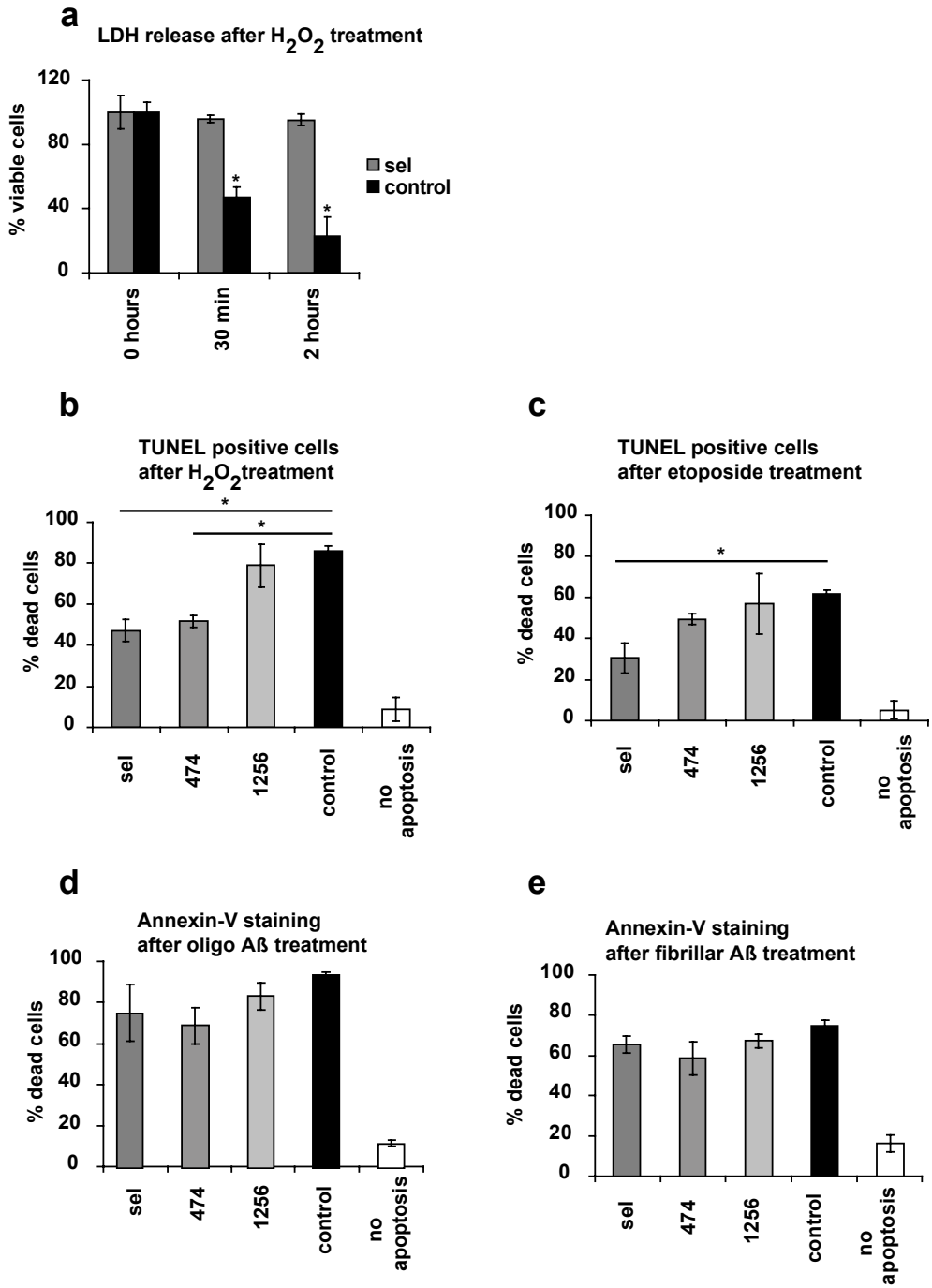


**Figure 3 Anti-apoptotic role of seladin-1**

Seladin-1 overexpressing cultures survive significantly better after 30 minutes and 2 hours $H_2O_2$ treatment when compared to control cultures (**a**). After 5 hours of $H_2O_2$ treatment overexpressing seladin-1 and 474 cells reveal a significant increase in survival when compared to 1256 and control cultures (**b**). 18 hours of etoposides treatment shows no differences between the four groups (**c**). Cultures incubated with oligo and fibrillar $A\beta_{40}$ do not reveal significant differences in cell survival (**d,e**).

**Expression levels of seladin-1 after induction of apoptosis**

To investigate the expression of the endogenous seladin-1 during apoptosis we treated SH-SY5Y cells with 200μM $H_2O_2$ and harvested the cells during 8 hours at different time points. An increase of the endogenous seladin-1 protein level was already detectable 1 hour after the insult and the levels remained elevated during the entire treatment. (**Fig 4**).

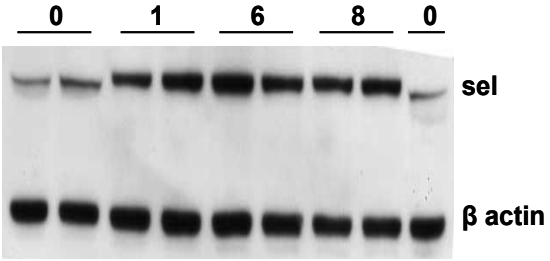


**Figure 4 Seladin-1 protein levels during apoptosis induced with $H_2O_2$**

SH-SY5Y cells show increased seladin-1 protein levels after an apoptotic insult. Already 1 hour after $H_2O_2$ treatment endogenous seladin-1 levels are elevated and remain increased during 8 hours of treatment.

**Intracranial injection of SH-SY5Y cells overexpressing seladin-1HA and EGFP**

Given the anti-apoptotic function of seladin-1 in a cell culture system we next analyzed whether the overexpression of seladin-1 in SH-SY5Y cells affects their survival *in vivo*. We injected wildtype seladin-1 overexpressing and control cells expressing EGFP intracranially into c57bl/6 mice. The cells were plated the day before the injection at a confluency of 40% in normal culture medium (**Fig 5 left panels**). Cells were trypsinized and resuspended in MEM without FCS, HS or antibiotics, and diluted to 3,500 cells per microliter. The mice were anesthetized and injected with 3,500 cells with a rate of 0.2µl per minute. Two and four weeks after the injections the mice were perfused with PBS followed by 4% PFA. 15µm cryosections were cut and analyzed.

No differences were detected in proliferation and in the distribution of the cells. Both cultures proliferated to the same extend and after two weeks seladin-1 and EGFP cells revealed the ability to grow as tumors (**Fig 5a**). The cells were not removed by the mouse immune system, suggesting that these cells are able to exhauste the mouse defence system independently of the expressed transgene. Taken together, these data suggest that seladin-1 overexpression did not affect their survival rate *in vivo.* Moreover, when a mixture of seladin-1 and EGFP overexpressing cells were injected into the brain, no difference was observed in their survival rate. (**Fig 5b**). Furthermore

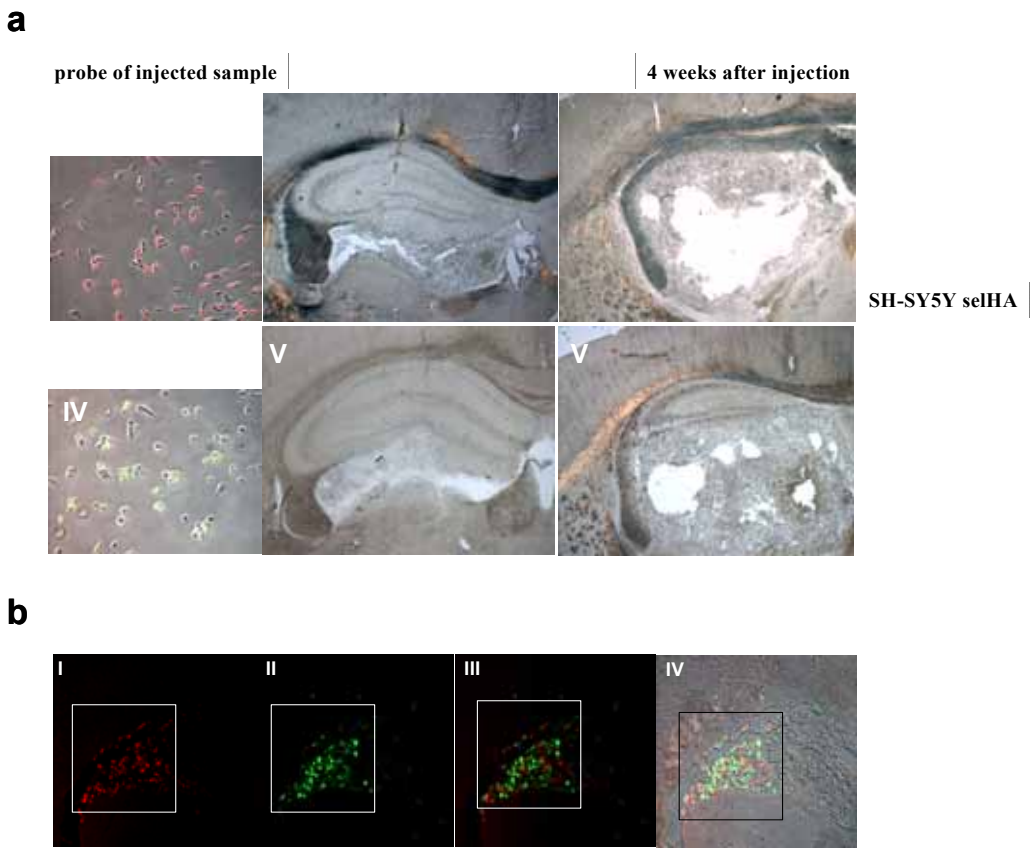


**Figure 5 Stereotactic injections of SH-SY5Y cells into c57BL/6 mice**

**(a)** SH-SY5Y cells over expressing seladin-1 and EGFP were injected intracranially into c57Bl/6. The left panel (I and IV) shows a representative culture of injected cells. The middle and right panels show the injected brains with the grown tumor 2 (II and V) and 4 (III and VI) weeks after injection, respectively. Upper pictures show seladin-1 and lower pictures show EGFP implanted brains. **(b)** Brain sections from injected mice with a mix of SH-SY5Y cells overexpressing seladin-1(HA) and EGFP. Pictures represent hippocampus section containing the mix of injected cells stained with HA antibody (red) for seladin-1(HA) (I) and EGFP antibody (green) (II); the same section in overlay (III) and overlay in contrast phase light is shown in (IV). No differences are visible in growth and distribution of seladin-1 and EGFP overepresssing cells.

to ensure that this fact is only valid for growing tumor cells, we predifferentiated the seladin-1 and EGFP cells, culturing them in medium containing 15nM retinoic acid during 5 day and used them for injections. In both groups no cells were detected in the injected region one week after the injections. These data show that predifferentiated cells do not develop into tumors and that overexpression of seladin-1 cannot rescue predifferentiated cells when injected into a mouse brain with a functional immune system.

**Semliki Forest Virus (SFV) transduction of primary neuronal cultures**

We designed semliki forest virus containing wildtype seladin-1, 474 and 1256 RNA to overexpress seladin-1 in primary neuronal culture. The obtained maximal virus titer in our system was $7.10^7$ infectious units per µl (stock concentration). Primary neuronal cultures were incubated with different virus concentrations. Neurons infected with virus titers smaller than $7.10^4$ survived the treatment but revealed an infection efficiency of only 1-4% (**Fig 6**). Neuronal cultures infected with greater virus titers did not survive the treatment independently of the transgene. Due to the low transfection efficiency, this gene transfer system would only allow immunocytochemical analysis of the small amount of transfected cells. For any biochemical analysis this system was not suitable within this protocol.

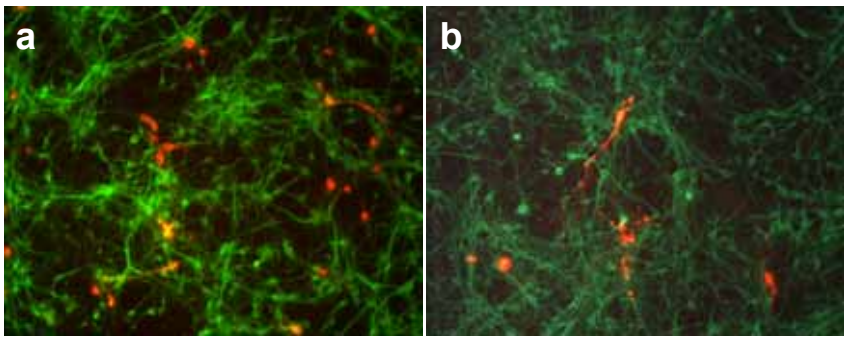


**Figure 6 Primary neuronal cultures infected with selmiki forest virus (SFV)**

Two representative pictures of primary neuronal culture from wildtype c57Bl/6 mice infected with SFV containing seladin-1 (**a**) and 474 (**b**), respectively (red). The infection efficiency of the SFV was about 1 to 4%. Neurons were stained using anti MAP2 antibody (green).

To ensure that the obtained results were not only an *in vitro* effect, we stereotactically injected the virus containing EGFP into mouse brains. We found a minor amount of EGFP expressing cells around the injection tract but no transfected cells could be detected in other regions of the hippocampus. These results confirmed the *in vitro* data and led us to the conclusion that the infection efficiency in our system was too low to obtain enough transfected cells to analyse the effect of seladin-1 overexpression in primary neurons or in mouse brains.

### Modifications of seladin-1

To determine whether seladin-1 is post-translationally modified, the gycosylation- patterns of seladin-1 were analyzed in seladin-1 overexpressing SH-SY5Y cells. Figure 7 shows a 70kDa prominent band appearing in all blots stained with the different agglutinins; GNA, SNA, MAA, PNA, DSA. The positive control, a Western blot probed with an anti-HA antibody, shows the real size of seladin-1 and revealed that the stained band on the agglutinin blot is not seladin-1. This strongly suggested that seladin-1 is not glycosylated in our conditions.

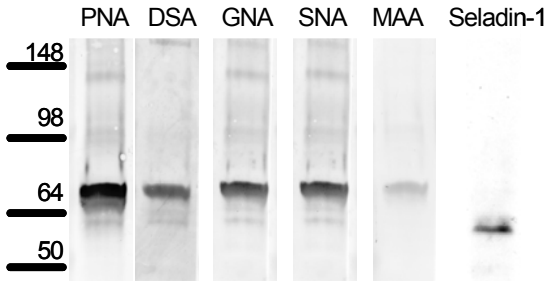


**Figure 7 Glycosylation analysis of seladin-1 overexpressing cells**

Membranes were stained using different agglutinins to detect sugars bound to seladin-1. Lane 1 to 5: a prominent band at about 70kDa appears in all tested lectine membrane stripes. Last lane: Western blot probed with anti-HA antibody to detect seladin-1 as positive control. Seladin-1 is significantly smaller than the detected 70kDa band, suggesting that seladin-1 is not glycosylated.

### Seladin-1 regulates the levels of total and membrane cholesterol in cultured human neuroblastoma cells

To determine to which extent the levels of neuronal cholesterol depend on seladin-1 we first analyzed the effects of seladin-1 (sel) overexpression in human neuroblastoma SH-SY5Y cells. Quantitative Real-Time PCR of seladin-1 mRNA revealed a significant increase (684±121% mean ±SE, P=0.0001, n=3) in the seladin-1 overexpressing cultures when compared to control cultures (**Fig 8a**). Significant increases of 1.9 fold in membrane cholesterol (P=0.003, n=3, **Fig 8b,**) and 1.7 fold in total cellular cholesterol (P=0.001, n=3, **Fig 8c**) were found in seladin-1 overexpressing cells when

compared to the control cultures. Desmosterol levels were dramatically reduced in cells overexpressing seladin-1 (43±5.2% mean ±SE, P=0.001, n=3, **Fig 8d**) while 24-OH-cholesterol amounts were increased (172±2.3% mean ±SE, P=0.00001) when compared to control cultures demonstrating a normal catabolism of cholesterol in both conditions. The ratio of desmosterol to cholesterol was 2.8 fold (p=0.001, n=4) lower in the seladin-1 overexpressing cultures (**Fig 8e**) indicating a dramatic decrease of desmostero,l in addition to a drastic increase in cholesterol under conditions of seladin-1 overexpression and therefore reconfirming the bioactivity of the transgene. The ratio of the catabolic product 24OH-cholesterol to cholesterol did not differ in both cell lines (**Fig 8g**) demonstrating a normal catabolism of cholesterol in both conditions.

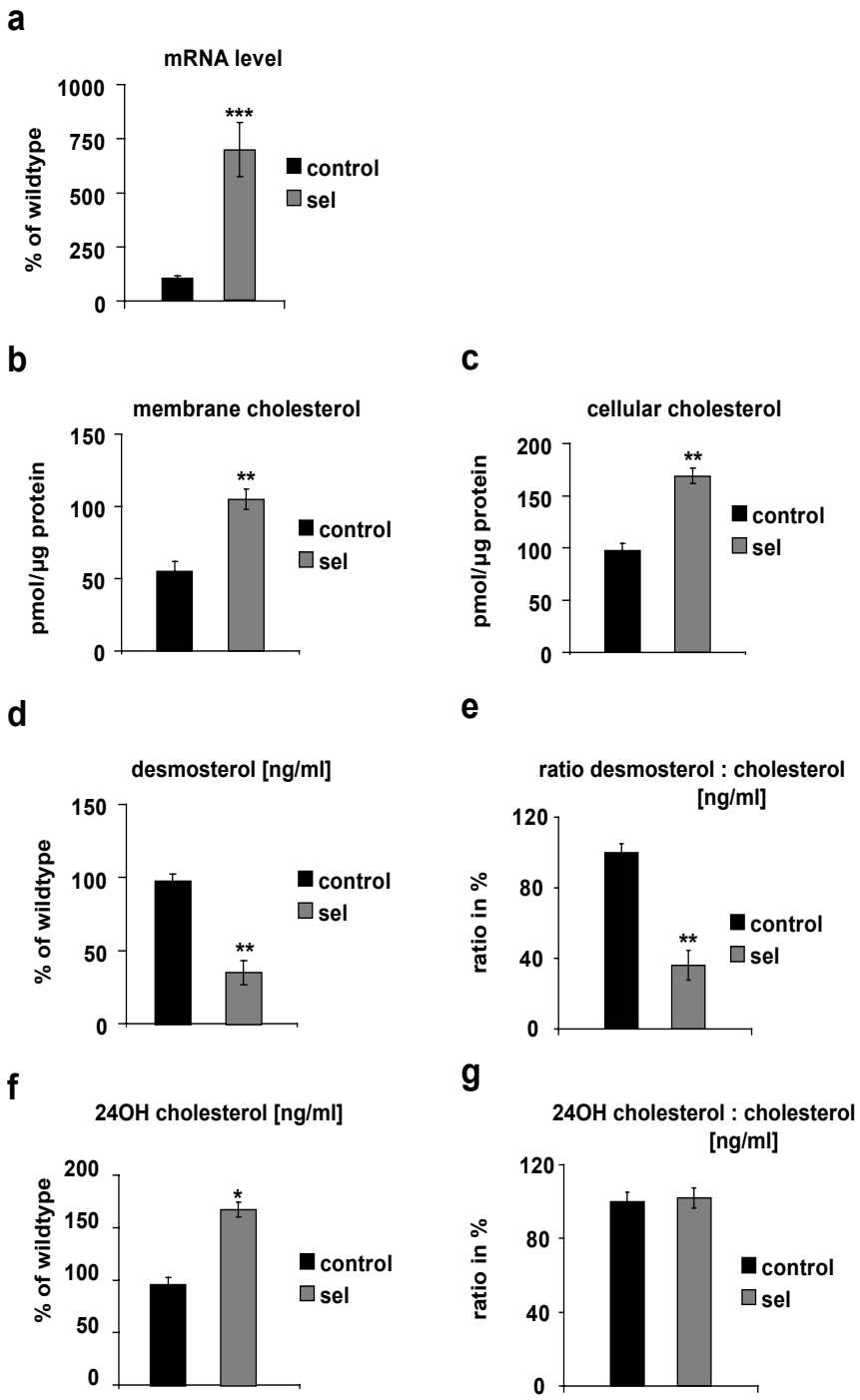


**Figure 8 The levels of total and membrane cholesterol depend on seladin-1 expression *in vitro***

Seladin-1 overexpressing SH-SY5Y cultures exhibited significantly higher seladin-1 mRNA levels when compared to control cultures (**a**). Amount of cholesterol expressed in pmol/µg protein in membrane (**b**) and cellular (**c**) extracts of control and seladin-1 overexpressing SH-SY5Y neuroblastoma cells. Amount of desmosterol (**d**) and 24OH-cholesterol (**f**) as well as ratios of desmosterol (**e**) and 24OH-cholesterol to cholesterol (**g**) in control and seladin-1 overexpressing SH-SY5Y cells. Values were expressed in percentage change to the corresponding values in control cells that were considered as 100%. Data in all graphs are mean values and standard error from three independent cell cultures.

**Seladin-1 contributes to the specific recruitment of DRM proteins and lipids into DRMs**

Given the above results and that cholesterol is a main component of DRMs we next hypothesized that changes in seladin-1 expression would affect the protein and lipid composition of these membrane domains. To test this, total extracts of control and seladin-1 overexpressing SH-SY5Y cells were incubated with 1% Triton X-100 at 4°C and centrifuged on a sucrose gradient. Measurement of the amount of total protein in the different gradient fractions revealed a significant increase in the light fractions 6-4, which correspond to detergent resistant membranes, in the seladin-1 overexpressing cells compared to control cells (31.6±3.5% and 22.2±3.5% mean ±SE, respectively, P=0.01, **Fig 9a**). To determine whether this increment in protein content was the consequence of general or DRM specific protein recruitment the flotation profiles of the DRM markers flotillin 1 (**Fig 9b**) and the GPI-anchored cellular prion protein ($PrP^c$) (**Fig 9d**) and of the non-DRM marker transferrin receptor (TfR) were analyzed (**Fig 9f**). In agreement with a specific recruitment, flotilin1 and $PrP^c$ were enriched in fractions 6-4 of seladin-1 overexpressing cell gradients than in control cells while TfR remained in the detergent soluble heavy fractions (8-10) in both conditions (**Fig 9b,d,f**). Quantitative analysis showed that while 4.8±2% of total flotillin 1 and 10.4±3% of total $PrP^c$ float to DRMs in control cells these percentages increase to 18.7±4.6% and 30.5±5% (mean ±SE), respectively, in seladin-1 overexpressing cells (P=0.004 and P=0.001, **Fig 9c,e**). To establish whether changes in protein content in DRMs were paralleled by changes in lipid composition, the levels of cholesterol, sphingomyelin (SPM) and the ganglioside GM1, were analyzed in the different gradient fractions (**Fig 10**). Thin Layer chromatography (TLC) (to detect cholesterol and SPM) and slot-blot using cholera toxin subunit B (that binds to GM1 with high affinity [142]) revealed that seladin-1 overexpression leads to the recruitment of more cholesterol (56±6%, **Fig 10a,b**), SPM (68.7±11%, **Fig 10c,d**) and GM1 (67.4±5.5%, **Fig 10e,f**) in detergent-insoluble fractions 6-4 compared to control cells (42±5% cholesterol, 48.3±12.3% SPM and 57±4% GM1, P<0.05).

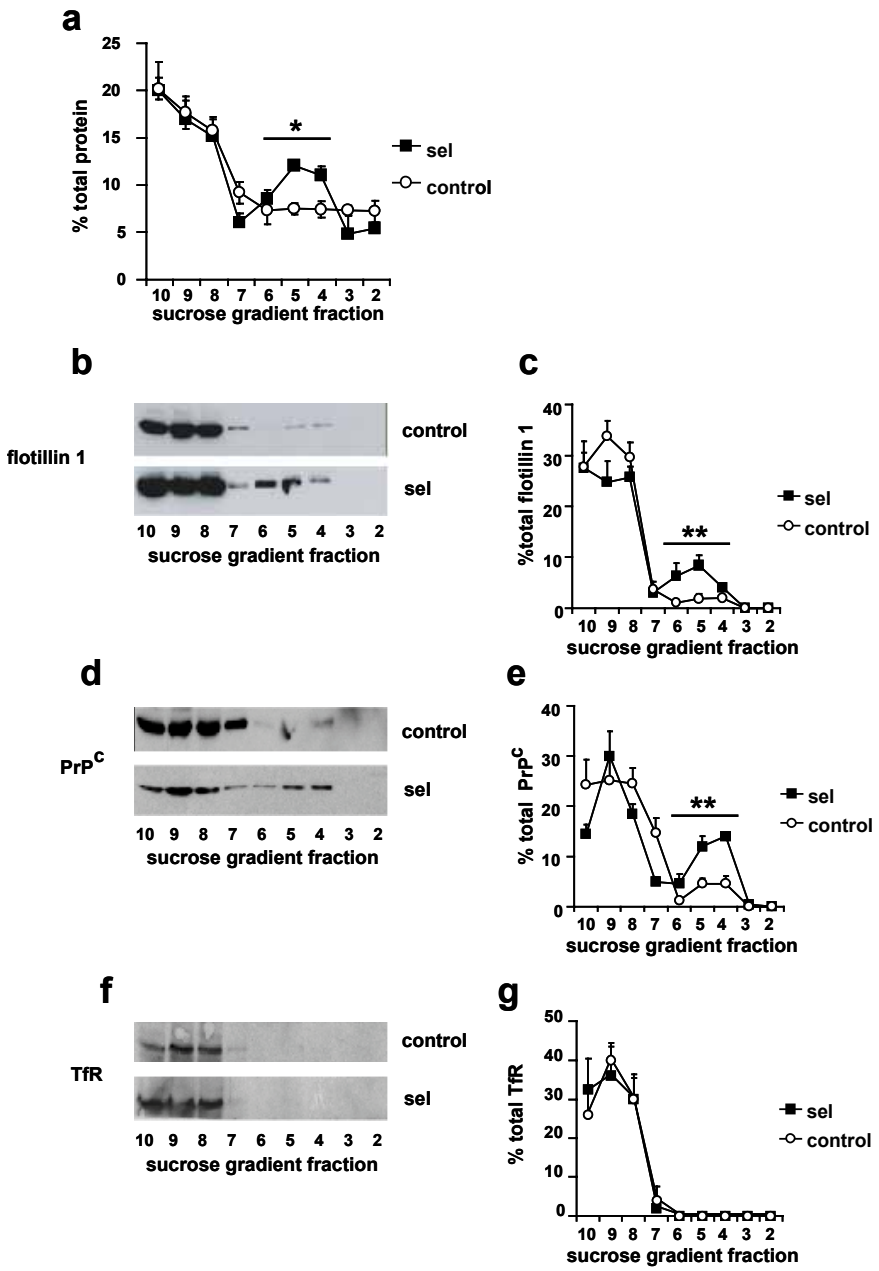


**Figure 9 Seladin-1 regulates the specific recruitment of DRM proteins to DRM microdomains**

Total cell extracts containing 100μg of protein from control and seladin-1 overexpressing SH-SY5Y cells were centrifuged in a sucrose gradient. Fractions containing equal volume were collected and numbered from the lightest to the heaviest (2 to 10). The amount of protein in each gradient fraction is expressed as percentage of the total protein along the gradient (**a**). Representative Western blots of the gradient fractions using antibodies against the DRM proteins flotillin 1 (**b**) and $PrP^c$ (**c**), and the non-DRM protein TfR (**d**). The graphs show the distribution of flotillin 1, $PrP^c$ and TfR in each fraction as percentage of the total amount of flotillin 1, $PrP^c$ and TfR, respectively, along the entire gradient (**c,e,g**). control: mock transfected SH-SY5Y cells; seladin-1: overexpressing SH-SY5Y cells. The graphs show the average and standard error from three independent SH-SY5Y cultures. Asterisks show statistical significance of the differences found in combined fractions 6-4 that correspond to DRMs.

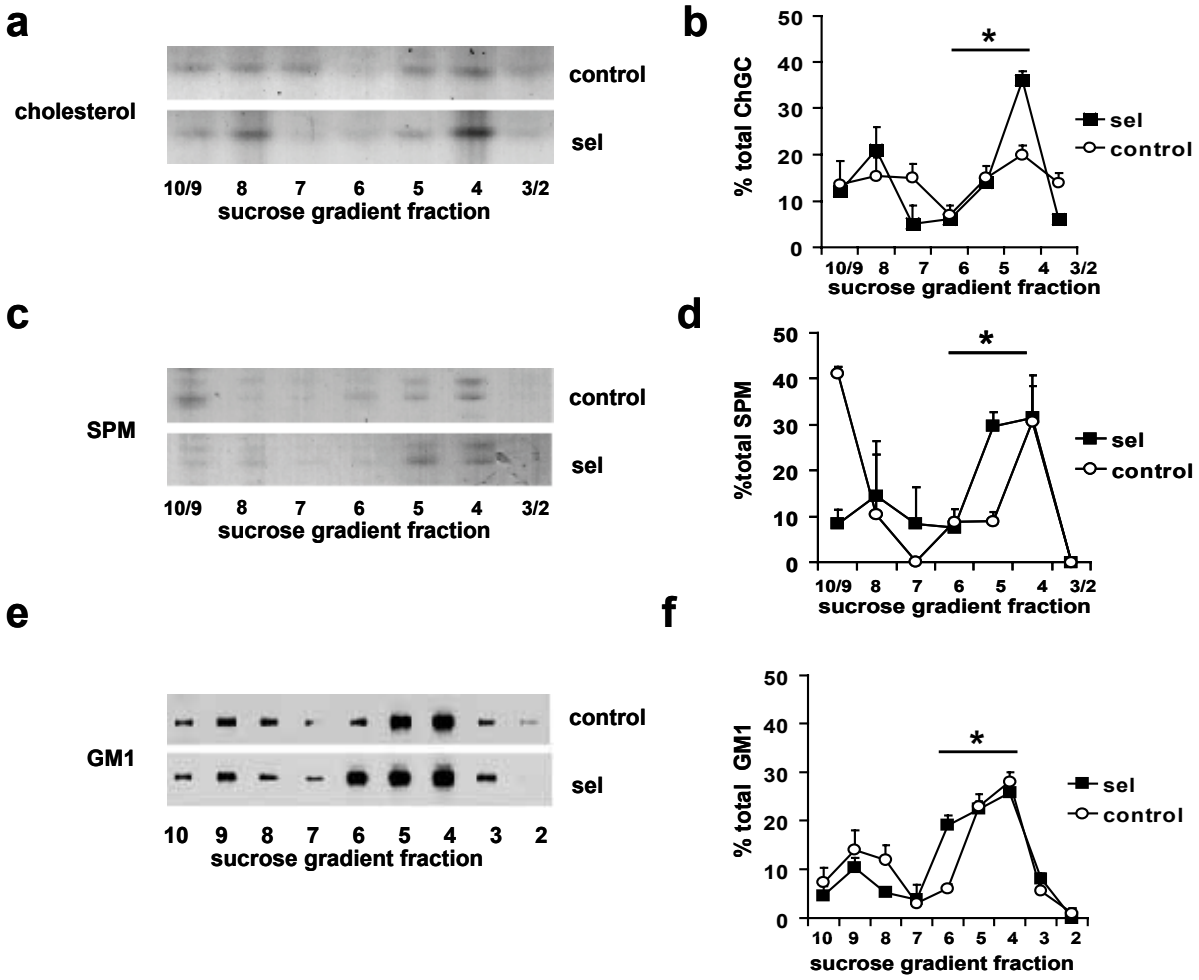


**Figure 10 Seladin-1 expression affects the amount of lipids in DRMs**

Total extracts containing 100μg of protein from control and seladin-1 overexpressing SH-SY5Y cells were prepared as described for Figure 15. Where indicated fractions 2-3 and 9-10 were pooled and analyzed together. The distribution of cholesterol (**a**) and SPM (**c**) was examined by TLC while slot blot and cholera toxin B linked to peroxidase were used to detect GM1 (**e**). Left panels show representative examples of the gradients. The graphs show the amount of cholesterol (**b**), SPM (**d**) and GM1 (**f**) in each fraction as the percentage of total cholesterol, SPM and GM1, respectively, along the entire gradient. Control: mock transfected S
a

Altogether these results indicate that seladin-1 is required for the specific recruitment of DRM protein and lipids into detergent insoluble membrane domains.

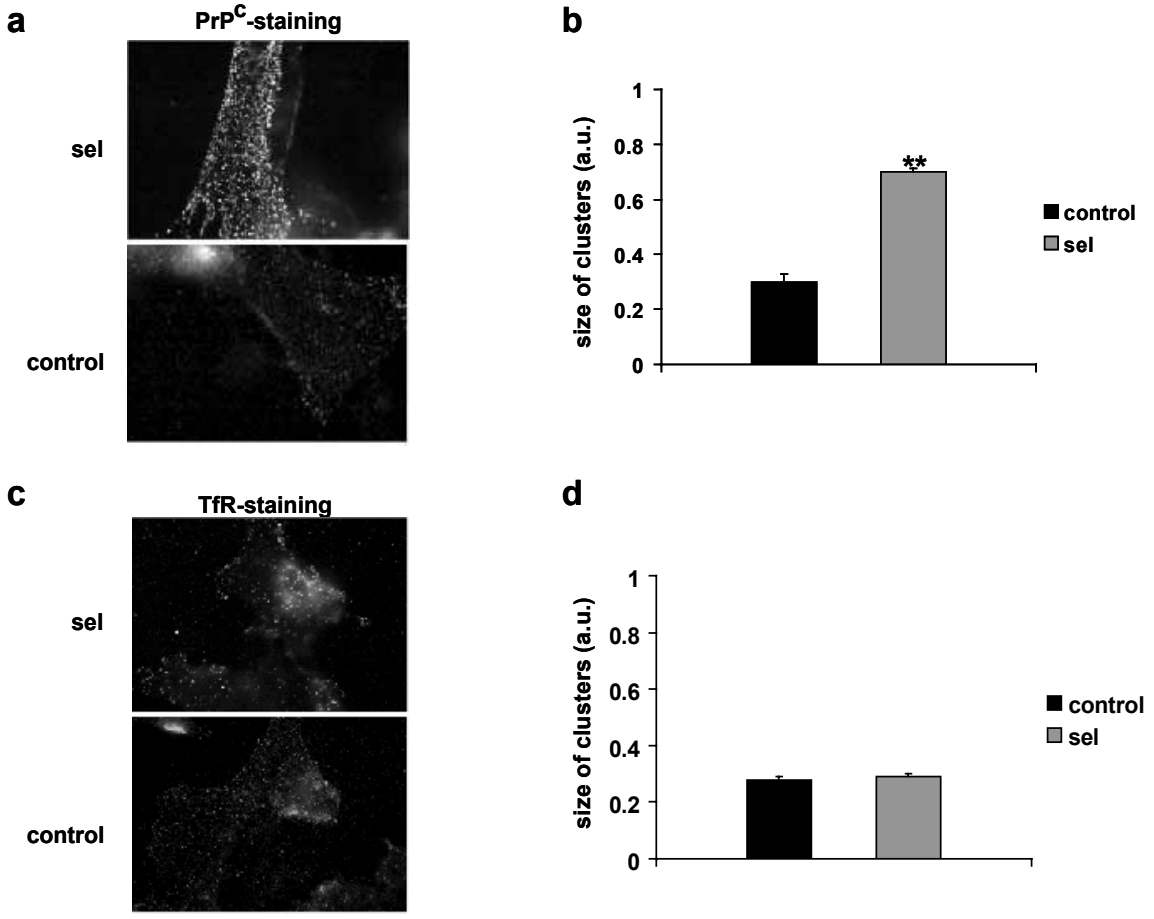


**Figure 11 increased DRM size in seladin-1 overexpressing cells**

Seladin-1 overexpression increases DRM size at the cell surface as determined by the antibody co-patching method. Living control SH-SY5Y neuroblastoma cells or overexpressing seladin-1 were incubated with antibodies against the DRM protein $PrP^c$ (**a**) or against the non-DRM protein TfR (**c**). Images show the immunofluorescence and phase contrast of representative examples in each condition. The graphs indicate the size of clusters observed for $PrP^c$ or TfR by immunofluorescence in arbitrary units (**b,d**). The data represent mean values and standard deviation from the analysis of 20 cells in each of three independent cultures per condition.

To determine the significance of the biochemical data obtained using cold detergent extraction in the context of intact, non detergent extracted cells, co-patching experiments[143] were performed in living cells using antibodies against the DRM-enriched protein $PrP^c$ and the non-DRM protein TfR. Control and seladin-1 overexpressing SH-SY5Y cells were incubated with the above antibodies and the size of $PrP^c$ and TfR clusters were determined by microscopy (**Fig 11a,c**). This study revealed a significant increase ($p<0.05$) in

the size of $PrP^c$ co-patches on the surface of seladin-1 overexpressing cells (0.7±0.06 arbitrary units/cluster) in comparison to control cells (0.3±0.1arbitrary units/cluster, **Fig 11b**). In contrast, the size of the non-DRM protein TfR clusters were not significantly altered by seladin-1 overexpression (**Fig 11d**). Quantitative analysis revealed that their average size was 0.29±0.05 and 0.28±0.05 arbitrary units/cluster in seladin-1 overexpressing and control cells, respectively. Based on these results, we conclude that seladin-1 specifically enhances DRM formation at the surface of living cells.

**Seladin-1 regulates DRM dependent plasminogen binding and activation**

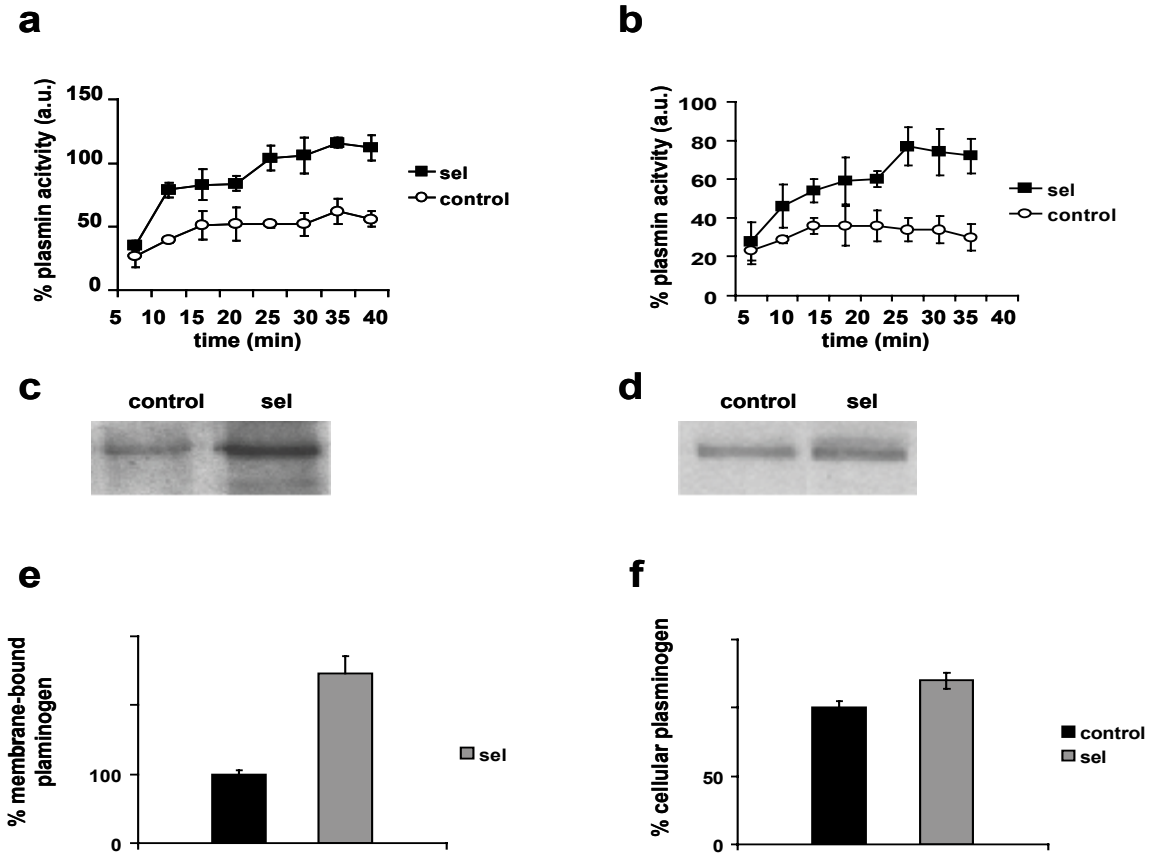


**Figure 12 The DRM-dependent plasminogen binding and plasmin activation rely on seladin-1 levels**

Plasmin activity (expressed in arbitrary units) was measured at the indicated times in membranes isolated from control and seladin-1 overexpressing SH-SY5Y cells (**a**). To monitor plasminogen binding exogenous plasminogen was added to the cellular membranes (**b**). Membrane extracts (**c,e**) and endogenous levels of cellular and membrane bound plasminogen were analyzed by Western blot (**d,f**) from control and seladin-1 overexpressing SH-SY5Y. Control: mock transfected SH-SY5Y cells; seladin-1: overexpressing SH-SY5Y cells. Data in all the graphs correspond to mean value and standard error from three independent SH-SY5Y cultures.

Given the influence of seladin-1 in DRM composition we reasoned that changes in its expression would affect DRM-dependent functions. Because plasminogen binding to the membrane leads to the activation of the Aβ degrading enzyme plasmin in a DRM-dependent manner[144], we decided to analyze the plasminogen content and plasmin activity in our experimental setup.

DRMs seggregate a major pool of the APP-β-secretase BACE1 from its non-DRM substrate APP, restricting APP-β-cleavage and Aβ production in cultured primary neurons[145]. in a first step, we therefore analyzed plasmin activity and plasminogen binding in conditions of seladin-1 overexpression. Endogenous plasmin activity was measured using a specific chromogenic substrate in membranes derived from control and seladin-1 overexpressing SH-SY5Y cells. Seladin-1 overexpressing cells exhibited a clear increase in plasmin activity (**Fig 12a**). To analyze plasminogen binding exogenous plasminogen was added to isolated membranes and plasmin activity was measured as above. Plasmin activity upon addition of exogenous plasminogen was higher in seladin-1 overexpressing cells than in control cells, indicating an increased ability of seladin-1 overexpressing cell-derived membranes to bind plasminogen (**Fig 12b**). This was further confirmed in endogenous conditions by Western blot of SH-SY5Y cell extracts. We observed significant differences in the amount of plasminogen bound to the membrane (247±14.7% mean ±SE, P=0.004, **Fig 12e**) while there were no changes in the endogenous levels of cellular plasminogen in control compared to seladin-1 overexpressing cells (**Fig 12f**).

### Seladin-1 overexpression reduces APP β-cleavage in cultured human neuroblastoma cells

Although much attention has been given to the effects that a reduction of membrane cholesterol has on APP processing, the consequences of higher cholesterol levels on APP processing are not known. Hence, we utilized control and seladin-1 overexpressing SH-SY5Y cells to determine how the induced cholesterol increase would affect BACE1-APP membrane segregation and their functional interaction. The flotation profile of BACE1 and

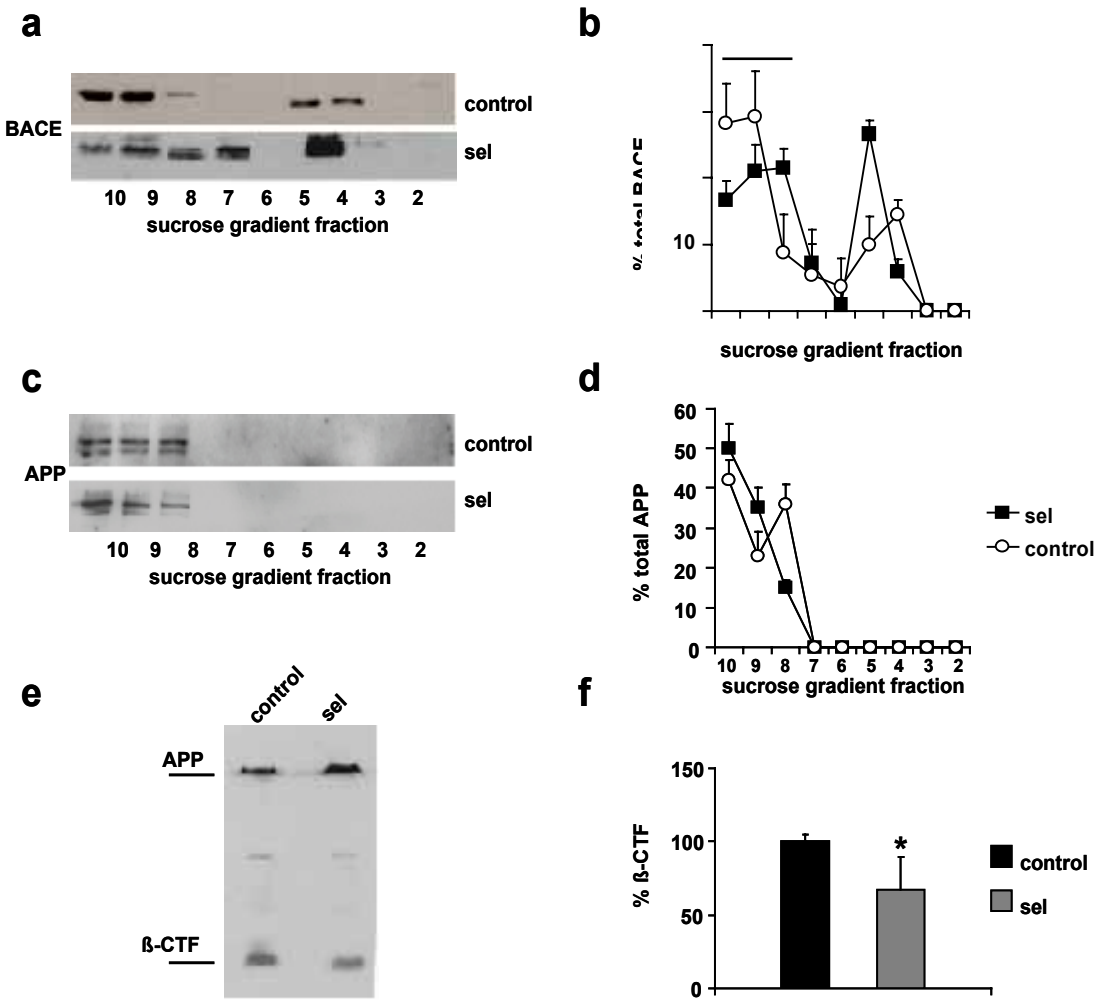


**Figure 13 Seladin-1 regulates BACE1-APP membrane segregation and APP-β cleavage**

Total extracts containing 100μg of protein from control and seladin1 overexpressing SH-SY5Y cells (**a,c**) were extracted in 1% Triton X-100 at 4°C and centrifuged in sucrose gradients. Fractions containing equal volume were collected according to increasing density and numbered from the lightest to the heaviest (2 to 10). APP and BACE1 distribution along the gradients were analyzed by Western blot using specific antibodies. a,c,e show representative examples. Graphs indicate the amount of APP and BACE1 in each fraction as a percentage of total APP and BACE1, respectively (**b,d**). APP β-cleavage was analyzed by Western blot of cellular extracts containing equal amount of protein from control and seladin-1 overexpressing SH-SY5Y cells as shown on Western blot (**e**). The graphs show the percentage of β-C-terminal fragment normalized to the amount of APP (**f**).

APP after Triton X-100 extraction at 4°C showed that while APP always remained in the heavy fractions more BACE1 was recruited in the light fractions (especially the DRM fraction 5) upon seladin-1 overexpression (**Fig 13a,c**).Quantitative analysis of the Western blots revealed that while

57.4±8.9% of BACE1 is in the APP containing fractions 10-9 in the control cells, the percentage diminishes to 35.6±4.3% in seladin-1 overexpressing cells (P=0.04, **Fig 13b**). Consistent with the enhanced membrane segregation of BACE1 from APP the generation of APP β-C-terminal fragment was significantly reduced (34%, P=0.04) in seladin-1 overexpressing cells (**Fig 13f**). Altogether these data demonstrate for the first time that high cholesterol levels decrease APP β-cleavage and that this is modulated by seladin-1.

### $A\beta_{40}$ and $A\beta_{42}$ ELISA

To confirm the results achieved by Western blot analysis we performed a ELISA using antibodies, that specifically recognize $A\beta_{40}$ and $A\beta_{42}$. In seladin-1 overexpressing cells the generation of both $A\beta_{40}$ and $A\beta_{42}$ were reduced to

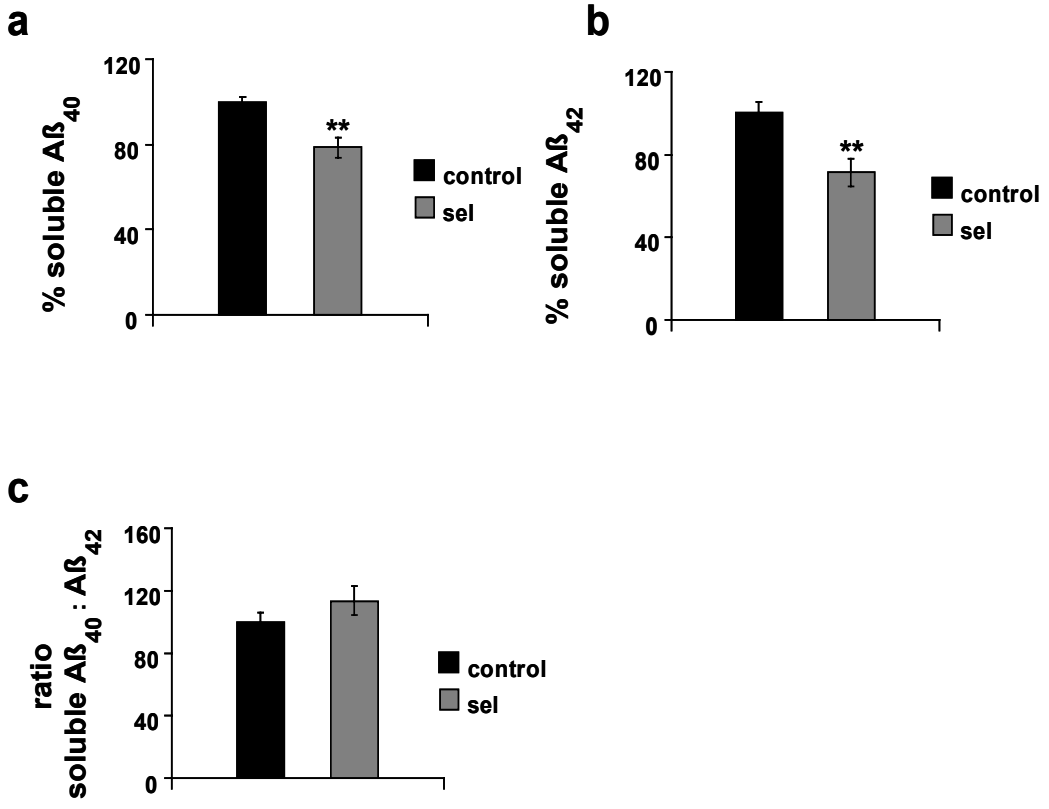


**Figure 14 Quantification of $A\beta_{40}$ and $A\beta_{42}$ in control and seladin-1 overexpressing cells**

In seladin-1 overexpressing SH-SY5Y cultures $A\beta_{40}$ (**a**) and $A\beta_{42}$ (**b**) was significantly decreased when compared to control cultures, whereas the ratio of $A\beta_{40}$ to $A\beta_{42}$ levels did not reveal significant differences between the two groups (**c**).

78.5±4.8 and 71.48±6.7%, respectively (**Fig. 14a,b**, P=0.001 and 0.003, respectively), whereas the ratio of $A\beta_{40}$ to $A\beta_{42}$ revealed no significant difference (**Fig. 14c**). These data emphasize the crucial role of seladin-1 protein in regulating Aβ generation and reconfirm a BACE-dependent mechanism for this effect.

**Functional mutagenesis of seladin-1 cDNA**

To determine the functionality of seladin-1 in the biosynthesis of cholesterol and to investigate possible partners involved in its activation and function, we mutated seladin-1 according to the published mutations found in desmosterolosis patients [4]. These mutations diminish the efficiency of seladin-1 to reduce sterols at the $\Delta^{24}$ position. If there is one or more essential binding partner(s) of seladin-1, it would be possible to induce a dominant negative effect by overexpressing a non-functional enzyme interacting with these partners and therefore inhibiting the binding of the functional protein and the

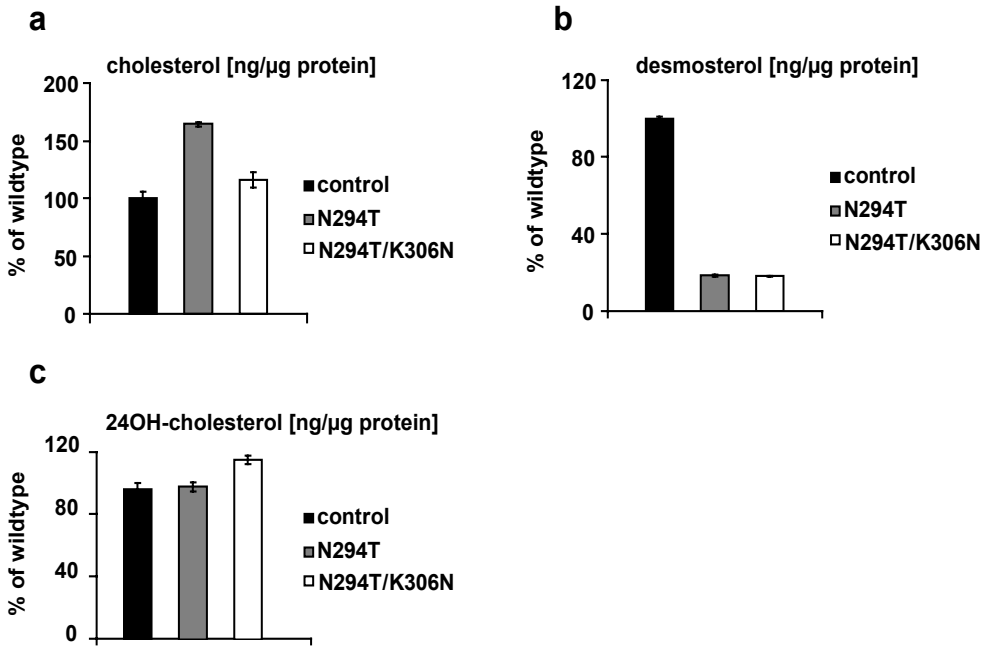


**Figure 15 Amount of different sterols in control and mutant seladin-1 (N294T, N294T/K306N) transfected cells**

Amount of cholesterol (**a**) desmosterol (**b**) and 24OH-cholesterol (**c**) in control, seladin-1 containing either single N294T or double N294T/K306N overexpressing SH-SY5Y cells. Significant differences in the two overexpressing cell (N294T, N294T/K306N) lines were detected in cholesterol and desmosterol levels when compared to control. No differences in total amount of the degradation product 24OH-cholesterol were observed.

conversion of the precursor desmosterol. Seladin-1 was cloned into an expression vector and mutated using the Qiagen Kit. One construct contained a single point mutation leading to a threonin replacing an asparagin at position 294. The second construct contained the asparagin at position 294 and a second mutation resulting in a lysin replacing an asparagin at position 306. In desmosterolosis patients, the single and the double mutation led to an inhibition of enzyme activity of about 80%, whereas the remaining 20% enzyme activity enabled the cells to reduce desmosterol to cholesterol[4]. Seladin-1 overexpressing SH-SY5Y cells and SH-SY5Y cells overexpressing the single and the double mutation constructs were analysed using gas chromatography-mass spectrometry. The sterol composition in these cells revealed a change in the cholesterol and desmosterol levels when compared to control cells. SH-SY5Y cells overexpressing the single (N294T) or the double (N294T/K306N) mutation showed a significant decrease in desmosterol levels (**Fig 15a**) and in parallel a significant increase in cholesterol amount (**Fig 15b**) when compared to control cells. These results suggest that the partial activity of the transgenes in addition to the endogenous levels of seladin-1 - which is obviously lacking in desmosterolosis patients - are sufficient to reduce desmosterol to cholesterol. Moreover, the levels of the degradation product 24OH-cholesterol (**Fig 15c**) did not change in any of the groups. This suggests that seladin-1 does not need a binding partner to be activated.

### Seladin-1 regulates membrane and cellular cholesterol levels in mouse brains

To determine to which extent the levels of brain cholesterol depend on seladin-1 we analyzed the effects of genetic seladin-1 depletion on steady-state cholesterol levels *in vivo*. The analysis of seladin-1 mRNA levels in the brain of wildtype mice, heterozygous mice with depletion of one (heterozygous) or knock-out mice with depletion of both (homozygous) seladin-1 alleles[94] revealed a gene-dose dependent reduction in the heterozygous mice compared to their wildtype littermates (43.8±3.3%, mean ±SE, P=0.009). There was no seladin-1 mRNA expression detectable in the

homozygous mice (**Fig 16a**). The brains of seladin-1 heterozygous mice exhibited an average reduction of 29% in the membrane (**Fig. 16b**, P=0.02) and 15% in total cellular cholesterol (**Fig 16c**, P=0.042) compared to wildtype brains. Furthermore, cholesterol amount was undetectable in the homozygous mouse brains (**Fig 16b,c**). To characterize the effect of seladin-1 expression on cholesterol metabolism we analyzed the effects of seladin-1 depletion on the levels of the cholesterol precursor desmosterol and of the major degradation product of cholesterol in the brain, 24OH-cholesterol. Desmosterol was 5.7- (P=0.012) and 50-fold (P=0.00006) increased in heterozygous and homozygous mouse brains, respectively (**Fig 16d**), indicating that desmosterol accumulates upon seladin-1 deficiency. Moreover, decreased seladin-1 expression led to a significant reduction in the catabolic product 24OH-cholesterol in heterozygous (24.6±4.3%, mean ±SE, P=0.017) and knock-out mice (97.6±0.47%, mean ±SE, P=0.0004, **Fig 16e**) compared to control brains. Altogether, these results confirm the observations from the *in vitro* studies with seladin-1 overexpressing SH-SY5Y cells overexpressing seladin-1 showing for the first time the key role of seladin-1 in the regulation of brain cholesterol metabolism and homeostasis *in vivo.*

**Seladin-1 regulates Aβ generation *in vivo***

To determine whether the alterations in membrane cholesterol (shown in Figure 15) affect the levels of Aβ, we peformed an ELISA to measure Aβ peptides in brain homogenates. Because the endogenous mouse Aβ levels are extremely low in young wildtype mice as previously reported[146], we analyzed aged-matched wildtype and seladin-1 heterozygous mice overexpressing the SwAPP mutations[147] (SwAPP/seladin-1). Both $A\beta_{40}$ (270±31%, mean ±SE, P=0.024, **Fig 17a**) and $A\beta_{42}$ (159±0.3%, mean ±SE, P=0.015, **Fig 17b**) levels were significantly higher in SwAPP mice with a seladin-1 deficiency when compared to SwAPP littermates, whereas the ratio

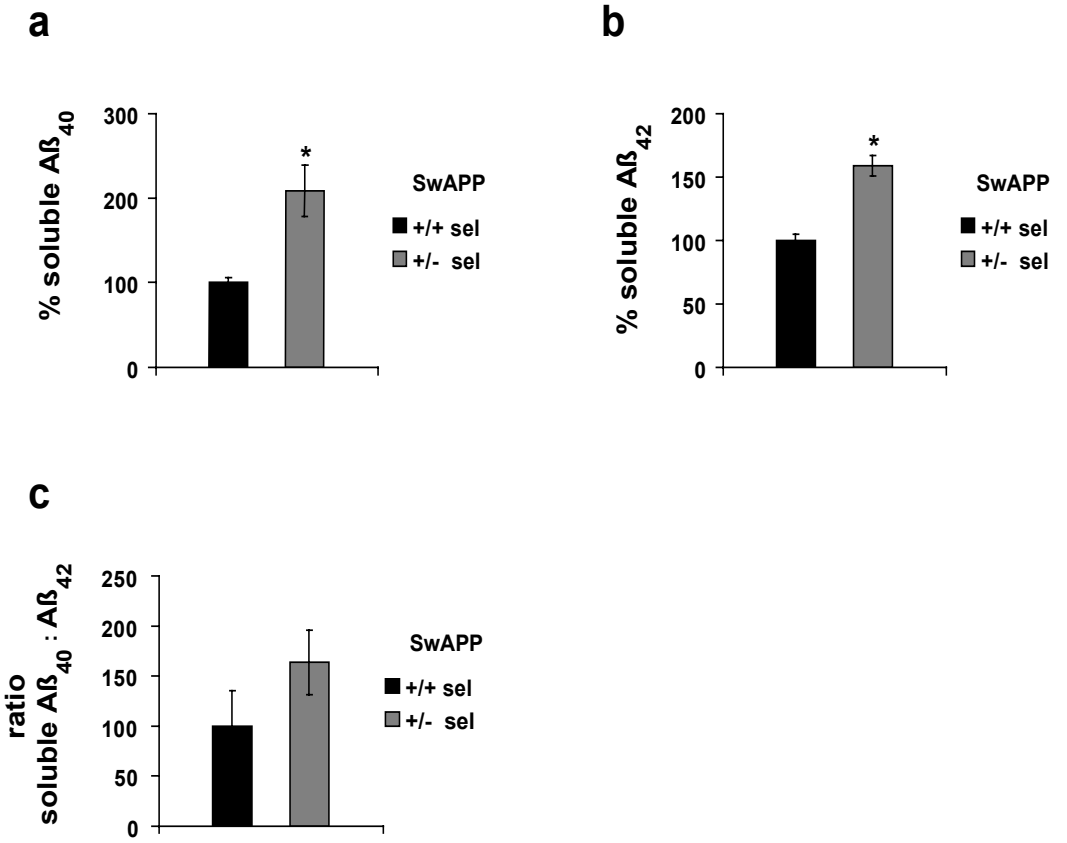


**Figure 17 Levels of $A\beta_{40}$ and $A\beta_{42}$ in SwAPP/sel mouse brains**

Quantification of $A\beta_{40}$ and $A\beta_{42}$ in brains of seladin-1 wildtype and heterozygous mice with the simultaneous overexpression of SwAPP confirmed that seladin-1 deficiency leads to higher Aβ steady-state levels. Brain $A\beta_{40}$ levels showed a significant increase in heterozygous (SwAPP/+/- sel) mouse brains compared to seladin-1 wildtype littermates expressing solely the SwAPP transgene (SwAPP/+/+ sel) (**a**). Levels of soluble $A\beta_{42}$ were also significantly increased in heterozygous (SwAPP/+/- sel) mouse brains (**b**). The ratio of $A\beta_{40}$ to $A\beta_{42}$ levels revealed no significant differences between the two genotypes (**c**).

of $A\beta_{40}$ to $A\beta_{42}$ did not significantly differ between the two groups (136±31%, mean ±SE, **Fig 17c**). These data suggest that seladin-1 deficiency favored the β–cleavage of APP and led to a pronounced increase of Aβ generation *in vivo*. These data show unequivocally that seladin-1 deficiency leads to an increased production and accumulation of Aβ in the brain.

**Generation of seladin-1 overexpressing mouse line**

The aim of the project was to generate an *in vivo* model which will confirm the neuroprotective role of seladin-1 results demonstrated *in vitro.* This model should allow to reproduce the data showing the role of seladin-1 in cholesterol biosynthesis and in DRM organization and function.

To generate seladin-1 overexpressing mice, the cDNA of human seladin-1 was cloned into the BamHI/XhoI site of the plasmid pEX-12. Expression of the transgene was under the control of the neuronal mThy1.2-promoter. Before injection into the pronucleus of oocytes the construct was sequenced, linearized and purified. Mice were tested for the presence of the transgene by PCR of mouse tail genomic DNA. For the PCR reaction the sense primer annealing to the mThy1.2 promoter (O-340(mThy1) ATCATGTGCTCCGTGGATC) and the reverse primer annealing to the 5' end of seladin-1 (0-339-selR GCCGCTGGGACTCGTGGGTGAACTT) were used. The PCR product was analysed on a 0.7% agarose gel and the predicted band for a positive result was 900bp. The first generation of mice (F1) tested for the human seladin-1 cDNA showed that the trangene was transmitted to the progeny (**Fig 18**). In order to detect the next step in the production of the trangene we performed a Northern blot analysis of total RNA isolated from PCR positve seladin-1 transgenic mice and their wildtype littermates at the age of 5 weeks.

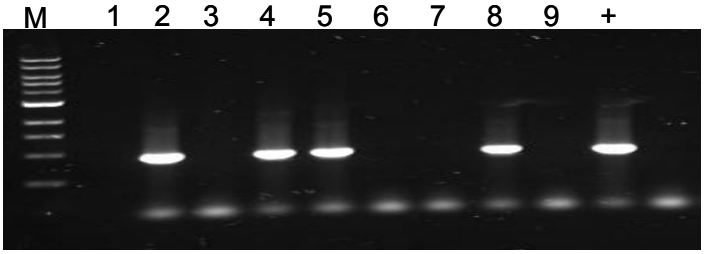


**Figure 18 Screening of seladin-1 trangenic mice using PCR**

Screening of the F1 generation of trangenic mice line containing human seladin-1 gene using PCR. M: marker 1kB DNA ladder marker ; lanes 2, 4, 5, 8, 9 PCR positive mice for seladin-1 trangene; Lane +: positive control using the original plasmid.

Northern blot applying a radioactive randomly labelled probe using the seladin-1 as template was performed to detect the mRNA of the transgene. Human seladin-1 cDNA was used as positive control. All the positive mice detected on the DNA level were negative for mRNA in the Northern blot, suggesting that the trangene is not transcripted (**Fig 19a**). A Western blot conclued that the mice did not express the exogenous seladin-1, although the

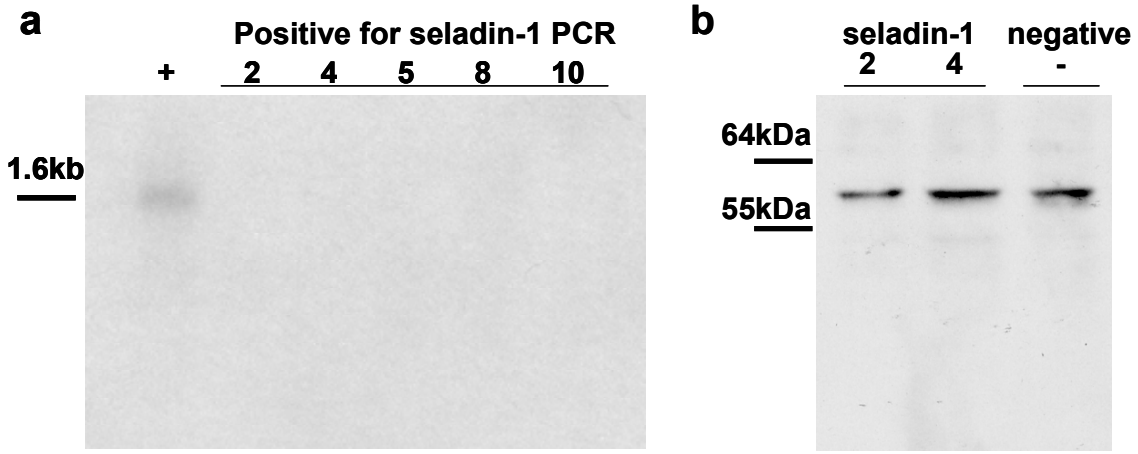


**Figure 19 Northern blot and Western blot of transgenic seladin-1 mice**

Northern blot of the PCR positive mice (2,4,5,8,10). No bands are visible at the size of the positive control using the human seladin-1 cDNA as template. None of these mice show expression of the transgene at the mRNA level (**a**). Western blot probed with anti seladin-1 specific antibody (**b**). 40µg total protein was loaded per lane. No differencies were found between seladin-1 PCR positive mice and wildtype mice. These data suggest that seladin-1 mRNA and protein is not present in the transgenic mice.

mice were positive in the PCR reaction (**Fig 19b**). We also performed an immunohistological staining using a specific anti-seladin-1 antibody (Ab40) (**Fig 20**). The result of the staining confirmed the absence of the transgene

observed in the Northern blot. In light of these accumated negative data we concluded that these mice did not express the transgene and therefore were not further investigated.

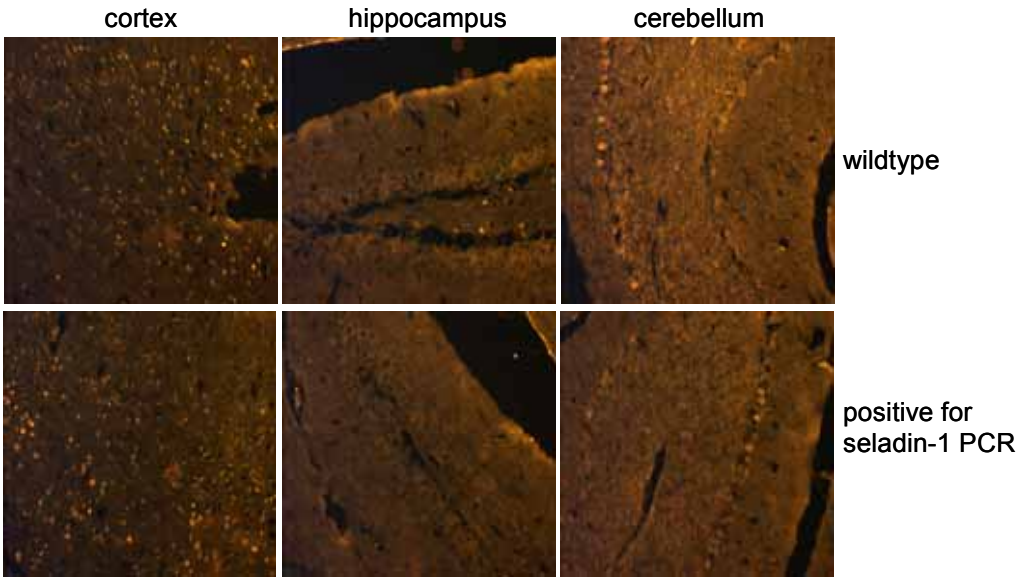


**Figure 20 Cryosections of seladin-1 transgenic mice stained with anti Ab40 antibody**

Immunohistochemistry of brain sections of wildtype and seladin-1 PCR positive mice. Staining with the anti seladin-1 specific antibody (Ab40) in cortex hippocampus and cerebellum; no differencies are visible, suggesting that human seladin-1 protein is not produced although the mice were PCR positive for the trangene.

### Generation of a seladin-1 (HA) overexpressing mouse line

To generate seladin-1 (HA) overexpressing mice, the cDNA of human seladin-1 containing an HA tag at the 3' end was cloned into the BamHI/XhoI site of

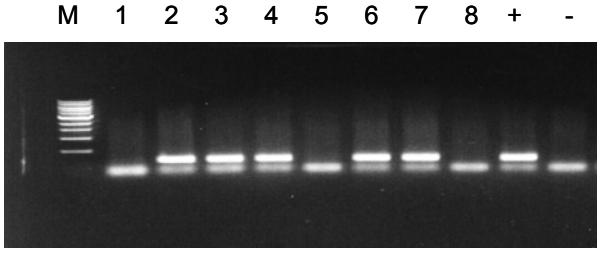


**Figure 21 Screening of seladin-1 HA trangenic mice using PCR**

PCR screening of the F1 generation of transgenic mice containing human seladin-1 gene tagged with an haemagglutinin sequence at the 3' end. M: marker 1kB DNA ladder marker lanes 2, 3, 4, 6, 7 PCR positive mice for seladin-1(HA) transgene; Lane +, -: positive and negative control, respectively.

the plasmid pEX-12. Expression of the transgene was under control of the neuronal mThy1.2-promoter. Mice were tested as previously described for the presence of the transgene by PCR of mouse tail genomic DNA using the same primers. The construct was sequenced to confirm the presence of the HA tag in frame at the 3' end of the seladin-1 cDNA. Several mice were found PCR positive (**Fig 21**).

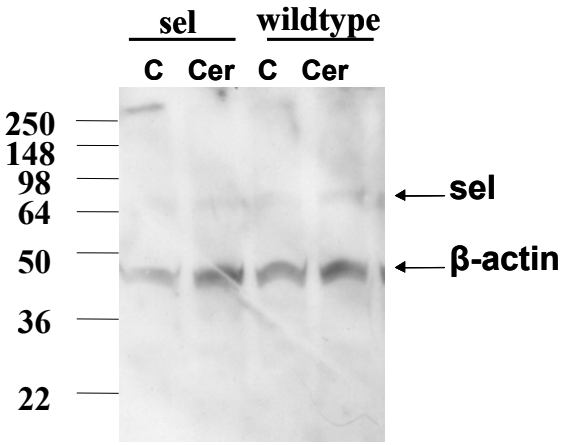


**Figure 22 Western blot of seladin-1(HA) transgenic mice probed with anti HA antibody**

Western blot of seladin-1(HA) and wildtype mice probed with anti haemagglutinin antibodies. No HA staining was detected suggesting that the transgene was not expressed. The β-actin band shows that the same amount of total protein was loaded.

This finding lead us to the next step in the characterisation of the mouse line performing a Western blot. However, the membranes probed with anti-HA antibodies did not reflect the result found in the DNA level (**Fig 22**).

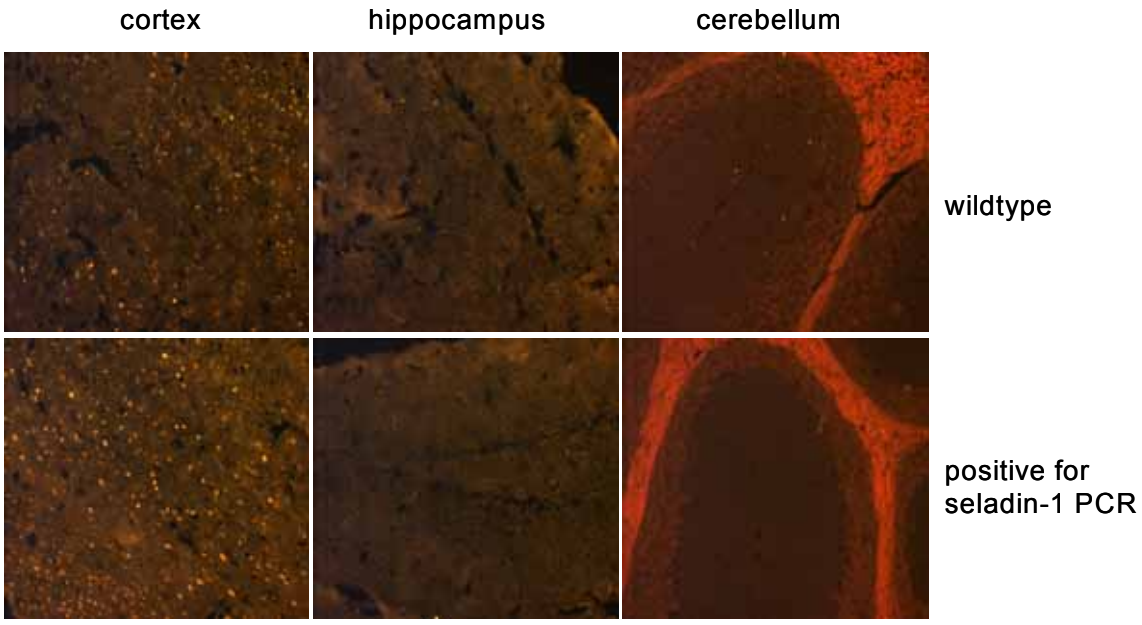


**Figure 23 Paraffin sections of seladin-1 transgenic mice stained with anti HA antibody**

Immmunohistochemistry of brain sections of seladin-1(HA) and wildtype mice. No differencies between the transgenic and the wildtype mice were detected.

Furthermore, immunohistochemical staining (**Fig 23**) revealed no differences between the seladin-1(HA) and the wildtype mice. These last data conducted us to discard the second trangene defining as unserviceable for our proposition.

**Generation of a seladin-1 EGFP overexpressing mouse line**

To generate mice overexpressing seladin-1 EGFP, the human seladin-1 cDNA was fused to an enhanced green fluorence protein (EGFP) tag at the 3'end cloned into the XhoI site of the plasmid PrP-MO. Expression of the transgene was under the control of the neuronaly active PrP-promoter. The construct was sequenced to confirm the presence of the EGFP tag in frame at the 3' end of the seladin-1 cDNA. Mice were genotyped as previously described for the presence of the transgene by PCR of mouse tail genomic DNA. The primers used were designed to cover the 3'end of seladin-1 containing the EGFP-tag with the forward primer (pSelEGFP,R1:CTTGAACACCACCCAGG) and the 5' end of the PrP-MO plasmid with a complementary reverse primer (Prp3(5-3): GGTTCTCATTCTTGCTTCTC). The PCR revealed some positive mice, confirming the introduction of the transgene into the genome (**Fig 24**). We characterized the PCR positive mice using Western blot and immunohistochemical analyses as described above. No seladin-1 transgene could be detected in these mice. Based on the fact that in both cases the results were negative we concluded that also in this case the transgenic mouse lines produced were useless.for our prupose.

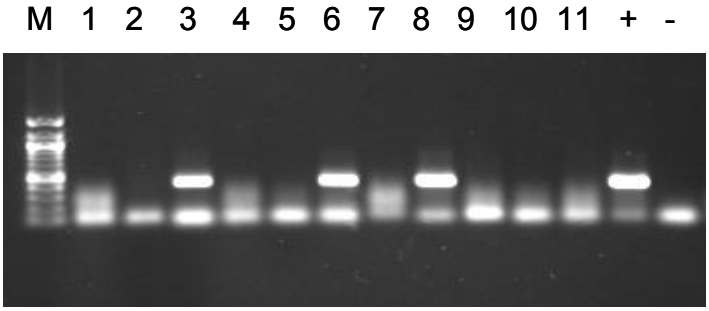


**Figure 24 Screening of seladin-1 EGFP mice using PCR**

PCR pictures using primer on seladin-1 EGFP tagged cDNA and the plasmid PrP-MO. M: 2 log marker; lane 3, 6, 8, are PCR positive mice for human seladin-1 cDNA; lane + and – are positive and negative controls, respectively.

# Discussion



### Anti apoptotic function of seladin-1

In 2000, Greeve and colleagues identified seladin-1, the selective Alzheimers disease indicator-1, a protein that shares domain homologies with a gene family of FAD-dependent oxidoreductases. This study showed that seladin-1 mRNA was highly expressed in neuronal cells throughout mammalian brains, and its expression was low in neurons within selectively vulnerable regions of AD brains[5]. Reduced levels of seladin-1 mRNA in affected areas of AD brains were related to reduced amounts of seladin-1 mRNA within remaining neurons and did not simply reflect neuronal cell loss. Reduced brain tissue levels of seladin-1 mRNA were paralleled by reduced levels of seladin-1 protein in affected regions. The reduced expression of seladin-1 in vulnerable brain regions in AD is in line with results of previous studies on antioxidant enzyme activities in AD brains; the activities of catalase and superoxide dismutase in temporal cortices from AD brains were lower when compared with temporal cortices from non-demented normal controls[148]. Differential activity of antioxidant enzymes in nerve cell populations may be one important cause for the selective resistance of specific cells against degeneration by toxic factors such as Aβ, which is distributed throughout the brain in both vulnerable and protected regions. Previous experiments showed that overexpression of seladin-1 in human H4 neuroglioma cells protected these cells from apoptosis induced by oxidative stress, and high expression of endogenous seladin-1 was associated with resistance against Aβ-induced toxicity. Moreover, functional expression of seladin-1 in H4 cells resulted in the inhibition of caspase-3 activation after either Aβ-mediated toxicity or oxidative stress and protected the cells from apoptotic cell death. In apoptotic cells, however, endogenous seladin-1 was cleaved to a 40 kDa derivative in a caspase-dependent manner[5]. In 2002, Iivonen and colleagues studied the relative transcription of seladin-1 in temporal and occipital cortices in demented and non-demented subjects and found a decrease in the transcription of seladin-1 in temporal cortex when compared to occipital cortex in AD[123]. Moreover, the seladin-1 transcription was inversly associated with

neuritic plaques and neurofibrillary tangles. In addition, these authors investigated the changes in seladin- 1 transcription in relation to amyloid accumulation and aging using a transgenic mouse model of AD. Results from these studies revealed that the transcription of mouse seladin-1 fluctuates during aging and this fluctuation was enhanced in double APP/PSEN-1 transgenic mice[123]. In 2004, Wu *et al*. identified seladin-1 as a key mediator of Ras induced senescence[1]. Activated Ha-RasV12 (Ras) is usually associated with cancer, but it also produces paradoxical premature senescence in primary cells by inducing reactive oxygen species followed by accumulation of tumour suppressors p53 and p16INK4a[149]. They found that following oncogenic and oxidative stress, seladin-1 binds p53 amino terminus and displaces E3 ubiquitin ligase mdm2 from p53, thus resulting in p53 accumulation. Additionally, seladin-1 was shown to cause the bypass of Ras-induced senescence in rodent and human fibroblasts, and allowed Ras to transform these cells. Wildtype seladin-1, but not its mutant form disrupted the association with p53 and suppressed the transformed phenotype. The same mutants were also inactive in directing p53-dependent oxidative stress response. These results determined an additional role for seladin-1 in integrating cellular response to oncogenic and oxidative stress. We overexpressed wildtype seladin-1 in human neuroblastoma SH-SY5Y cells and consistent with previous findings[5], these cells revealed a greater resistence against oxidative stress induced by $H_2O_2$. We also analyzed the two additional cultures, which carry point mutations in the seladin-1 construct at the presumed cleavage sites of either caspase-3 or caspase-6 (474 and 1256 cultures) respectively. These mutations were proposed to block the caspase activity. Our results, after inflicting oxidative stress, show that the expression of wildtype or 474 mutated seladin-1 significantly protects the cells against $H_2O_2$ toxicity, whereas the 1256 mutation did not confer greater resistance to the cells. The point mutation at the 1256 position is located in the p53 binding site of the protein[1]. Therefore it is possible that an amino acid substitution in this region prevents p53 binding and defeats the anti apoptotic function of the protein. This explanation is supported by the fact that the survival of 1256 culture did not show any statistical differences compared to control cells.

Depending on the apoptotic inductor utilized, various mechanisms are involved in the apoptotic cell death. While $H_2O_2$ induces oxidative stress in a general manner, etoposides block the topoisomerase II activity, an enzyme crucial for DNA replication. 14 hours after etoposide treatment seladin-1 overexpressing cultures exhibited a significantly larger number of surviving cells than the control cultures. In this experiment, the surviving rate of the 474 culture was smaller compared to the wildtype seladin-1 overexpressing cells, but more cells survived the insult when compared to control cells, even if not statistically significant. Independent of the apoptotic insult, the percentage of surviving cells in the 1256 culture was similar to those in the control cultures, suggesting that this mutation affected the anti-apoptotic function of seladin-1. All cell lines were non clonal lines with different percentages of transfected cells stably expressing the transgene. In the seladin-1 overexpressing culture 30% of the cells overexpressed the transgene, whereas in the 474 and 1256 cultures only 22% and 16% of the cells were shown to express the transgene on IHC level, respectively. The seladin-1 overexpressing culture consistently appeared to be the most robust and fastest growing culture, whereas 474 cells also seemed to proliferate more rapidly than the 1256 and the control cultures. These data are in agreement with published results, showing an anti-apoptotic and growth promoting role for seladin-1[1,150]. Resistance of cultured cells to Aβ toxicity was previously found to be attributable to the transcriptional activation of antioxidant enzymes, including glutathione peroxidase or catalase[78,151]. Greeve *et al*. extended that proposal by adding seladin-1, which may function in concert with these enzymes in protecting cells from oxidative stress and Aβ toxicity. In our system, the overexpression of neither wildtype nor mutated seladin-1 in SH-SY5Y cells resulted in a significantly higher resistance against Aβ induced toxicity when compared to control cells. A general trend, however, was observable, suggesting that a smaller number of cells underwent apoptosis in seladin-1 and 474 cultures. In an additional experiment we could show that the endogenous level of seladin-1 in wildtype SH-SY5Y cells was upregulated after induction of apoptosis. These results are consistent with previous observations, where seladin-1 transcription was found to be up-regulated in mouse N2a cells induced to undergo apoptosis

with okadaic acid[123]. Taken together, we conclude that seladin-1 has an anti-apoptotic role *in vitro*. It is upregulated by apoptotic stimuli and protects the cells against apoptotic cell death induced by different inductors.

Intracranial injections of seladin-1 overexpressing cells in c57Bl/6 mice were performed to examine the effect of elevated seladin-1 levels on cell survival *in vivo*. Earlier studies showed that seladin-1 is upregulated in different types of tumors: Expression analysis in benign functioning adrenocortical adenomas reveal that seladin-1 mRNA was overexpressed in the adenoma tissue of 14 patients with Cushing's syndrome in comparison to the adjacent nontumorous adrenal gland[150]. Di Stasi *et al*. found an elevation of seladin-1 gene expression in melanoma metastases that was associated to resistance to oxidative stress-induced apoptosis[152]. Given that seladin-1 overexpression can protect cells against apoptosis *in vitro*, we tested whether seladin-1 could also be protective under conditions, where external physiological factors (i.e. components of the immune system) are the inductors of the apoptotic insults. We expected that seladin-1 overexpressing SH-SY5Y cells are more resistant against the defensive mechanisms of the murine host. Eventhough the survival of seladin-1 oveexpressing cells was higher four days after implantation, tumors has developed equally four weks later. We could not detect any apparent differences in tumor growth or profile between seladin-1 overexpressing and control SH-SY5Y cells. Because the brain is an immune-privileged organ, this can be explained by the fact that the immunosystem of the brain might not be potent enough to protect the host against extraneous cells that are thoroughly immortalized. In this scenario the surviving rate of the injected SH-SY5Y cells would be independent of seladin-1 overexpression, since there is no requirement for an anti-apoptotic function. With our experiments it still remained elusive as to which role seladin-1 plays in terms of oncogenic signaling and Ras-induced senescence. Wu and colleagues in 2004 could show that injections of seladin-1 deficient fibroblasts with depleted seladin-1 expression in immuno-suppressed nude mice resulted in tumorous proliferation of the cells two weeks after inoculation, indicating that they were oncogenically transformed[1]. In contrast, cells with normal levels of seladin-1

failed to proliferate as tumours. This observation is somehow contradictive to previous findings, where seladin-1 was hightly upregulated in tumor cells[152].

**Production of a mouse model overexpressing seladin-1**

Based on our findings concerning the role of seladin-1 *in vitro* and *in vivo* we next tried to generate mice overexpressing seladin-1 to study the effect of seladin-1 overexpression *in vivo*. To achieve our goal we encountered a sequence of problems which we are trying to solve. All experiments of determining a transgenic overexpression led to negative results indicating that the seladin-1 transgene was not expressed in these mouse lines even though PCR screenings for detection of the insertion of the transgene were positive. The reason for lack of transgenic expression were not further investigated. Results from our laboratory show that the promoters used (mThy1.2 and PrP) are functional, because they drive the expression of other transgenes in transgenic mice[48,61]. Seladin-1 is normally expressed in all brain neurons. To avoid the possibility to miss low levels of transgene expression in neurons of our mice we also tried to generate mouse lines expressing an HA-tag or EGFP fused to the seladin-1 cDNA. Again, no transgene expression could be found in these mice. The lack of transgenic seladin-1 expression in these mice led us to speculate that an elevation of seladin-1 levels during neurogenesis can not be tolerated, probably because of the interferance with normal elimination of excessive neurons of with cholesterol metabolism. Therefore, we are now trying, as a last resort, to use a tet-on system to be able to switch on the expression of seladin-1 in neurons at an adult age, thus eliminating a possible obstruction of seladin-1 function in neuronal development.

**The role of seladin-1 in cholesterol biosynthesis, raft composition and function, Aβ generation and AD pathology**

Desmosterolosis is a rare autosomal recessive disorder characterized by multiple congenital anomalies. Patients with desmosterolosis have elevated levels of the cholesterol precursor desmosterol, in plasma, tissue and cultured cells. The only two known patients homozygous for these mutations died shortly after birth and in early childhood[125].

In 2001, Waterham *et al*. published that this abnormality suggested a deficiency of the enzyme 3β-hydroxysterolΔ24-reductase (DHCR24), also named seladin-1. Isoprenoid/cholesterol biosynthesis starts with the $C_2$ compound acetyl-CoA, which, in a series of different enzyme reactions, is converted to isopentenyl-pyrophosphate, the basic $C_5$ isoprene unit used for the synthesis of all subsequent isoprenoids[153,154]. The first intermediate committed to the production of sterols is $C_{30}$ squalene, which is converted to lanosterol. To eventually produce cholesterol from lanosterol a series of enzyme reactions is required. Consequently, two major routes involving the same enzymes have been proposed, the Bloch synthesis pathway with desmosterol as the ultimate precursor of cholesterol and the Kandutsch-Russell pathway with 7-dehydrocholesterol as the direct precursor. Seladin-1 is crucial for cholesterol biosynthesis, as it is the mediating enzyme between the two pathways – reducing the Δ24 double bond of the bloch-pathway precursors to finally produce cholesterol. Bloch synthesis occur principally during the development and at young age, whereas the Kandutsch-Russell pathway is active in adulthood.

Sterol analysis in seladin-1 overexpressing SH-SY5Y cells revealed dramatically reduced desmosterol levels and significantly elevated membrane and cellular cholesterol levels when compared to control cells. These results gave evidence for the bioactivity of the transgene and suggested that seladin-1 is the limitting factor in modulation and regulation of cholesterol biosynthesis.

Cholesterol is a prominent modulator of the integrity and functional activity of physiological membranes - and hence plays an essential role in the regulation of synaptic function and membranous signal transduction pathways. Within the plasma membrane, cholesterol is strictly organized into structual and kinetic pools such as leaflet domains and lipid rafts[155]. Lipid rafts are specialized plasma membrane micro-domains, so called detergent resistant membrane domains (DRMs of rafts), floating on the exofacial side of the membrane bilayer[156]. Regarding their physicochemical and structural characteristics, they clearly differ from the adjacent non-raft lipid environement. They are highly loaded with glycosphingolipids, choelsterol and

multiple membrane proteins and play a crucial role in cell-signaling pathways[157].

Biochemical analysis of DRMs prepared from seladin-1 overexpressing SH-SY5Y cells revealed a significant change in raft composition and function. DRM specific proteins (like $PrP^c$ and flotilin 1), and lipids (like cholesterol, sphingomyelin and the ganglioside GM1) also showed elevated levels in the fractions corresponding to DRMs when compared to control cells. Co-patching experiment revealed that the size of DRMs in seladin-1 overexpressing cells was greater than in control cells. These data imply that the composition of rafts is determined by the amount of membrane and/or cellular cholesterol and that the expression level of seladin-1 can modulate these cholesterol concentrations and therefore determine raft composition and size. Functional analysis revealed a higher plasmin activity in seladin-1 overexpressing cells and the ability of plasminogen to bind to the membrane was significantly increased in these cells. These results suggest that the amount of cholesterol in a membrane determines not only the composition and the size of DRM's but also their functional properties.

A large body of literature indicates that alterations in cholesterol levels affect APP metabolism. The two important enzymes involved in amyloidogenic APP processing, BACE and the $\gamma$-secretase, were found to reside within DRMs of the late Golgi and endosomes[158]. APP, however, is found exclusively in non-raft membrane compartiment. Whether the membrane or cellular cholesterol levels play the crucial role in affecting APP processing has not yet studied to date *in vivo*. Serveral studies in the last years could show that reducing cholesterol resulted in increased membrane fluidity and shifted APP processing toward the APPs$\alpha$ pathway. The common observation in these studies was that lowering cholesterol levels resulted in a strong decrease in A$\beta$ production[159,160]. Others proposed that lipids, by participating in producing raft domains, might build an invisible boundary, corralling the $\gamma$-secretase complex and BACE away from their substrate, APP. Their surveillance was that moderate lowering of cholesterol led to an increased $\beta$-cleavage and

elevated Aβ levels in primary neuronal cultures.[145] Consistently, these alterations also resulted in diminished activity of the Aβ degrading enzyme plasmin, which is normally produced in these domains[161]. Our data revealed clearly that APP processing was affected in seladin-1 overexpressing cells. We found reduced β-CTF generation in seladin-1 overexpressing cells that exhibited elevated cholesterol concentrations and the production of Aβ was significantly decreased in these cells when compared to control cells.

These findings are consistent with the hypothesis that elevated cholesterol levels and therefore greater DRMs immobilize the β-secretase within the lipid rafts and prohibit its interaction with APP leading to a decrease in β-cleavage of APP, an integral membrane protein that does not reside within rafts. We therefore put forward the idea that BACE1 in cholesterol-rich raft domains may represent an inactive pool of the protein, at least in terms of APP cleavage, which can be delivered when required to soluble domains where APP resides. In support of this view, a mild reduction of membrane cholesterol results in more BACE1 in the soluble fractions, higher BACE1-APP colocalization and enhanced β-processing, as was shown in a cell culture system[145].

The seladin-1 knock-out mice were published in december 2003 by Wechsler and co-workers. These mice are viable even though almost no cholesterol was found in plasma and tissue of three months old knock-out mice[94]. In our colony, homozygous mice were born to the published frequency of about 15%, but these mice, however, were dramatically smaller in size and extremely weak under normal husbandary conditions, and most of them died before reaching the age of 3 weeks, probably because of the inconsistency of vertebrate life with total lack of cholesterol or due to insufficient maternal care. The heterozygous knock-out mice in our colony developed normally and had no problem of health, fertility or longevity (up to 16 months). In this study we sacrificed the only two seladin-1 knock-out mice that were born in our colony, three weeks after birth and compared them to their heterozygous and wildtype littermates. We found a gene-dose dependent effect: The heterozygous mice exhibited a 50% reduction of seladin-1 expression on mRNA level. In the knock-out mice, seladin-1 expression was abolished. Next, we could show

that modulated seladin-1 expression influeced membrane and cellular cholesterol levels and cholesterol homeostasis in the mouse brains: In seladin-1 knock-out mice cholesterol undetectable. As a consequence of abolished seladin-1 expression, desmosterol was not sufficiently catabolized in these mice, resulting in vast amounts of the accumulated choelsterol precursor in knock-out brains. According to the negligible levels of cholesterol, only minor concentrations of the oxysterol 24OH-cholesterol was detected in the knock-out mice. Heterozygous mice with 50% less seladin-1 expression exhibited a significant reduction of membrane and cellular brain cholesterol, and considerablely elevated concentrations of desmosterol. In addition, a non-significant reduction of the catabolic product 24OH-cholesterol was observed in brains of heterozygous mice. Regarding the findings that overexpression of seladin-1 led to decreased Aβ production in our study and taking into account that the reduction of cholesterol *in vitro* resulted in increased Aβ generation as previously demonstrated[145], we crossed the seladin-1 deficient mice with mice, overexpressing the human APP carrying the Swedish (Sw) mutation (SwAPP mice)[162]. This mutation leads to an increased β-cleavage of transgenic APP and therefore resulting in elevated Aβ levels in these mice that develop the first Aβ deposits as early as 6 months after birth in the cerebral cortex. As expected, no seladin-1 knock-out mice survived, overexpressing the SwAPP. Probably vbecause of an additive effect of seladin-1 knock-out and Sw mutation. Nevertheless, we could show for the first time, that the depletion of seladin-1 in heterozygous knock-out mice overexpressing SwAPP results in increased brain amyloidogenic APP processing and in significantly augmented $A\beta_{40}$ and $A\beta_{42}$ generation when compared to wildtype seladin-1 SwAPP mice. Because seladin-1 is down-regulated in vulnerable areas of brains in AD patients [5] it is reasonable to think that low levels of seladin-1, promoted by yet to be identified causes, are responsible for the membrane cholesterol reduction found in such brains[144]. This would consequently lead to Aβ accumulation via a combination of increased APP amyloidogenic cleavage and possibly reduced activity of Aβ degrading enzymes like plasmin. Moreover, the observation of unchanged ratios of $A\beta_{40}$ and $A\beta_{42}$ levels supports the involvement of a BACE-mediated

mechanism. Furthermore, our data of a reduction of cholesterol catabolites in seladin-1 deficient mouse brains are supported by a study showing that cholesterol degradation products, especially 24OH-cholesterol, inhibit the production of Aβ in neurons by a liver-X-receptor (LXR) dependent mechanism[163].

In conclusion, our results establish a role of seladin-1 in the formation of DRMs and suggest that seladin-1-dependent cholesterol synthesis may be involved in lowering Aβ levels. Furthermore, pharmacological increases in seladin-1 activity may be a novel Aβ-lowering approach for the treatment of AD.

**Outlook**

In conclusion, our results show that seladin-1 plays an important role in apoptosis and in cholesterol metabolism *in vitro* and *in vivo.* The link to AD was found in the ability of seladin-1 to regulate DRM composition and function via cholesterol. Aβ was reduced in seladin-1 overexpressing cells and increased in seladin-1 deficient mouse brains. These findings promote a new cholesterol based mechanism, which propose the membrane cholesterol as a essential factor to prevent AD. Further studies must clarify the implication of seladin-1 in NFT formation and neurodegeneration. Overexpressing seladin-1 in animal models will advance our understanding of the roles of seladin-1 and identify potential disease-modifying factors in AD. Studies of knock-out and overexpressing seladin-1 mice will also provide novel strategies for the treatment and prevention of AD and related disorders.

## Solutions

**Blocking buffer**
1x PBS
5% Horse serum
0.05% Triton X-100

**Coomassie staining solution**
0.16%(w/v) coomassie Blue R250
40%(v/v) methanol
10%(v/v) acetic acid

**Coomassie destaining solution**
45%(v/v) methanol
10%(v/v) glacial acetic acid

**Culturing DMEM-F12 medium**
2mM L-glutamine
1 mM sodium pyruvate
10% fetal calf serum (FCS)
5% horse serum (HS)
5 U/ml penicillin
50µg/ml strepavidiC

**DEPC-$H_2O$**
0.2 ml DEPC
100 ml H2O
stir under a fume hood overnight
autoclave

**DNA sample buffer**
0.25%(w/v) bromophenol blue
0.25%(w/v) xylene cyanol FF
30%(w/v) glycerol

**Extraction buffer (rafts prep)**
25mM MES pH=7.0
5mM DTT
2mM EDTA

**Formaldehyde Gel**
1% agarose
7% formaldehyde

**Hybridization Wash-buffer**
0.25 M Na2HPO4 (pH 7.2)
1 % (w/v) SDS
1 mM EDTA

**Ketalar/Rompun**
Ketamin 12.5mg/ml
Xylazin 2.5mg/ml
in PBS
peritoneally injected: 8µl/g mouse

**LB agar**
LB medium
15g/L Bacto Agar

**LB medium**
10g/L Bacto Tryptone
5g/L Bacto Yeast extract
10g/L NaCl pH=7.0

**Loading buffer 6x**

10mM EDTA, pH 8.0
0.25% (w/v) bromphenol blue
0.25% (w/v) xylene cyanol
50% (v/v) glycerol+ EtBr

**Loading buffer 2x (NB)**

1x running buffer
50% deionized formamide
6.6% formaldehyde

**Loading buffer 4x (WB)**

100 mM Tris-Base
100mM Tris-HCl
4 % (v/v) ß-mercaptoethanol
40 % (v/v) glycerol
0.08 % (w/v) serva blue G250
0.025 phenol red
0.6‰ EDTA
1.92 M glycine

**Ly**

137mM NaCl
20mM Tris pH=7.6
1% Triton X-100
25x protease inhibitors

**MBS for sucrose gradient**

25mM MES pH=7.0
150mM NaCl
add (w/v) sucrose for
90%, 35%, 5%

**[redacted]**

0.2 M MOPS [ 3-(N-morpholino)-
propanesulfonic acid] (pH 7.0)
0.5 M sodium acetate
0,01 M EDTA

**NuPage running buffer 20x**

1M MOPS
1M Tris-Base
69.3 mM SDS
20.5mM EDTA

**Paraformaldehyde (PFA) 4%**

Heat dd$H_2O$ 200ml 65°C
4g PFA
few drops NaOH till clear
up to 1 litre pH=7.4

**PBS 1x**

8g NaCl
0.2g KCl
0.2g KH2PO4
0.765g Na2HPO4*2H2O
Adjust pH to 7.4
up to 1 liter

**Permeabilizition buffer**

1x PBS
0.1% Triton X-100
25x proteinase inhibitors

**Ponceau S solution**

0.2%(w/v) Ponceau-S red
3%(w/v) sulfonic acid
0.1%(v/v) glacial acid

**Protein sample buffer 2x**

450mM Tris-HCl pH=8.45
12%(v/v) Glycerol
4%(w/v) SDS
7.5‰ Coomassie brillant Blue
2.5‰ Phenol Red

**RNA sample buffer 6x**

10mM EDTA pH=8
0.25%(w/v) bromphenol blue
0.25%(w/v) xylenecyanol
50%(v/v) glycerol

**SSC 20x**

175g NaCl
88g (tri-)Sodium Citrate Dihydrate
900 ml $H_2O$
Adjust pH=7.0 with HCl
up to 1 litre

**SSPE 20x**

3M NaCl
0.2 M $NaH_2PO_4$ x $H_20$
20 mM EDTA
adjust pH to 7.4 with NaOH

**Stripping solution**
**(for WB membrane)**

Tris 62.5 mM pH=6.7
β mercaptoethanol 100mM
SDS 2%
30' 56°C

**TAE Buffer 50X**

242 gr. Tris
57.1 ml glacial acetic acid
100 ml 0.5 M EDTA pH=8.0
up to 1 litre

**TBS (Tris Buffered Saline) 10x**

25 mM Tris
0.8% NaCl
pH 8.0

**Transfer buffer 10x**

25 mM Tris
0.192 M glycine
20 % (v/v) methanol
1% (w/v) SDS

**Freezing medium**

DMEM-F12
20 % (v/v) FCS
5% HS
10 % (v/v) DMSO

**Plasmids**

| | |
|---|---|
| pcDNA3+ (CMV promoter) | Invitrogen |
| pEX-12 (mThy1.2 promoter) | Kusters JG[164] |
| pPrP-MO (PrP promoter) | Borchelt DR[165] |
| pSFV2gen | Life Technologies[166] |
| pSFVHelper | Life Technologies |

**Antibodies**

**Primary antibodies**

| | |
|---|---|
| Annexin-V-FITC (direct conjugated) | LabForce |
| Anti HA (rat) | Santa Cruz |
| Anti HA (mouse) | Santa Cruz |
| Anti APP C-terminal (rabbit) | Sigma |
| Anti APP N-terminal (mouse) | Roche |
| Anti $A\beta_{(40,42)}$ (BNT77) | Takeda |
| Anti $A\beta_{40}$ HRP (BA27) | Takeda |
| Anti $A\beta_{42}$ HRP (BC05) | Takeda |
| Anti BACE1 (rabbit) | C.Dingwall Glaxo Smith Kline |
| Anti MAP-2 (mouse) | Sigma |
| Anti seladin-1 N-Terminal (rabbit) | Nano-tools |
| Anti seladin-1 C-Terminal (rabbit) | Nano-tools |
| Anti EGFP (rat) | Santa Cruz |
| Anti $PrP^c$ POM-1 (mouse) | A.Aguzzi Zürich |
| Anti Flotilin 1 (mouse) | Transduction Laboratories |
| Anti Transferrin Receptor (mouse) | Santa Cruz |
| 6E10 | Signet |

**Secondary conjugated antibodies**

| | |
|---|---|
| Anti mouse-HRP | Amersham |
| Anti rabbit HRP | Pierce |
| Anti rat HRP | Amersham |
| Anti mouse FITC | Alexia |
| Anti rabbit FITC | Alexia |
| Anti rat FITC | Alexia |
| Anti mouse Cy5 | Jackson |
| Anti rabbit TRITC | Jackson |
| Anti rat TRITC | Alexia |

**Primers**

**Primer for caspase cleavage site mutations**

| primer name | aim | 5'→3' |
|---|---|---|
| Sel1F,D474E,gaC→gaA | site mutation of Caspase-3 cleavage | GGA CAT TCT GGA AGT GGA AAC CAA GAa ACA GAT TGT CCG |
| Sel1R,D474E,ctG→ctT | site mutation of Caspase-3 cleavage | CGG ACA ATC TGT TTC TTG GTT TCC ACT tCC AGA ATG TCC |
| Sel1F,D1256E,gaC→gaA | site mutation of Caspase-6 cleavage | CCA CGT GGT GCA GGA AAT GCT GGT GCC CAT GAa GTG CC |
| Sel1R,D1256E,ctG→ctT | site mutation of Caspase-6 cleavage | GGC ACT tCA TGG GCA CCA GCA TTT CCT GCA CCA CGT GG |

**Primer for desmosterolosis mutations**

| primer name | aim | 5'→3' |
|---|---|---|
| Sel1F, A to C mutation N294T | Desmosterolosis mutation | AGA GCC CAG CAA GCT GAc TAG CAT TGG C |
| Sel1R, A to C mutation N294T | Desmosterolosis mutation | GCC AAT GCT AgT CAG CTT GCT GGG CTC T |
| Sel1F,G to C mutation K306N | Desmosterolosis mutation | CAA GCC GTG GTT CTT TAA cCA TGT GGA GAA C |
| Sel1R,G to C mutation K306N | Desmosterolosis mutation | GTT CTC CAC ATG gTT AAA GAA CCA CGG CTT G |

| | | |
|---|---|---|
| Sel1F,G to A mutation E191K | Desmosterolosis mutation | TCT GCA CTG CTT ACa AGC TGG TCC TGG CTG |
| Sel1R,G to A mutation E191K | Desmosterolosis mutation | CAG CCA GGA CCA GCT tGT AAG CAG TGC AGA |

**Primer for HA tag in human seladin-1cDNA insertion**

| | | |
|---|---|---|
| Primer HA F sel1 | for HA tag | CAA GCT GGT ACC GAG CTC G |
| Primer HA R sel1 | for HA tag | A GCC TCT AGA AGC TCG AGC TCA *AGC GTA ATC TGG AAC ATC GTA TGG GTA GTG* CCT GGC GGC CTT GCA G |

**Primers for sequencing**

| | |
|---|---|
| primer2,F,sel1 | GG ACA TCC AGA AGC A |
| primer2,R,sel1 | CTG TGC CCA TGA TCA A |
| primer3,F,sel1 | CGT GTT GCC TGA GCT T |
| primer3,R,sel1 | TGA ACT TGG CAC AGA T |
| primer4,F,sel1 | TCA AGC TGC GTT TCG AG |
| primer4,R,sel1 | GCT CCC AGA AGA TGC T |
| primer5,F,sel1 | ATT CCC TTG AGA CAC T |
| primer5,R,sel1 | ACG GAC ACA GCC AGA T |
| primer6,F,sel1 | CCT GCA CAC CTT CCA A |
| primer6,R,sel1 | AGG AGC CAT CAA ACA T |
| primer7,F,sel1 | GTA TGC CGA CTG CTA C |
| primerT7,R,sel1 | CAC GGC GGG CTC CAT |

## Devices and Chemicals

| product | company |
|---|---|
| ABI Prism 310 Genetic Analyzer | Applied Biosystems |
| ABI Prism 7700 Sequence Detector | Applied Biosystems |
| Centrifuge 5417C | eppendorf |
| Centrifuge 5417R | eppendorf |
| Concentrator 5301 | eppendorf |
| Gel Dryer Model 583 | BioRAD |
| Gene Pulser II Electroporation System | BioRAD |
| Gene Quant pro (Photometer) | Amersham Pharmacia |
| GeneAmp PCR System 9700 | PE Applied Biosystems |
| Horizontal Electrophoresis System | owl |
| Leica DMRXE | Leica |
| Leica RM 2135 | Leica |
| MP 220 pH Meter | Mettler Toledo |
| RoboCycler Gradient 96 | Stratagene |
| Rotor GSA | Sorvall |
| Rotor SS-34 | Sorvall |
| β-mercaptoethanol | Sigma |
| 10-20% TrisTricine gels | Novex |
| 4-12% TrisTricine gels | Novex |
| Agarose | Gibco BRL |
| Biomax MR film | Kodak |

| | |
|---|---|
| Bromphenol blue | Sigma |
| BSA | Sigma |
| CaCl2 | Sigma |
| Calf intestinal phosphatase (CIAP) | Promega |
| Cell culture dishes | TTP |
| Cell culture flasks | Falcon |
| Cell culture media | Gibco BRL |
| Chloroform | Merck |
| Complete Protease Inhibitor | Roche |
| Coomassie brilliant blue | Merck |
| DEPC | Sigma |
| DMSO | Sigma |
| DNA ladder | New England Biolabs |
| DNase I | Roche |
| dNTPs | Sigma |
| EDTA | Sigma |
| EndoFree Maxi Kit | QIAGEN |
| Ethanol | Kantonsapotheke Zurich |
| ExpressHyb | Clontech |
| FCS | Biochrom KG |
| Formaldehyde | Fluka |
| Formamide | Calbiochem |
| Glacial acid | Merck |

| | |
|---|---|
| Glycerol | Sigma |
| Glycine | Merck |
| Hybond+ | Amersham Pharmacia |
| Isopropanol / Ketamin | Sigma, Streuli Uznach |
| LF2000 | Invitrogen |
| Methanol | Merck |
| MgCl2 | Sigma |
| Milk powder | Migros |
| MOPS | Sigma |
| MuLV reverse transcriptase | Perkin Elmer |
| Na2HPO4 | Merck |
| NaAc | Merck |
| NaCl | Sigma |
| NaOH | Sigma |
| Nitrocellulose-membrane 0.1µm | Schleicher&Schuell |
| Nitrocellulose-membrane 0.45µm | BioRAD |
| Oligonucleotides | Metabion<br>Microsynth |
| Paraformaldehyde | Elctron Microscopy Sciences |
| Pfu polymerase | Stratagene |
| Phenol | Merck |
| Ponceau-S | Merck |
| Proteinase K | Roche |
| PVDF-membrane | Millipore |

| | |
|---|---|
| QIAGEN DNeasy Kit | QIAGEN |
| QIAGEN Nucleotide Removal Kit | QIAGEN |
| QIAGEN PCR purification kit | QIAGEN |
| QIAGEN Plasmid Maxi Kit | QIAGEN |
| QIAGEN Plasmid Midi Kit | QIAGEN |
| QIAGEN RNeasy Kit | QIAGEN |
| Rapid DNA Ligation Kit | Roche |
| Restriction Endonucleases | New England Biolabs / Roche |
| Salmon sperm DNA | Roche |
| SDS | Sigma |
| T4 DNA ligase | New England Biolabs |
| Tricine | Sigma |
| Tris | Sigma |
| Triton X-100 | Sigma |
| Trizol | Gibco BRL |
| Trypsin/EDTA | Gibco BRL |
| Tryptone | Becton Dickinson |
| Tween20 | Sigma |
| Xylazin<br>Yeast extract | Streuli Uznach<br>Becton Dickinson |
| Kodak X-OMAT 2000 Processor | Kodak |
| Memmert waterbath | Fisher Scientific |
| Microtome Leica RM 2135 | Leica |
| MP 220 pH meter | Mettler Toledo |

| | |
|---|---|
| Nikon Eclipse E800 | Nikon |
| Nikon Eclipse TE300 | Nikon |
| Nikon TMS F | Nikon |
| NUAIRE Autoflow $CO_2$ Incubator | Inotech |
| Rotor GSA | Sorvall |
| Rotor SS34 | Sorvall |
| SKAN VSE 2000-120 sterilhood | Skan |
| Sorvall RC 26 Plus | Kendro |
| Thermomixer | Eppendorf |
| Universal 32 Hettich centrifuge | Fisher Scientific |
| Vibratome Leica VT 1000S | Leica |
| | |

| | |
|---|---|
| aa | amino acids |
| Aβ | β-amyloid peptide |
| $Aβ_{40}$ | β-amyloid peptide of 40aa |
| $Aβ_{42}$ | β-amyloid peptide of 42aa |
| AD | Alzheimer's disease |
| apoE | apolipoprotein E |
| APP | amyloid precursor protein |
| α APPs | soluble domain of APP after α-secretase cleavage |
| β APPs | soluble domain of APP after β-secretase cleavage |
| BACE1 | β amyloid APP cleavage enzyme (β-secretase) |
| bp | base pair |
| cDNA | complementary DNA |
| C-Term | APP C-Terminal |
| C-Term-α | APP C-Terminal fragment produced by α- secretase cleavage |
| C-Term-β | APP C-Terminal fragment produced by β- secretase cleavage |

| | |
|---|---|
| dATP | deoxy ATP |
| dCTP | deoxy CTP |
| DEPC | diethylpyrocarbonate |
| dGTP | deoxy GTP |
| DMEM | Dulbecco's Modified Eagle Medium |
| DMSO | dimethylsulfoxid |
| DNA | Deoxyribonucleic acid |
| DNase | deoxy ribonuclease |
| dNTP | deoxy nucleotide triphosphate |
| DRM | detergent resistant cholesterol-rich membrane microdomain |
| DTT | dithiothreitol |
| dTTP | deoxy TTP |
| *E. coli* | *Escherichia coli* |
| ECL | enhanced chemiluminescence |
| EDTA | Ethylendiamintetra acetic acid |
| EGFP | enhanced green fluorescent protein |
| FAD | familial Alzheimer's disease |
| FAD | Flavin adenine dinucleotide |

| | |
|---|---|
| FCS | fetal calf serum |
| GFAP | glial fibrillary acidic protein |
| g | acceleration of gravity |
| HS | horse serum |
| HPLC | high performance liquid chromatography |
| Kbp | kilo basepair |
| kDa | kilo Dalton |
| LDH | Lactate dehydrogenase |
| MOPS | 3-N-morpholinpropansulfonic acid |
| NFT | neurofibrillary tangles |
| Ntera-2 | human teratoma cell line |
| OD | optical density |
| Oligo | oligonucleotide |
| ORF | open reading frame |
| PCR | polymerase chain reaction |
| PFA | paraformaldehyde |
| pfu | proof reading |
| PS1 | presenilin 1 |
| PS2 | presenilin 2 |
| RNA | ribonucleic acid |
| RNase | ribonuclease |
| rpm | rotations per minute |
| SAP | shrimp alcaline phosphatase |
| SDS | sodium dodecyl sulphate |
| Sel-1 | seladin-1 |
| SH-SY5Y | a human neuroblastoma cell line |
| Sw APP | APP Swedish mutation |
| TAE | Tris acetate EDTA buffer |
| TBS | Tris buffer saline |
| TUNEL | terminal deoxyribonucleotidyl transferase (TdT)-mediated dUTP nick-end labelling |
| UTR | untranslated region |
| U | Unit |
| UV | Ultra-violet |
| V | Volt |
| v/v | volume per volume |
| w/v | weight per volume |
| WB | Western blot |
| Wt | wild-type |

# Acknowledgements



At the end of this work I thank without reservation all members of my family who have supported me during this long journay, from my mother and my sister, *Dolores & Dolores* up to my father in heaven, *Carlo*.

I thank Dr. *M. Hasan Mohajeri,* who introduced me into the exciting field of Alzheimer's disease. His patience, support and great efforts have made these years most rewarding.

My thanks go to Prof. Dr. *Roger M. Nitsch* for the opportunity to do my PhD work in his department and for his valuable suggestions; to Prof. Dr. *Peter Sonderegger* for his kindness to accept me as an external student and to Prof. Dr. *Josef Jiricny* for refereeing my thesis.

Likewise, I am very greateful to Dr. *Dolores Ledesma* and Prof. Dr. *Carlos Dotti* from the Cavalieri Ottolenghi Institute in Torino and Prof. Dr. *Dieter Lütjohann* from the University of Bonn for a fruitful cooperation and inspiring communication.

I would like to express my thanks to all the people in the lab, in particular *Danielle Gretener, Fabienne Brunner* and *Dr. Fred Hoerndli* for restorative coffee-talks and *Jay Tracy* for reading this manuscript carefully.

Particular gratitude goes to *Katrin Kuehnle* for excellent teamwork during the daily bench battle, for her intellectual support in the planning scuffle and for never-ending patience, encouragement and high spirits.

# Curriculum Vitae

## Personal data


| | |
|---|---|
| First name: | Arames |
| Last name | Crameri |
| Born: | 3 October 1969 |
| Origin: | Poschiavo 7742, Graubünden, Switzerland |
| Actual address: | Zweierstrasse 139, 8003 Zürich, Switzerland |
| Phone numbers: | (H) ++41-1-461 30 79 |
| | (Lab) ++41-1-634 88 64 |


| | |
|---|---|
| Languages: | Italian mother language |
| | German written and spoken |
| | French written and spoken |
| | English written and spoken |

## Education

| | |
|---|---|
| 2001-2005 | PhD degree at the Department of Psychiatry Research, University of Zürich, Switzerland, entitle: “Analysis of Seladin-1 Role in Apoptosis and Cholesterol Metabolism” |
| | Supervisors: Dr. M. Hasan Mohajeri, Prof. Dr. Peter Sonderegger, Prof. Dr. Josef Jiricny, Prof. Dr. Roger M. Nitsch. |
| 2000-2001 | Research project at the Institute of Molecular Neurogenetics at the Harvard Medical School (partner with the Massachusetts General Hospital) by Prof. Vijaya Ramesh PhD. Topic of the research: Identification of novel proteins that might specifically bind to merlin which is involved in the pathology of the neurofibromatosis. |
| 1999-2000 | Master degree in molecular biology, at the Department of Psychiatry Research, University of Zürich, Switzerland, entitle: “Effects of Dominant |

| | |
|---|---|
| | Expression of PP2Ac-α Mutants on Phosphorylation Status of Tau *in vitro* and *in vivo"* |
| | Supervisors: Dr. Jürgen Götz, Dr. M. Hasan Mohajeri and Prof. Dr. Walter Schaffner |
| 1995-1999 | Student of biology in molecular biology and immunology at the University of Zürich, Switzerland |
| 1994-1995 | Work as an assistant at a youth educational center, Zürich, Switzerland |
| 1992-1993 | Medical student at the University of Zürich, Switzerland |
| 1987-1992 | College major in life science, Zuoz, Graubünden, Switzerland |
| 1986-1987 | Introductory courses in Economics, Graubünden, Switzerland |
| 1976-1985 | Primary and high school in Graubünden, Switzerland |

## Publications

**Crameri, A.**, Biondi, E., Kuehnle, K.,Lütjohann, D., Thelen, K. M., Dotti, C. G., Nitsch, M. R., Ledesma, M. D., Mohajeri, M. H. Seladin-1 regulates cholesterol levels, APP processing and Aβ generation *in vivo.* Nat Med *in review* June 2005

Gaugler, M. N.; Tracy, J.; Kuhnle, K.; **Crameri, A**.; Nitsch, R. M.; Mohajeri, M. H. (2005). "Modulation of Alzheimer's pathology by cerebro-ventricular grafting of hybridoma cells expressing antibodies against Abeta in vivo." FEBS Lett 579(3): 7536.

Mohajeri, M. H.; Gaugler, M. N.; Martinez J.; Tracy J., Li, H.; **Crameri, A**.; Kuehnle, K.; Wollmer M. A.; Nitsch, R. M. (2004) Assessment of the Bioactivity of Antibodies against β-Amyloid Peptide *in vitro* and *in vivo* Neurodegenerative Diseases;1:160-167

Mohajeri, M. H.; Saini, K.; Li, H.; **Crameri, A.**; Lipp, H. P.; Wolfer, D. P.; Nitsch, R. M. (2003). "Intact spatial memory in mice with seizure-induced partial loss of hippocampal pyramidal neurons." Neurobiol Dis 12(3): 174-81.

Kins, S.; **Crameri, A.**; Evans, D. R.; Hemmings, B. A.; Nitsch, R. M.; Gotz, J. (2001). "Reduced protein phosphatase 2A activity induces hyperphosphorylation and altered compartmentalization of tau in transgenic mice." J Biol Chem 276(41): 38193-200.

## References


1. Wu, C., Miloslavskaya, I., Demontis, S., Maestro, R. & Galaktionov, K. Regulation of cellular response to oncogenic and oxidative stress by Seladin-1. *Nature* **432**, 640-5 (2004).
2. Mauch, D.H. et al. CNS synaptogenesis promoted by glia-derived cholesterol. *Science* **294**, 1354-7 (2001).
3. Pfrieger, F.W. Outsourcing in the brain: do neurons depend on cholesterol delivery by astrocytes? *Bioessays* **25**, 72-8 (2003).
4. Waterham, H.R. et al. Mutations in the 3beta-hydroxysterol Delta24-reductase gene cause desmosterolosis, an autosomal recessive disorder of cholesterol biosynthesis. *Am J Hum Genet* **69**, 685-94 (2001).
5. Greeve, I. et al. The human DIMINUTO/DWARF1 homolog seladin-1 confers resistance to Alzheimer's disease-associated neurodegeneration and oxidative stress. *J Neurosci* **20**, 7345-52 (2000).
6. De Strooper, B. & Annaert, W. Proteolytic processing and cell biological functions of the amyloid precursor protein. *J Cell Sci* **113 (Pt 11)**, 1857-70 (2000).
7. Seubert, P. et al. Secretion of beta-amyloid precursor protein cleaved at the amino terminus of the beta-amyloid peptide. *Nature* **361**, 260-3 (1993).
8. Selkoe, D.J. Translating cell biology into therapeutic advances in Alzheimer's disease. *Nature* **399**, A23-31 (1999).
9. Busciglio, J., Gabuzda, D.H., Matsudaira, P. & Yankner, B.A. Generation of beta-amyloid in the secretory pathway in neuronal and nonneuronal cells. *Proc Natl Acad Sci U S A* **90**, 2092-6 (1993).
10. Haass, C. et al. Amyloid beta-peptide is produced by cultured cells during normal metabolism. *Nature* **359**, 322-5 (1992).
11. Shoji, M. et al. Production of the Alzheimer amyloid beta protein by normal proteolytic processing. *Science* **258**, 126-9 (1992).
12. Haass, C., Hung, A.Y., Schlossmacher, M.G., Teplow, D.B. & Selkoe, D.J. beta-Amyloid peptide and a 3-kDa fragment are derived by distinct cellular mechanisms. *J Biol Chem* **268**, 3021-4 (1993).
13. Lansbury, P.T., Jr. Structural neurology: are seeds at the root of neuronal degeneration? *Neuron* **19**, 1151-4 (1997).
14. Steiner, H. et al. PEN-2 is an integral component of the gamma-secretase complex required for coordinated expression of presenilin and nicastrin. *J Biol Chem* **277**, 39062-5 (2002).
15. Gu, Y. et al. APH-1 interacts with mature and immature forms of presenilins and nicastrin and may play a role in maturation of presenilin.nicastrin complexes. *J Biol Chem* **278**, 7374-80 (2003).
16. De Strooper, B. et al. A presenilin-1-dependent gamma-secretase-like protease mediates release of Notch intracellular domain. *Nature* **398**, 518-22 (1999).

17. Okochi, M. et al. Presenilins mediate a dual intramembranous gamma-secretase cleavage of Notch-1. *Embo J* **21**, 5408-16 (2002).

18. Marambaud, P. et al. A CBP binding transcriptional repressor produced by the PS1/epsilon-cleavage of N-cadherin is inhibited by PS1 FAD mutations. *Cell* **114**, 635-45 (2003).

19. De Strooper, B. Aph-1, Pen-2, and Nicastrin with Presenilin generate an active gamma-Secretase complex. *Neuron* **38**, 9-12 (2003).

20. Borchelt, D.R. et al. Familial Alzheimer's disease-linked presenilin 1 variants elevate Abeta1-42/1-40 ratio in vitro and in vivo. *Neuron* **17**, 1005-13 (1996).

21. Duff, K. et al. Increased amyloid-beta42(43) in brains of mice expressing mutant presenilin 1. *Nature* **383**, 710-3 (1996).

22. Selkoe, D.J. Toward a comprehensive theory for Alzheimer's disease. Hypothesis: Alzheimer's disease is caused by the cerebral accumulation and cytotoxicity of amyloid beta-protein. *Ann N Y Acad Sci* **924**, 17-25 (2000).

23. Giovanni, A. et al. E2F1 mediates death of B-amyloid-treated cortical neurons in a manner independent of p53 and dependent on Bax and caspase 3. *J Biol Chem* **275**, 11553-60 (2000).

24. Saido, T.C. Alzheimer's disease as proteolytic disorders: anabolism and catabolism of beta-amyloid. *Neurobiol Aging* **19**, S69-75 (1998).

25. Qiu, W.Q. et al. Insulin-degrading enzyme regulates extracellular levels of amyloid beta-protein by degradation. *J Biol Chem* **273**, 32730-8 (1998).

26. Selkoe, D.J. Alzheimer's disease: genes, proteins, and therapy. *Physiol Rev* **81**, 741-66 (2001).

27. Lijnen, H.R., Okada, K., Matsuo, O., Collen, D. & Dewerchin, M. Alpha2-antiplasmin gene deficiency in mice is associated with enhanced fibrinolytic potential without overt bleeding. *Blood* **93**, 2274-81 (1999).

28. Collen, D. Ham-Wasserman lecture: role of the plasminogen system in fibrin-homeostasis and tissue remodeling. *Hematology (Am Soc Hematol Educ Program)*, 1-9 (2001).

29. Sappino, A.P. et al. Extracellular proteolysis in the adult murine brain. *J Clin Invest* **92**, 679-85 (1993).

30. Baranes, D. et al. Tissue plasminogen activator contributes to the late phase of LTP and to synaptic growth in the hippocampal mossy fiber pathway. *Neuron* **21**, 813-25 (1998).

31. Seeds, N.W., Williams, B.L. & Bickford, P.C. Tissue plasminogen activator induction in Purkinje neurons after cerebellar motor learning. *Science* **270**, 1992-4 (1995).

32. Wu, Y.P. et al. The tissue plasminogen activator (tPA)/plasmin extracellular proteolytic system regulates seizure-induced hippocampal mossy fiber outgrowth through a proteoglycan substrate. *J Cell Biol* **148**, 1295-304 (2000).

33. Chen, Z.L. et al. Neuronal death and blood-brain barrier breakdown after excitotoxic injury are independent processes. *J Neurosci* **19**, 9813-20 (1999).

34. Werb, Z. ECM and cell surface proteolysis: regulating cellular ecology. *Cell* **91**, 439-42 (1997).

35. Nicole, O. et al. The proteolytic activity of tissue-plasminogen activator enhances NMDA receptor-mediated signaling. *Nat Med* **7**, 59-64 (2001).

36. Rogove, A.D., Siao, C., Keyt, B., Strickland, S. & Tsirka, S.E. Activation of microglia reveals a non-proteolytic cytokine function for tissue plasminogen activator in the central nervous system. *J Cell Sci* **112 (Pt 22)**, 4007-16 (1999).

37. Mrak, R.E., Sheng, J.G. & Griffin, W.S. Glial cytokines in Alzheimer's disease: review and pathogenic implications. *Hum Pathol* **26**, 816-23 (1995).

38. Wood, P.L. Microglia as a unique cellular target in the treatment of stroke: potential neurotoxic mediators produced by activated microglia. *Neurol Res* **17**, 242-8 (1995).

39. Binder, L.I., Frankfurter, A. & Rebhun, L.I. The distribution of tau in the mammalian central nervous system. *J Cell Biol* **101**, 1371-8 (1985).

40. Neve, R.L., Harris, P., Kosik, K.S., Kurnit, D.M. & Donlon, T.A. Identification of cDNA clones for the human microtubule-associated protein tau and chromosomal localization of the genes for tau and microtubule-associated protein 2. *Brain Res* **387**, 271-80 (1986).

41. Goedert, M., Spillantini, M.G., Jakes, R., Rutherford, D. & Crowther, R.A. Multiple isoforms of human microtubule-associated protein tau: sequences and localization in neurofibrillary tangles of Alzheimer's disease. *Neuron* **3**, 519-26 (1989).

42. Goedert, M., Spillantini, M.G., Potier, M.C., Ulrich, J. & Crowther, R.A. Cloning and sequencing of the cDNA encoding an isoform of microtubule-associated protein tau containing four tandem repeats: differential expression of tau protein mRNAs in human brain. *Embo J* **8**, 393-9 (1989).

43. Sontag, E. et al. Molecular interactions among protein phosphatase 2A, tau, and microtubules. Implications for the regulation of tau phosphorylation and the development of tauopathies. *J Biol Chem* **274**, 25490-8 (1999).

44. Arriagada, P.V., Growdon, J.H., Hedley-Whyte, E.T. & Hyman, B.T. Neurofibrillary tangles but not senile plaques parallel duration and severity of Alzheimer's disease. *Neurology* **42**, 631-9 (1992).

45. Sperfeld, A.D. et al. FTDP-17: an early-onset phenotype with parkinsonism and epileptic seizures caused by a novel mutation. *Ann Neurol* **46**, 708-15 (1999).

46. Hardy, J. & Allsop, D. Amyloid deposition as the central event in the aetiology of Alzheimer's disease. *Trends Pharmacol Sci* **12**, 383-8 (1991).

47. Lewis, J. et al. Enhanced neurofibrillary degeneration in transgenic mice expressing mutant tau and APP. *Science* **293**, 1487-91 (2001).

48. Gotz, J., Chen, F., van Dorpe, J. & Nitsch, R.M. Formation of neurofibrillary tangles in P301l tau transgenic mice induced by Abeta 42 fibrils. *Science* **293**, 1491-5 (2001).

49. Hardy, J. & Selkoe, D.J. The amyloid hypothesis of Alzheimer's disease: progress and problems on the road to therapeutics. *Science* **297**, 353-6 (2002).

50. Lashuel, H.A., Hartley, D., Petre, B.M., Walz, T. & Lansbury, P.T., Jr. Neurodegenerative disease: amyloid pores from pathogenic mutations. *Nature* **418**, 291 (2002).

51. Games, D. et al. Alzheimer-type neuropathology in transgenic mice overexpressing V717F beta-amyloid precursor protein. *Nature* **373**, 523-7 (1995).

52. Moechars, D., Lorent, K., De Strooper, B., Dewachter, I. & Van Leuven, F. Expression in brain of amyloid precursor protein mutated in the alpha-secretase site causes disturbed behavior, neuronal degeneration and premature death in transgenic mice. *Embo J* **15**, 1265-74 (1996).

53. Sturchler-Pierrat, C. et al. Two amyloid precursor protein transgenic mouse models with Alzheimer disease-like pathology. *Proc Natl Acad Sci U S A* **94**, 13287-92 (1997).

54. Bornemann, K.D. & Staufenbiel, M. Transgenic mouse models of Alzheimer's disease. *Ann N Y Acad Sci* **908**, 260-6 (2000).

55. Lee, V.M., Goedert, M. & Trojanowski, J.Q. Neurodegenerative tauopathies. *Annu Rev Neurosci* **24**, 1121-59 (2001).

56. Gotz, J. et al. Somatodendritic localization and hyperphosphorylation of tau protein in transgenic mice expressing the longest human brain tau isoform. *Embo J* **14**, 1304-13 (1995).

57. Ishihara, T. et al. Age-dependent emergence and progression of a tauopathy in transgenic mice overexpressing the shortest human tau isoform. *Neuron* **24**, 751-62 (1999).

58. Probst, A. et al. Axonopathy and amyotrophy in mice transgenic for human four-repeat tau protein. *Acta Neuropathol (Berl)* **99**, 469-81 (2000).

59. Lewis, J. et al. Neurofibrillary tangles, amyotrophy and progressive motor disturbance in mice expressing mutant (P301L) tau protein. *Nat Genet* **25**, 402-5 (2000).

60. Gotz, J., Probst, A., Ehler, E., Hemmings, B. & Kues, W. Delayed embryonic lethality in mice lacking protein phosphatase 2A catalytic subunit Calpha. *Proc Natl Acad Sci U S A* **95**, 12370-5 (1998).

61. Kins, S. et al. Reduced protein phosphatase 2A activity induces hyperphosphorylation and altered compartmentalization of tau in transgenic mice. *J Biol Chem* **276**, 38193-200 (2001).

62. Datta, K., Biswal, S.S. & Kehrer, J.P. The 5-lipoxygenase-activating protein (FLAP) inhibitor, MK886, induces apoptosis independently of FLAP. *Biochem J* **340 (Pt 2)**, 371-5 (1999).

63. Zong, W.X., Edelstein, L.C., Chen, C., Bash, J. & Gelinas, C. The prosurvival Bcl-2 homolog Bfl-1/A1 is a direct transcriptional target of NF-kappaB that blocks TNFalpha-induced apoptosis. *Genes Dev* **13**, 382-7 (1999).

64. Zou, H., Li, Y., Liu, X. & Wang, X. An APAF-1.cytochrome c multimeric complex is a functional apoptosome that activates procaspase-9. *J Biol Chem* **274**, 11549-56 (1999).

65. Cregan, S.P. et al. Bax-dependent caspase-3 activation is a key determinant in p53-induced apoptosis in neurons. *J Neurosci* **19**, 7860-9 (1999).

66. Putcha, G.V., Deshmukh, M. & Johnson, E.M., Jr. BAX translocation is a critical event in neuronal apoptosis: regulation by neuroprotectants, BCL-2, and caspases. *J Neurosci* **19**, 7476-85 (1999).

67. Selimi, F., Campana, A., Weitzman, J., Vogel, M.W. & Mariani, J. Bax and p53 are differentially involved in the regulation of caspase-3 expression and activation during neurodegeneration in Lurcher mice. *C R Acad Sci III* **323**, 967-73 (2000).

68. Gagliardini, V. et al. Prevention of vertebrate neuronal death by the crmA gene. *Science* **263**, 826-8 (1994).

69. Kang, S.J. et al. Dual role of caspase-11 in mediating activation of caspase-1 and caspase-3 under pathological conditions. *J Cell Biol* **149**, 613-22 (2000).

70. Nakagawa, T. et al. Caspase-12 mediates endoplasmic-reticulum-specific apoptosis and cytotoxicity by amyloid-beta. *Nature* **403**, 98-103 (2000).

71. Barbacid, M. Structural and functional properties of the TRK family of neurotrophin receptors. *Ann N Y Acad Sci* **766**, 442-58 (1995).

72. Fruman, D.A., Meyers, R.E. & Cantley, L.C. Phosphoinositide kinases. *Annu Rev Biochem* **67**, 481-507 (1998).

73. Philpott, K.L., McCarthy, M.J., Klippel, A. & Rubin, L.L. Activated phosphatidylinositol 3-kinase and Akt kinase promote survival of superior cervical neurons. *J Cell Biol* **139**, 809-15 (1997).

74. Bonni, A. et al. Cell survival promoted by the Ras-MAPK signaling pathway by transcription-dependent and -independent mechanisms. *Science* **286**, 1358-62 (1999).

75. Su, J.H., Anderson, A.J., Cummings, B.J. & Cotman, C.W. Immunohistochemical evidence for apoptosis in Alzheimer's disease. *Neuroreport* **5**, 2529-33 (1994).

76. Troncoso, J.C., Sukhov, R.R., Kawas, C.H. & Koliatsos, V.E. In situ labeling of dying cortical neurons in normal aging and in Alzheimer's disease: correlations with senile plaques and disease progression. *J Neuropathol Exp Neurol* **55**, 1134-42 (1996).

77. Small, D.H. & McLean, C.A. Alzheimer's disease and the amyloid beta protein: What is the role of amyloid? *J Neurochem* **73**, 443-9 (1999).

78. Behl, C., Davis, J.B., Lesley, R. & Schubert, D. Hydrogen peroxide mediates amyloid beta protein toxicity. *Cell* **77**, 817-27 (1994).

79. Mattson, M.P., Tomaselli, K.J. & Rydel, R.E. Calcium-destabilizing and neurodegenerative effects of aggregated beta-amyloid peptide are attenuated by basic FGF. *Brain Res* **621**, 35-49 (1993).

80. Yaar, M. et al. Binding of beta-amyloid to the p75 neurotrophin receptor induces apoptosis. A possible mechanism for Alzheimer's disease. *J Clin Invest* **100**, 2333-40 (1997).

81. Yan, S.D. et al. RAGE and amyloid-beta peptide neurotoxicity in Alzheimer's disease. *Nature* **382**, 685-91 (1996).

82. Lee, M.S. et al. Neurotoxicity induces cleavage of p35 to p25 by calpain. *Nature* **405**, 360-4 (2000).

83. Harada, J. & Sugimoto, M. Activation of caspase-3 in beta-amyloid-induced apoptosis of cultured rat cortical neurons. *Brain Res* **842**, 311-23 (1999).

84. Troy, C.M. et al. beta-Amyloid-induced neuronal apoptosis requires c-Jun N-terminal kinase activation. *J Neurochem* **77**, 157-64 (2001).

85. Snipes, G.J. & Suter, U. Cholesterol and myelin. *Subcell Biochem* **28**, 173-204 (1997).

86. Bjorkhem, I. et al. Cholesterol homeostasis in human brain: turnover of 24S-hydroxycholesterol and evidence for a cerebral origin of most of this oxysterol in the circulation. *J Lipid Res* **39**, 1594-600 (1998).

87. Panzenboeck, U. et al. ABCA1 and scavenger receptor class B, type I, are modulators of reverse sterol transport at an in vitro blood-brain barrier constituted of porcine brain capillary endothelial cells. *J Biol Chem* **277**, 42781-9 (2002).

88. Bjorkhem, I., Lutjohann, D., Breuer, O., Sakinis, A. & Wennmalm, A. Importance of a novel oxidative mechanism for elimination of brain cholesterol. Turnover of cholesterol and 24(S)-hydroxycholesterol in rat brain as measured with 18O2 techniques in vivo and in vitro. *J Biol Chem* **272**, 30178-84 (1997).

89. Edwards, P.A. & Ericsson, J. Signaling molecules derived from the cholesterol biosynthetic pathway: mechanisms of action and possible roles in human disease. *Curr Opin Lipidol* **9**, 433-40 (1998).

90. Gimpl, G., Burger, K. & Fahrenholz, F. Cholesterol as modulator of receptor function. *Biochemistry* **36**, 10959-74 (1997).

91. Thiele, C., Hannah, M.J., Fahrenholz, F. & Huttner, W.B. Cholesterol binds to synaptophysin and is required for biogenesis of synaptic vesicles. *Nat Cell Biol* **2**, 42-9 (2000).

92. Burns, M. & Duff, K. Cholesterol in Alzheimer's disease and tauopathy. *Ann N Y Acad Sci* **977**, 367-75 (2002).

93. Sparks, D.L. et al. Induction of Alzheimer-like beta-amyloid immunoreactivity in the brains of rabbits with dietary cholesterol. *Exp Neurol* **126**, 88-94 (1994).

94. Wechsler, A. et al. Generation of viable cholesterol-free mice. *Science* **302**, 2087 (2003).

95. Ignatius, M.J. et al. Expression of apolipoprotein E during nerve degeneration and regeneration. *Proc Natl Acad Sci U S A* **83**, 1125-9 (1986).

96. Poirier, J., Hess, M., May, P.C. & Finch, C.E. Astrocytic apolipoprotein E mRNA and GFAP mRNA in hippocampus after entorhinal cortex lesioning. *Brain Res Mol Brain Res* **11**, 97-106 (1991).

97. Mahley, R.W. Apolipoprotein E: cholesterol transport protein with expanding role in cell biology. *Science* **240**, 622-30 (1988).

98. Corder, E.H. et al. Gene dose of apolipoprotein E type 4 allele and the risk of Alzheimer's disease in late onset families. *Science* **261**, 921-3 (1993).

99. Greenberg, S.M., Rebeck, G.W., Vonsattel, J.P., Gomez-Isla, T. & Hyman, B.T. Apolipoprotein E epsilon 4 and cerebral hemorrhage associated with amyloid angiopathy. *Ann Neurol* **38**, 254-9 (1995).

100. Biere, A.L. et al. Co-expression of beta-amyloid precursor protein (betaAPP) and apolipoprotein E in cell culture: analysis of betaAPP processing. *Neurobiol Dis* **2**, 177-87 (1995).

101. Ma, J., Yee, A., Brewer, H.B., Jr., Das, S. & Potter, H. Amyloid-associated proteins alpha 1-antichymotrypsin and apolipoprotein E promote assembly of Alzheimer beta-protein into filaments. *Nature* **372**, 92-4 (1994).

102. Rebeck, G.W., Reiter, J.S., Strickland, D.K. & Hyman, B.T. Apolipoprotein E in sporadic Alzheimer's disease: allelic variation and receptor interactions. *Neuron* **11**, 575-80 (1993).

103. Schmechel, D.E. et al. Increased amyloid beta-peptide deposition in cerebral cortex as a consequence of apolipoprotein E genotype in late-onset Alzheimer disease. *Proc Natl Acad Sci U S A* **90**, 9649-53 (1993).

104. Nathan, B.P. et al. Differential effects of apolipoproteins E3 and E4 on neuronal growth in vitro. *Science* **264**, 850-2 (1994).

105. Muller, W. et al. Apolipoprotein E isoforms increase intracellular Ca2+ differentially through a omega-agatoxin IVa-sensitive Ca2+-channel. *Brain Pathol* **8**, 641-53 (1998).

106. Aono, M. et al. Apolipoprotein E protects against NMDA excitotoxicity. *Neurobiol Dis* **11**, 214-20 (2002).

107. Lee, Y., Aono, M., Laskowitz, D., Warner, D.S. & Pearlstein, R.D. Apolipoprotein E protects against oxidative stress in mixed neuronal-glial cell cultures by reducing glutamate toxicity. *Neurochem Int* **44**, 107-18 (2004).

108. Gee, J.R. & Keller, J.N. Astrocytes: regulation of brain homeostasis via apolipoprotein E. *Int J Biochem Cell Biol* **37**, 1145-50 (2005).

109. Igbavboa, U., Avdulov, N.A., Chochina, S.V. & Wood, W.G. Transbilayer distribution of cholesterol is modified in brain synaptic plasma membranes of knockout mice deficient in the low-density lipoprotein receptor, apolipoprotein E, or both proteins. *J Neurochem* **69**, 1661-7 (1997).

110. Igbavboa, U., Avdulov, N.A., Schroeder, F. & Wood, W.G. Increasing age alters transbilayer fluidity and cholesterol asymmetry in synaptic plasma membranes of mice. *J Neurochem* **66**, 1717-25 (1996).

111. Wood, W.G., Schroeder, F., Avdulov, N.A., Chochina, S.V. & Igbavboa, U. Recent advances in brain cholesterol dynamics: transport, domains, and Alzheimer's disease. *Lipids* **34**, 225-34 (1999).

112. Kirsch, C., Eckert, G.P., Koudinov, A.R. & Muller, W.E. Brain cholesterol, statins and Alzheimer's Disease. *Pharmacopsychiatry* **36 Suppl 2**, S113-9 (2003).

113. Simons, K. & Ikonen, E. Functional rafts in cell membranes. *Nature* **387**, 569-72 (1997).

114. Eckert, G.P., Igbavboa, U., Muller, W.E. & Wood, W.G. Lipid rafts of purified mouse brain synaptosomes prepared with or without detergent reveal different lipid and protein domains. *Brain Res* **962**, 144-50 (2003).

115. Simons, K. & Toomre, D. Lipid rafts and signal transduction. *Nat Rev Mol Cell Biol* **1**, 31-9 (2000).

116. Laux, T. et al. GAP43, MARCKS, and CAP23 modulate PI(4,5)P(2) at plasmalemmal rafts, and regulate cell cortex actin dynamics through a common mechanism. *J Cell Biol* **149**, 1455-72 (2000).

117. Kronke, M. Involvement of sphingomyelinases in TNF signaling pathways. *Chem Phys Lipids* **102**, 157-66 (1999).

118. Billis, W., Fuks, Z. & Kolesnick, R. Signaling in and regulation of ionizing radiation-induced apoptosis in endothelial cells. *Recent Prog Horm Res* **53**, 85-92; discussion 93 (1998).

119. Choo-Smith, L.P., Garzon-Rodriguez, W., Glabe, C.G. & Surewicz, W.K. Acceleration of amyloid fibril formation by specific binding of Abeta-(1-40) peptide to ganglioside-containing membrane vesicles. *J Biol Chem* **272**, 22987-90 (1997).

120. Klahre, U. et al. The Arabidopsis DIMINUTO/DWARF1 gene encodes a protein involved in steroid synthesis. *Plant Cell* **10**, 1677-90 (1998).

121. Bishop, G.J. et al. The tomato DWARF enzyme catalyses C-6 oxidation in brassinosteroid biosynthesis. *Proc Natl Acad Sci U S A* **96**, 1761-6 (1999).

122. McMorris, T.C. Recent developments in the field of plant steroid hormones. *Lipids* **32**, 1303-8 (1997).

123. Iivonen, S. et al. Seladin-1 transcription is linked to neuronal degeneration in Alzheimer's disease. *Neuroscience* **113**, 301-10 (2002).

124. Bae, S.H. & Paik, Y.K. Cholesterol biosynthesis from lanosterol: development of a novel assay method and characterization of rat liver microsomal lanosterol delta 24-reductase. *Biochem J* **326 (Pt 2)**, 609-16 (1997).

125. Andersson, H.C., Kratz, L. & Kelley, R. Desmosterolosis presenting with multiple congenital anomalies and profound developmental delay. *Am J Med Genet* **113**, 315-9 (2002).

126. Luciani, P. et al. Expression of the novel adrenocorticotropin-responsive gene selective Alzheimer's disease indicator-1 in the normal adrenal cortex and in adrenocortical adenomas and carcinomas. *J Clin Endocrinol Metab* **89**, 1332-9 (2004).

127. Fitzky, B.U. et al. 7-Dehydrocholesterol-dependent proteolysis of HMG-CoA reductase suppresses sterol biosynthesis in a mouse model of Smith-Lemli-Opitz/RSH syndrome. *J Clin Invest* **108**, 905-15 (2001).

128. Birnboim, H.C. & Doly, J. A rapid alkaline extraction procedure for screening recombinant plasmid DNA. *Nucleic Acids Res* **7**, 1513-23 (1979).

129. Saiki, R.K. et al. Enzymatic amplification of beta-globin genomic sequences and restriction site analysis for diagnosis of sickle cell anemia. *Science* **230**, 1350-4 (1985).

130. Sanger, F., Nicklen, S. & Coulson, A.R. DNA sequencing with chain-terminating inhibitors. *Proc Natl Acad Sci U S A* **74**, 5463-7 (1977).

131. Chomczynski, P. A reagent for the single-step simultaneous isolation of RNA, DNA and proteins from cell and tissue samples. *Biotechniques* **15**, 532-4, 536-7 (1993).

132. Tooyama, I. et al. Correlation of the expression level of C1q mRNA and the number of C1q-positive plaques in the Alzheimer Disease temporal cortex. analysis of C1q mrna and its protein using adjacent or nearby sections. *Dement Geriatr Cogn Disord* **12**, 237-42 (2001).

133. Lowry, O.H., Rosebrough, N.J., Farr, A.L. & Randall, R.J. Protein measurement with the Folin phenol reagent. *J Biol Chem* **193**, 265-75 (1951).

134. Fukumoto, H., Cheung, B.S., Hyman, B.T. & Irizarry, M.C. Beta-secretase protein and activity are increased in the neocortex in Alzheimer disease. *Arch Neurol* **59**, 1381-9 (2002).

135. Crocker, I.P., Cooper, S., Ong, S.C. & Baker, P.N. Differences in apoptotic susceptibility of cytotrophoblasts and syncytiotrophoblasts in normal pregnancy to those complicated with preeclampsia and intrauterine growth restriction. *Am J Pathol* **162**, 637-43 (2003).

136. Bligh, E.G. & Dyer, W.J. A rapid method of total lipid extraction and purification. *Can J Biochem Physiol* **37**, 911-7 (1959).

137. Lutjohann, D. et al. Profile of cholesterol-related sterols in aged amyloid precursor protein transgenic mouse brain. *J Lipid Res* **43**, 1078-85 (2002).

138. Ledesma, M.D., Da Silva, J.S., Schevchenko, A., Wilm, M. & Dotti, C.G. Proteomic characterisation of neuronal sphingolipid-cholesterol microdomains: role in plasminogen activation. *Brain Res* **987**, 107-16 (2003b).

139. Lundstrom, K. & Ehrengruber, M.U. Semliki Forest virus (SFV) vectors in neurobiology and gene therapy. *Methods Mol Med* **76**, 503-23 (2003).

140. Berglund, P. et al. Semliki Forest virus expression system: production of conditionally infectious recombinant particles. *Biotechnology (N Y)* **11**, 916-20 (1993).

141. Butterfield, D.A. & Boyd-Kimball, D. Amyloid beta-peptide(1-42) contributes to the oxidative stress and neurodegeneration found in Alzheimer disease brain. *Brain Pathol* **14**, 426-32 (2004).

142. Fishman, P.H., Pacuszka, T. & Orlandi, P.A. Gangliosides as receptors for bacterial enterotoxins. *Adv Lipid Res* **25**, 165-87 (1993).

143. Harder, T., Scheiffele, P., Verkade, P. & Simons, K. Lipid domain structure of the plasma membrane revealed by patching of membrane components. *J Cell Biol* **141**, 929-42 (1998).

144. Ledesma, M.D. et al. Raft disorganization leads to reduced plasmin activity in Alzheimer's disease brains. *EMBO Rep* **4**, 1190-6 (2003a).

145. Abad-Rodriguez, J. et al. Neuronal membrane cholesterol loss enhances amyloid peptide generation. *J Cell Biol* **167**, 953-60 (2004).

146. Refolo, L.M. et al. A cholesterol-lowering drug reduces beta-amyloid pathology in a transgenic mouse model of Alzheimer's disease. *Neurobiol Dis* **8**, 890-9 (2001).

147. Hsiao, K. et al. Correlative memory deficits, Abeta elevation, and amyloid plaques in transgenic mice. *Science* **274**, 99-102 (1996).

148. Marcus, D.L. et al. Increased peroxidation and reduced antioxidant enzyme activity in Alzheimer's disease. *Exp Neurol* **150**, 40-4 (1998).

149. Serrano, M., Lin, A.W., McCurrach, M.E., Beach, D. & Lowe, S.W. Oncogenic ras provokes premature cell senescence associated with accumulation of p53 and p16INK4a. *Cell* **88**, 593-602 (1997).

150. Sarkar, D. et al. The human homolog of Diminuto/Dwarf1 gene (hDiminuto): a novel ACTH-responsive gene overexpressed in benign cortisol-producing adrenocortical adenomas. *J Clin Endocrinol Metab* **86**, 5130-7 (2001).

151. Sagara, Y., Dargusch, R., Klier, F.G., Schubert, D. & Behl, C. Increased antioxidant enzyme activity in amyloid beta protein-resistant cells. *J Neurosci* **16**, 497-505 (1996).

152. Di Stasi, D. et al. DHCR24 gene expression is upregulated in melanoma metastases and associated to resistance to oxidative stress-induced apoptosis. *Int J Cancer* **115**, 224-30 (2005).

153. Goldstein, J.L. & Brown, M.S. Regulation of the mevalonate pathway. *Nature* **343**, 425-30 (1990).

154. Waterham, H.R. & Wanders, R.J. Biochemical and genetic aspects of 7-dehydrocholesterol reductase and Smith-Lemli-Opitz syndrome. *Biochim Biophys Acta* **1529**, 340-56 (2000).

155. Wood, W.G., Schroeder, F., Igbavboa, U., Avdulov, N.A. & Chochina, S.V. Brain membrane cholesterol domains, aging and amyloid beta-peptides. *Neurobiol Aging* **23**, 685-94 (2002).

156. Schroeder, F. et al. Recent advances in membrane microdomains: rafts, caveolae, and intracellular cholesterol trafficking. *Exp Biol Med (Maywood)* **226**, 873-90 (2001).

157. Simons, K. & Ehehalt, R. Cholesterol, lipid rafts, and disease. *J Clin Invest* **110**, 597-603 (2002).

158. von Arnim, C.A. et al. The low density lipoprotein receptor-related protein (LRP) is a novel beta-secretase (BACE1) substrate. *J Biol Chem* **280**, 17777-85 (2005).

159. Ehehalt, R., Keller, P., Haass, C., Thiele, C. & Simons, K. Amyloidogenic processing of the Alzheimer beta-amyloid precursor protein depends on lipid rafts. *J Cell Biol* **160**, 113-23 (2003).

160. Simons, M. et al. Cholesterol depletion inhibits the generation of beta-amyloid in hippocampal neurons. *Proc Natl Acad Sci U S A* **95**, 6460-4 (1998).

161. Ledesma, M.D. et al. Brain plasmin enhances APP alpha-cleavage and Abeta degradation and is reduced in Alzheimer's disease brains. *EMBO Rep* **1**, 530-5 (2000).

162. Hsiao, K.K. et al. Age-related CNS disorder and early death in transgenic FVB/N mice overexpressing Alzheimer amyloid precursor proteins. *Neuron* **15**, 1203-18 (1995).

163. Brown, M.S. & Goldstein, J.L. Lowering plasma cholesterol by raising ldl receptors. 1981. *Atheroscler Suppl* **5**, 57-9 (2004).

164. Kusters, J.G., Jager, E.J. & van der Zeijst, B.A. Improvement of the cloning linker of the bacterial expression vector pEX. *Nucleic Acids Res* **17**, 8007 (1989).

165. Borchelt, D.R. et al. A vector for expressing foreign genes in the brains and hearts of transgenic mice. *Genet Anal* **13**, 159-63 (1996).

166. Liljestrom, P. & Garoff, H. A new generation of animal cell expression vectors based on the Semliki Forest virus replicon. *Biotechnology (N Y)* **9**, 1356-61 (1991).